

**REPUBLIC OF TURKEY
HACETTEPE UNIVERSITY
GRADUATE SCHOOL OF HEALTH SCIENCES**

**INVESTIGATING THE EFFECTS OF NEUROMETABOLIC DISEASE-
CAUSING GENES ON SYNAPSE FUNCTION IN DROSOPHILA
MELANOGASTER**

M.Sc. Rukiye KARATEPE

**Program of Molecular Metabolism
DOCTOR OF PHILOSOPHY THESIS**

**ANKARA
2022**

**REPUBLIC OF TURKEY
HACETTEPE UNIVERSITY
GRADUATE SCHOOL OF HEALTH SCIENCES**

**INVESTIGATING THE EFFECTS OF NEUROMETABOLIC DISEASE-CAUSING
GENES ON SYNAPSE FUNCTION IN DROSOPHILA MELANOGASTER**

Rukiye KARATEPE (M.Sc.)

**Program of Molecular Metabolism
DOCTOR OF PHILOSOPHY THESIS**

**ADVISOR OF THE THESIS
Prof. Dr. Rıza Köksal ÖZGÜL**

**ANKARA
2022**

HACETTEPE UNIVERSITY
GRADUATE SCHOOL OF HEALTH SCIENCES

Investigating The Effects Of Neurometabolic Disease-Causing Genes On Synapse Function
In *Drosophila Melanogaster*
Rukiye Karatepe
Supervisor: Prof. Rıza Köksal Özgül

This thesis study has been approved and accepted as a PhD dissertation in "Molecular Metabolism Program" by the assesment committee, whose members are listed below, on 20 July 2022.

Chairman of the Committee : *Prof. Dr. Nuhan Puralı*
Hacettepe University, Department of Biophysics
Member : *Prof. Dr. Ali Dursun*
Hacettepe University, Department of Pediatrics
Member : *Prof. Dr. Mehmet Karaca*
Aksaray University, Department of Biology
Member : *Assoc. Prof. Alexander M. Walter*
Copenhagen University, Department of Neuroscience
Member : *Dr. Mathias Böhme*
University of Leipzig, Department of Biochemistry

This dissertation has been approved by the above committee in conformity to the related issues of Hacettepe University Graduate Education and Examination Regulation.

12 August 2022

Prof. Müge YEMİŞÇİ ÖZKAN, MD, PhD

Director

YAYIMLAMA VE FİKRİ MÜLKİYET HAKLARI BEYANI

Enstitü tarafından onaylanan lisansüstü tezimin/raporumun tamamını veya herhangi bir kısmını, basılı (kağıt) ve elektronik formatta arşivleme ve aşağıda verilen koşullarla kullanıma açma iznini Hacettepe Üniversitesine verdiğimi bildiririm. Bu izinle Üniversiteye verilen kullanım hakları dışındaki tüm fikri mülkiyet haklarım bende kalacak, tezimin tamamının ya da bir bölümünün gelecekteki çalışmalarda (makale, kitap, lisans ve patent vb.) kullanım hakları bana ait olacaktır.

Tezin kendi orijinal çalışmam olduğunu, başkalarının haklarını ihlal etmediğimi ve tezimin tek yetkili sahibi olduğumu beyan ve taahhüt ederim. Tezimde yer alan telif hakkı bulunan ve sahiplerinden yazılı izin alınarak kullanılması zorunlu metinlerin yazılı izin alınarak kullandığımı ve istenildiğinde suretlerini Üniversiteye teslim etmeyi taahhüt ederim.

Yükseköğretim Kurulu tarafından yayınlanan **“Lisansüstü Tezlerin Elektronik Ortamda Toplanması, Düzenlenmesi ve Erişime Açılmasına İlişkin Yönerge”** kapsamında tezim aşağıda belirtilen koşullar haricince YÖK Ulusal Tez Merkezi / H.Ü. Kütüphaneleri Açık Erişim Sisteminde erişime açılır.

- Enstitü / Fakülte yönetim kurulu kararı ile tezimin erişime açılması mezuniyet tarihimden itibaren 2 yıl ertelenmiştir¹.
- Enstitü / Fakülte yönetim kurulunun gerekçeli kararı ile tezimin erişime açılması mezuniyet tarihimden itibaren .6.. ay ertelenmiştir².
- Tezimle ilgili gizlilik kararı verilmiştir³.

..... / /

Rukiye Karatepe

Lisansüstü Tezlerin Elektronik Ortamda Toplanması, Düzenlenmesi ve Erişime Açılmasına İlişkin Yönerge:

¹ Madde 6. 1. Lisansüstü teze ilgili patent başvurusu yapılması veya patent alma sürecinin devam etmesi durumunda, tez **danışmanın** önerisi ve **enstitü anabilim dalının** uygun görüşü üzerine **enstitü** veya **fakülte yönetim kurulu** iki yıl süre ile tezin erişime açılmasının ertelenmesine karar verebilir.

² Madde 6. 2. Yeni teknik, materyal ve metotların kullanıldığı, henüz makaleye dönüşmemiş veya patent gibi yöntemlerle korunmamış ve internetten paylaşılması durumunda 3. şahıslara veya kurumlara haksız kazanç imkanı oluşturabilecek bilgi ve bulguları içeren tezler hakkında tez **danışmanın** önerisi ve **enstitü anabilim dalının** uygun görüşü üzerine **enstitü** veya **fakülte yönetim kurulunun** gerekçeli kararı ile altı ayı aşmamak üzere tezin erişime açılması engellenebilir.

³ Madde 7. 1. Ulusal çıkarları veya güvenliği ilgilendiren, emniyet, istihbarat, savunma ve güvenlik, sağlık vb. konulara ilişkin lisansüstü tezlerle ilgili gizlilik kararı, **tezin yapıldığı kurum** tarafından verilir *. Kurum ve kuruluşlarla yapılan işbirliği protokolü çerçevesinde hazırlanan lisansüstü tezlere ilişkin gizlilik kararı ise, **ilgili kurum ve kuruluşun önerisi** ile **enstitü** veya **fakültenin** uygun görüşü üzerine **üniversite yönetim kurulu** tarafından verilir. Gizlilik kararı verilen tezler Yükseköğretim Kuruluna bildirilir.

Madde 7.2. Gizlilik kararı verilen tezler gizlilik süresince enstitü veya fakülte tarafından gizlilik kuralları çerçevesinde muhafaza edilir, gizlilik kararının kaldırılması halinde Tez Otomasyon Sistemine yüklenir

ETHICAL DECLARATION

In this thesis study, I declare that all the information and documents have been obtained in the base of the academic rules and all audio-visual and written information and results have been presented according to the rules of scientific ethics. I did not do any distortion in data set. In case of using other works, related studies have been fully cited in accordance with the scientific standards. I also declare that my thesis study is original except cited references. It was produced by myself in consultation with supervisor Prof. Dr. Rıza Köksal Özgül and written according to the rules of thesis writing of Hacettepe University Institute of Health Sciences .

(Signature)

Rukiye KARATEPE

ACKNOWLEDGEMENTS

First and foremost, I would like to express my sincere gratitude to my supervisor Prof. Dr. Rıza Köksal Özgül for his guidance and support with full encouragement. This thesis would not have been possible without Assoc. Prof. Dr. Alexander Walter: Thank you for giving me the opportunity to work in your lab, for sharing your expertise, and providing me invaluable guidance throughout the research. I would like to recognize the invaluable assistance of Dr. Mathias Böhme, whose guidance from the initial step in *Drosophila* research enabled me to develop an understanding of the subject. I would like to also thank him for his great empathy and patience. I would like express my deep and sincere gratitude to my thesis committee members for their efforts and contributions to this work. I would like to thank to Prof. Kadriye Kart Yaşar, Prof. Dr. Ali Dursun, Prof. Papatya Keleş, Dr. Tuba Canbaz, and Assoc. Prof. Basri Gülbakan for their unfailing support and continuous encouragement. I acknowledge the generous financial support from DAAD and TUBITAK and would like to thank to especially Mr. Joscha Seul from DAAD and to Marina Spors from FMP for their help in especially official issues. Heartfelt thanks goes to AG Walter and AG Sigrist lab members: Manon, Natalie, Kiana, Meida, Marc, Andreas, Torsten, Nika, Anthony, Niraja, Jason, Chengji, Sabine, Gabi, and Frau Stübner. Very special thanks to Hacettepe Molecular Metabolism Department members to especially Mümine, Esra, Neşe, Eda, Didem, and Esin; and to my colleagues from University of Health Sciences Rumeysa, Sena, Tuğba, Fatima, Sude, Hande, Burak, and Sibel. I am indebted to Şeyma, Fatma abla, Fırat abi, Mehmet amca and his family, Asya, and Bayram for their hospitality, and help in every issue during my stay in Berlin. And, to my close friends Eda, Güliz, and Aysel. Last years were hard yet it strengthened our friendship! Lastly, my family deserves endless gratitude: my father and mother for raising me in a crepuscular manner, according to religious acts, your raising style helped me in building the method section of the project. And to all of my family members, Rabia, Vildan, Zeliha, Yusuf Berâ, and Gül Nevâ: Without your support I would not be able to finish the thesis!

ABSTRACT

Karatepe, R., Investigating the Effects of Neurometabolic Disease-Causing Genes on Synapse Function in *Drosophila melanogaster*, Program of Molecular Metabolism Doctor of Philosophy Thesis, Ankara, 2022. Our group has identified several patients that harbor mutations in genes that hold the potential for being important players of synapse function, UNC79 and MBOAT7 being two of them. UNC79 is one of the accessory subunits of a sodium leak channel, NALCN, which is composed of NALCN, UNC80 and UNC79 subunits. It is widely expressed in the brain and known to inhabit neuropils in *Drosophila*. MBOAT7, on the other hand, is an enzyme that attaches preferentially arachidonic acid to sn-2 positions of phosphoinositide (PI) in specifically brain tissues of mammals. PIs, are renown players of synapse function. In the light of information, we aimed to reveal the effects of UNC79 and MBOAT7 knockdowns on synapse size, number and morphology via combination of molecular biology and imaging techniques by using fruit fly as a model organism.

Pan-neuronal and motoneuronal silencing of NALCN channel components - NALCN, UNC79, and UNC80- and motoneuronal silencing MBOAT7 ortholog in *Drosophila* 3rd instar larvae resulted in discrepancies in both brp and glutamate receptor levels and morphologies compared to control groups. Besides, pan-neuronal silencing MBOAT7 ortholog has no effect on brp and glutamate receptor intensities.

Dissecting wild-type larvae in a time-dependent fashion showed that brp and glutamate receptor levels oscillate in 1b neuromuscular junctions. Dissecting motoneuronally silenced na in a time dependent fashion showed a shift in brp and glutamate receptor intensities compared to control groups. On the other hand no changes in both brp and glutamate receptor levels were observed in pan-neuronally silenced frj larvae.

Keywords: Rare metabolic disease, GAL4/UAS, RNAi, brp, Glutamate receptor.

(*) This work was supported by TUBITAK 1002 (Project Number: 120Z189) and The German Academic Exchange Service (DAAD) Scholarship (57442045).

ÖZET

Karatepe, R., Nörometabolik Hastalık Nedeni Olan Mutasyonların *Drosophila Melanogaster*'da Modellenmesi ve Sinaps Fonksiyonu Üzerine Etkilerinin Araştırılması, Moleküler Metabolizma Programı Doktora Tezi, Ankara, 2022.

Grubumuz tarafından son yıllarda sinaptopati ile ilişkilendirilebilecek UNC79 ve MBOAT7 gibi patojenik olduğu değerlendirilen yeni varyantlar saptanmıştır. UNC79 geni, NALCN ve UNC80 proteinleri ile birleşerek NALCN sızıntı kanalı olarak isimlendirilen bir kanalı oluşturmaktadır. MBOAT7 geni ise Lands lipid modelleme yolağında yer alan önemli ve sinaps fonksiyonu üzerine önemli etkileri olabilecek enzimlerden biridir. Yukarıda verilen bilgiler ışığında UNC79 geni ve etkileşim içerisinde olduğu NALCN kanal bileşenleri (UNC80 ve NALCN) ile MBOAT7 geninin sinaps fonksiyonu ve sinaptik iletimde önemli rolleri olabileceği fikri güçlenmektedir. Fakat, proteinlerin yokluğunda sinaptik iletim, sinaps büyüklüğü ve şeklinin nasıl etkilendiği bilinmemektedir. Bu soruların cevaplanabilmesi için ilgili genler *Drosophila melanogaster*'de motor nöronlarında ve tüm beyinde doku bazlı susturulmuştur. Bahsi geçen genlerin moto-nöronal ve pan-nöronal olarak susturulması sonucunda *Drosophila* 3. instar larva nöromusküler kavşağında bulunan brp ve glutamat reseptör miktarlarının kontrol grubuna göre arttığı/azaldığı yani sabit olmadığı gözlenmiştir. Sonucun sirkadiyen ritim ile ilişkili olup olmadığının anlaşılması için yabancı tip sinek larvasının zamana bağlı olarak disekte edilmesi sonucunda brp ve glutamat reseptörünün zamana bağlı olarak osile ettiği ve bu osilasyon paterninin literatürde bahsi geçen sinek lokomotor aktivitesine benzediği gözlenmiştir. Son olarak NALCN *Drosophila* ortoloğu na motonöronal olarak susturulup zamana bağlı brp ve glutamat reseptör miktarı incelendiğinde proteinlerin zamana bağlı olarak osile ettiği, fakat osilasyonun kontrol grubuna göre kaydığı gözlenmiştir.

Anahtar Kelimeler: Gal4/UAS, RNAi, brp, glutamate reseptörü, metabolik hastalık.

(*) Bu çalışma TÜBİTAK 1002 (Proje Numarası: 120Z189) ve DAAD Araştırma Bursu (57442045)) ile desteklenmiştir.

CONTENTS

ABSTRACT	vii
ÖZET	viii
SYMBOLS AND ABBREVIATIONS	xi
FIGURES	xii
TABLES	xiv
1. INTRODUCTION	1
2. LITERATURE REVIEW	4
2.1. Inborn Errors of Metabolism	4
2.2. Synaptic Transmission and <i>Drosophila</i> Neuromuscular Junction	5
2.3. <i>Drosophila</i> Locomotor Behavior	7
2.4. Synaptic Plasticity	8
2.5. Cyto-matrix at the Active Zone (CAZ)	9
2.6. Synaptopathies of Interest	11
2.6.1. UNC79	11
2.6.2. MBOAT7	15
2.7. <i>Drosophila</i> Melanogaster as a Model Organism	21
2.8. GAL4-UAS System	22
2.9. Problem Statement and Aim	23
3. MATERIALS METHODS	25
4. RESULTS	36
4.1. Motoneuronal and Pan-neuronal Silencing of NALCN Channel Components	36
4.2. Motoneuronal and Pan-neuronal Silencing of NALCN Channel Components -Na, Unc79, and Unc80- Produced Discrepant Results	39

4.3.	Motoneuronal Silencing of Farjavit	48
4.4.	Pan-Neuronal Silencing of Farjavit has no Effect on Brp and Glutamate Receptor Intensities	51
4.5.	BRP and Glutamate Receptor Levels are not Constant in Wild-Type (w1118) <i>Drosophila melanogaster</i> at 29 °C	54
4.6.	BRP and Glutamate Receptor Levels are not Constant in Wild-Type (W1118) <i>Drosophila Melanogaster</i> at 25 °C	56
4.6.1.	BRP and Glutamate Receptor Levels Fluctuate in a Time-Dependent Manner	60
4.7.	Shifting Dissection Time for Only One-Two Hours Results in Non-Significant Change in Intensities	64
4.8.	Dissecting Larvae by Taking Sequential Time Points Results in Gradual Change in BRP and Glutamate Receptor Levels	69
4.9.	Motoneuronally Silencing na Produces Phase Shift in BRP/Glutamate Receptor Levels	71
5.	DISCUSSION	73
5.1.	Silencing NALCN Channel Components Produced Discrepant Results	73
5.2.	Not Pan-Neuronally but Motoneuronally Silencing MBOAT7 Ortholog <i>frj</i> Produced Discrepant Results	75
5.3.	BRP Oscillates at <i>Drosophila</i> Neuromuscular Junctions	76
6.	CONCLUSION	82
7.	REFERENCES	84
8.	APPENDIX	97
	Appendix 1: Summary of the Statistics	97
	Appendix 2: Thesis Originality Report	121
	Appendix 3: Digital Receipt	122
9.	Curriculum Vitae	123

SYMBOLS AND ABBREVIATIONS

AA	Arachidonic Acid
AZ	active zone
BRP	Bruchpilot
CaC	Cacophony (<i>Drosophila</i> Ca ²⁺ channel α 1 subunit)
CAST	CAZ-associated structural protein
CAZ	Cytomatrix at the active zone
CNS	Central nervous system
MBOAT7	Membrane-bound O-acyltransferase domain-containing protein 7
NALCN	Sodium Leak Channel, Non-Selective
NMJ	Neuromuscular junction
PI	Phosphoinositide
PIP	Phosphatidylinositol phosphate
RBP	RIM-binding protein
RIM	Rab3-interacting molecule
RNAi	RNA interference
Sn-2	Stereo-specifically numbered-2
SNARE	Soluble NSF attachment receptor proteins
SV	Synaptic vesicle
Syt	Synaptotagmin
Syx	Syntaxin
UAS	Upstream activating sequence
UNC79	Uncoordinated 79
UNC80	Uncoordinated 80

FIGURES

Figure	Page
2.1. Domain Structure of AZ Components.	9
2.2. NALCN channel components are mostly expressed at central nervous system and head of Drosophila.	15
2.3. General representation of a phospholipid.	16
2.4. PI Acyl Species are heterogeneously distributed among different sub-membranous compartments.	17
2.5. Phosphoinositide is a special type of phospholipid.	18
2.6. Acyl Chain Remodelling via Lands Cycle.	20
2.7. Depiction of Gal4-UAS System.	23
3.1. Representation of Magnitude and phase of intensity calculation from brp and glutamate receptor spots.	29
4.1. AZ intensities are lognormally distributed.	37
4.2. BRP and glutamate receptor spot areas and integrated intensity are directly proportional with each other.	37
4.3. Input NMJs and segmented NMJs.	38
4.4. Motoneuronal silencing of na results in altered morphology and altered brp and glutamate receptor intensities.	41
4.5. Pan-neuronal silencing of na results in altered morphology and intensity in both presynaptic and postsynaptic sides.	42
4.6. Motoneuronal silencing of the accessory subunit unc79 results in altered morphology and intensity in both presynaptic and postsynaptic sides.	44
4.7. Pan-neuronal silencing of the accessory subunit unc79 results in altered morphology and intensity in both presynaptic and postsynaptic sides.	45
4.8. Motoneuronal silencing of the accessory subunit unc80 resulted in inconsistent morphology and intensity.	46
4.9. Pan-neuronal silencing of the accessory subunit unc80 resulted in inconsistent morphology and intensity.	47

4.10. Motoneuronal silencing of frj results in altered morphology and intensity in both presynaptic and postsynaptic sides.	49
4.11. Motoneuronal silencing of frj results in altered morphology and intensity in both presynaptic and postsynaptic sides.	50
4.12. Pan-neuronal silencing of frj results in no change in brp and glutamate receptor intensities.	52
4.13. Gender dependent pan-neuronal silencing of frj has no effect on brp and glutamate receptor intensities.	53
4.14. BRP and glutamate receptor levels are not constant in 3rd instar larvae.	55
4.15. BRP and glutamate receptor oscillate with the same pattern.	59
4.16. Mean BRP and glutamate receptor changes at least two fold. Six separate experiments were analyzed and at least two fold change in both brp and glutamate receptor levels were observed between max and min brp and glutamate receptor mean intensities.	60
4.17. Dissecting larvae in two consecutive days resulted in approximately the same mean intensities at same time points.	62
4.18. Mean BRP and mean glutamate receptor intensities showed upside down shaped bell curve on both days.	63
4.19. Changing diet has an impact on AZ shape and intensity.	67
4.20. Tremendous changes in both spot shape of brp/glutamate receptor and intensity changes in brp/glutamate receptor were observed.	68
4.21. Dissecting larvae by taking consecutive times results in gradual brp and glutamate receptor intensity increase and a change in brp and glutamate receptor morphologies.	70
4.22. BRP/Glutamate Receptor Intensities that are dissected in a time-dependent fashion.	72

TABLES

Table	Page
2.1. Key Drosophila Active Zone Components	10
3.1. Genotypes of the 3rd instar larvae used in experiments	26
3.2. Solutions	31
3.3. Reagent and Resources	32
3.4. Software and Algorithms	33
3.5. Experimental Models: Organisms/Strains	34
3.6. Fly Food Ingredients	35
4.1. Description of the environmental cues for w1118 dissections.	57
4.2. Experimental Conditions for normal food and special food vials.	66

1. INTRODUCTION

Single-gene mutations that result in defects in metabolic pathways are known as inborn errors of metabolism (IEMs). Most of the IEMs are recessively inherited and clinical symptoms can be due to intoxication, defects in energy metabolism or due to complex molecules.(1)

Most of the IEMs are known to manifest neurological signs. Neurological findings may stem as early as the first neuronal differentiation which starts in the 1st half of gestation, however synapse wiring and synapse formation does not speed up until the last trimester where brain mass increases about three fold.(2) Hence, synaptic dysfunctions mostly stem from this time and beyond.

Any process that hinders the formation and/or wiring of synapses can result in epilepsy, movement disorders, and/or intellectual disability. Diseases that affect synapse formation/wiring or synaptic function are referred to as synaptopathies. Since, synapses possess unique composition and function, synaptopathies take an important place in IEMs. Still, very few studies exist concerning synaptopathies and little is known about the underlying molecular mechanisms.

Our research group has been working on the identification of the genes and pathways for undiagnosed IEM patients via whole-exome analysis. We identified several candidate genes that may have important tasks in synaptic function.(3-5) Besides, our database harbors strong candidate genes that may have important roles in synapse function -UNC79 and MBOAT7 being two of them.

UNC79, functions as the accessory subunit of NALCN sodium leak channel. The channel is composed of three subunits: NALCN forms the pore region whereas UNC79 and UNC80 form the accessory subunits.(6)

The channel is expressed in the whole brain and is known to be located close to neuropils (synaptic dense regions) (7) and expressed in parallel to a conserved active zone(AZ) component, bruchpilot (brp), in *Drosophila*.(8)

MBOAT7, on the other hand, is an enzyme that plays important roles in phosphoinositide(PI) remodeling: It preferentially attaches arachidonic acid(AA) to the sn-2 position of PIs.(9) Mammalian brain PIs show tissue specific tail composition, and mammalian brain PIs are enriched with AA on their sn-2 position. Besides, PIs are renowned regulators of synaptic function: AA, that is located in the sn-2 position of PIs is known to play a role in easing open syntaxin (Syx) formation and thus SNARE (Soluble NSF attachment receptor proteins) formation. Whereas Phosphatidylinositol phosphate (PIPs) modulate synapse function by recruiting important synaptic proteins.

In this study, by taking the aforementioned information into consideration, our first aim was to understand

1. How synapse morphology, and synaptic brp and postsynaptic glutamate receptor levels change at *Drosophila* neuromuscular junctions upon motoneuronal and pan-neuronal silencing of NALCN channel components and MBOAT7.

Afterwards we sought to understand

2. Whether presynaptic and postsynaptic brp and glutamate receptor levels cycle across the day in a time dependent fashion in *Drosophila* neuromuscular junctions (NMJs).
3. And if diet has an effect on brp/glutamate receptor levels and synapse morphology.

Lastly,

4. We dissected motoneuronally silenced NALCN ortholog in a time-dependent fashion to see if there is a change in oscillatory pattern of brp and glutamate receptor levels.

With this study we, for the first time:

1. Silenced NALCN channel components and MBOAT7 to see the effects on synapse morphology and pre- and post-synaptic brp and glutamate receptor levels respectively.
2. Analyzed brp and glutamate receptor levels in a time-dependent manner at *Drosophila* NMJs.
3. Analyzed presynaptic and postsynaptic morphologies/areas.
4. Observed how motoneuronally silencing na affected brp and glutamate receptor levels in a time-dependent fashion.
5. Analyzed putative environmental factors that may have an effect on synapse morphology and synaptic protein levels.

2. LITERATURE REVIEW

2.1. Inborn Errors of Metabolism

Inherited metabolic disorders are diseases that are estimated to be as high as 1 in 800 live births, but it varies greatly and depends on the population. Although rare, around 350 million people on earth live with rare disorders.(10) Among these patients, most of them have no treatment. On top of it, half of these patients came to the doctor's attention due to neurological deterioration possibly due to people taking neurological signs more seriously than other signs.

Inherited metabolic disorders mostly result from single-gene mutations, and, pathophysiologically, can be grouped into three main subgroups:

1. IEMs giving rise to intoxication
2. Energy metabolism defects
3. Complex molecule disorders

IEMs that give rise to intoxication mostly possess a symptom free period and afterwards proceed with the accumulation of toxin substrate. Removal of toxin via special diets or cleansing drugs i.e. sodium benzoate is mostly enough to treat the disease (i.e. inborn errors of neurotransmitter synthesis).(1)

Energy metabolism defects, on the other hand, can be grouped into mitochondrial (i.e. congenital lactic acidemias) and cytoplasmic energy defects (i.e. disorders of glycogen and glycolysis metabolism), and are more severe and mostly untreatable.(1)

The last group, complex molecule disorders, is mostly related with cellular organelles, i.e. lysosome and peroxisome, and dysfunction of any of the organelles affects many biochemical pathways in a more subtle way giving rise to a more complex pathophysiology.(11)

Besides, most of the IEMs result in molecular homeostasis defects, and hence mostly disrupt neuronal functioning and/or neurodevelopment and thus manifest neurological outcome:

Brain development starts in very early neonatal stages by differentiation of the cell to different types of neuronal cells and proceed with the proliferation of progenitor cells. Any disruption in this phase results mostly in microcephaly. This stage proceeds by the migration of neurons to their predefined locations (2-6 m gestation) and proceeds in postnatal stage with circuitry formation and myelination.(2) Disruptions in this stage will come with a broad disease manifestation: It can range from attention deficits to locomotor problems, epilepsy and developmental delay.

Synaptopathies, an umbrella term for diseases affecting synaptic transmission, add up to considerable amounts in rare metabolic diseases, perhaps due to synapses' unique composition and unique metabolic functions. Unfortunately, albeit their amounts, synaptopathies are also one of the least studied subgroups of metabolic diseases:

IEMs that lead to synaptopathies, may result from vitamin and purine defects (i.e. intracellular cobalamin defects), small molecule accumulation (i.e. galactosemia) small molecule deficiencies (i.e. GABA, GluR), complex molecule accumulations (i.e. Niemann Pick-C) or complex molecule defects (i.e. SNX14) or rarely may be a result of energy/mitochondrial defects.(2)

Before turning faces to synaptopathy of interest, it is of great importance to understand the principal players of synaptic transmission.

2.2. Synaptic Transmission and *Drosophila* Neuromuscular Junction

Neuronal lipid membranes surrounding axons and synaptic regions, host many channels, mostly voltage-gated, that are important players in signal propagation.

In *Drosophila*, action potentials that start from the axon hillock, travel all the way to the end of the axon by depolarizing the membrane and ultimately opening voltage-gated Ca^{2+} channels. This event results in Ca^{2+} rush into the neurons and eventually Ca^{2+} interacts with negatively charged amino acids located on Ca^{2+} sensor proteins, most notably synaptotagmin-1 (Syt-1).(12) This interaction facilitates the

formation of the SNARE complex which is composed of SNAP25, synaptobrevin, and Syx-1.(13) Cleavage of these molecules results in neurotransmitter release at specialized locations observed as dense bodies and named 'active zone' by Couteaux and Pecot-Dechavassine.(14) Released neurotransmitters at 1b motoneuron NMJs mostly bind to heteromeric glutamate receptors that are composed of GluRIIC, GluRIID, GluRIIE subunits alongside with either GluRIIA or GluRIIB subunit.(15)

All of the processes take no more than a few milliseconds indicating a fast and precise neuronal information flow. One can intuitively understand that the timing for neurotransmitter release is very fast indicating that synaptic vesicles (SVs) must be prepared beforehand. In fact, this is the case: AZs that host both SVs (some docked whereas others not) and conserved synaptic proteins (RIM, Munc13, RBP, a-liprin, and ELKS) bridge SVs with Ca^{2+} channels and eventually regulate short-term and long-term synaptic plasticity.(16) The precise amount of synaptic proteins and their spatial location plays a big role in defining the speed and precision of synaptic transmission.

Muscles are present on the other end of the NMJ and comprise substantial amount of body mass in *Drosophila* larvae. Motor neurons that exit the central nervous system (CNS), extend all the way till muscles to form glutamatergic synapses via type 1 boutons at neuromuscular junctions.(17, 18) Type 1 boutons can further be classified as 1b (big) and 1s (small) and are stereotypic.(17, 19) To no surprise, *Drosophila* larvae also share a stereotypic muscle anatomy which is distinct from its mammalian counterparts: The most important distinction between mammalian muscle and fly muscle is their formation style. One myotube forms one muscle in fly larvae (20) whereas in mammalian system a bundle of myotubes have to come together to form muscle fibers.(21, 22) In flies this feature results in shape and size signatures for each muscle: Each abdominal segment has approximately 30 muscles aligned in the same direction and innervated by special neuronal protrusions.(20, 21, 23) Besides, fly abdominal segments 2-7 share the same muscle pattern that allows the analysis of NMJs pretty easily.(24)

In short, NMJs process the messages they receive from upstream networks, send the signal to the muscles which eventually is observed as locomotor behavior.

Hence, neuromuscular junctions, due to their location and stereotypic pattern are notable hubs for not only understanding synaptic plasticity and synaptic function, but also for driving conclusions for synaptic function-locomotor output association.

2.3. *Drosophila* Locomotor Behavior

Drosophila, opposed to most of the mammals is crepuscular in controlled laboratory condition: They are active close to lights on-off and exhibit a siesta phase in between and another sleep phase approximately 12h later at midnight.(25) In other words, two sin waves form daily rhythm in *Drosophila*. Therebeside, the amplitude of the slope of the sin wave can be modulated by circadian rhythm factors, temperature, age of the animal, to name a few.(25)

After the morning peak (M), fly activity level declines with differing slopes and eventually a sleep phase is observed in the middle of the day. In the course of time another steep increase occurs resulting in evening (E) activity peak close to lights off phase. Of note, flies under natural conditions, behave in a totally different way: They house another activity peak in the middle of the day known as afternoon (A) peak.(26)

Studies have shown that evening and morning peaks are regulated differently by three different molecular mechanisms (27-29), yet light and circadian rhythm are the main drivers of the daily locomotor oscillations (30):

Circadian rhythm regulation is mostly achieved by three main mechanisms. Morning activity peak is regulated by PDF (Pigment-dispersing factor) positive small ventral lateral neurons, whereas dorsal lateral neurons (LNDs) and PDF negative sLNVs are necessary for evening peaks.(28, 31, 32)

One of the modulators of evening peak starting time is known to be the circadian clock and temperature.(26) The timing of the peaks are thus prone to changes in a daily basis. Evening to morning peak is reset everyday with morning light and another set of sin wave starts each day . On top of it, previous history such as sleep deprivation will have an effect on the locomotor pattern on consecutive days which is known as rebound state.(33-35)

Besides, similar to adult flies *Drosophila* larvae also exhibit circadian rhythms.(36-38) The first thing that comes into mind is whether *Drosophila* larvae' also sense light? Though larvae do not have eye, larvae sense light via their rhodopsin expressing bolwig organs (39, 40) and another highly interesting structure: cd4a dendritic arborizations.(41) Cd4a with their highly branched dendrites cover all of the muscles of *Drosophila* larvae and express extraocular photoreceptors.(41, 42) These receptors that are not rhodopsin are highly sensitive to UV and blue light and can sense light.(43, 44) Indeed high levels of light exposure induces the same locomotor pattern in larvae via extraocular receptors: a rolling behavior which is preceded by running from the light source.(41, 44)

2.4. Synaptic Plasticity

Synapses are dynamic structures. Their morphology and protein amount can change rapidly by outside and inside cues in a long-term and/or short-term fashion. These changes known as synaptic plasticity (45, 46) can be modulated by several agents i.e. synaptic activity, circadian rhythm, light amount, and locomotor behavior. Factors that change synaptic activity form a history at synapses, and later, synaptic response changes according to the history of its own activity (44, 45) thus synaptic activity results in learning and memory formation.(47, 48)

Synaptic plasticity may be the result of post-synaptic or presynaptic induction.(49) Synaptic depression and facilitation in a short-time scale are considered as short-term synaptic plasticity (50) while long-term synaptic changes are accompanied by transcription of new proteins.(51-53)

Due to the conserved molecules and their meticulous housing at AZs researchers tried to understand the relationship between morphology and synaptic plasticity.(54, 55) As expected there are numerous papers drawing correlation with synaptic molecular organization and synaptic plasticity.(56)

2.5. Cyto-matrix at the Active Zone (CAZ)

AZs, neurotransmitter release territories, are formed by a meshwork of detergent-insoluble proteins (57) with a predefined structure that can change from neuron to neuron or organism to organism. For instance, *Drosophila* neuromuscular junctions share a T-shaped CAZ, thus named T-bar (58) whereas vertebrate central synapse AZs have a disc-like shape.(59) *Drosophila* T-bars are formed by mainly five conserved proteins: BRP, RIM, RBP, Liprin- α , and UNC13 (Figure 2.1.). (16)

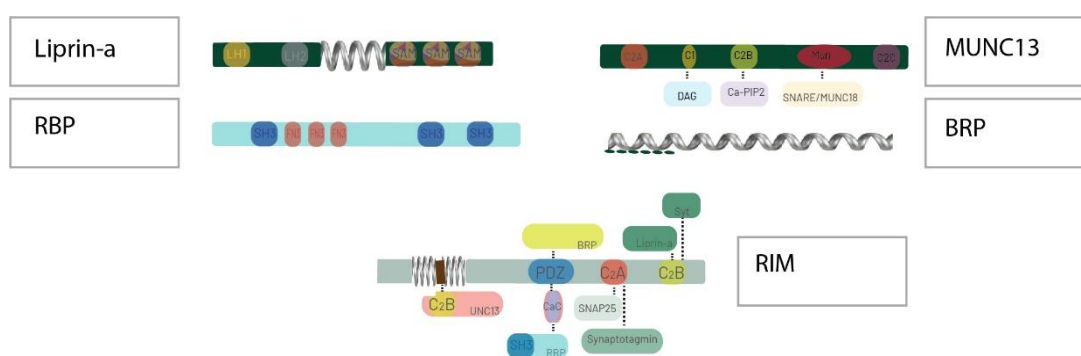


Figure 2.1. Domain Structure of AZ Components.

BRP is the main component that forms the T-shape and is thus used as a morphology marker of AZs.(60) It aligns and forms an elliptic shape, and with its C-terminal, interacts with SVs, while its N-terminal is in close contact with calcium channel cacophony (CaC).(54, 61) Several brp molecules come together to form a meticulous shape resembling a donut that wraps around CaC.(62) Furthermore, ultrastructural studies of CAZ revealed that nearly 1:4 of BRP molecules are freely standing at AZs and AZ intensities are gradually distributed which matches functional synaptic activity among synapses.(56)

BRP is in close contact with one UNC13 isoform, UNC13A, that is placed approximately 70nm away from CaC and is important in vesicle fusion; approximately 120nm away lies the other isoform UNC13B that is in close contact with liprin-a.(63) RIM and RBP on the other hand, have important tasks in AZ organization and BRP morphology (Please refer to Table 2.1. for other essential CAZ components).

Table 2.1. Key *Drosophila* Active Zone Components

AZ Component	Definition
BRP	Presynaptic AZ protein. Forms T-bar, the presynaptic dense region at AZs in which synaptic transmission occurs in <i>Drosophila</i> . BRP C-term binds to SVs and is highly homologous to vertebrate ELKS/CAST; whereas N term is in contact with Calcium channel CaC and is formed by coiled-coil sequences (54). BRP is in close contact with UNC13A which lies approximately 70nm away from CaC. (63)
RBP	Rim binding protein consists of three SH3 and three FN3 domains (64) and mutating RBP results in a change in AZ BRP morphology.(65)
Synaptotagmin-1	Syt is placed in lipid membrane in a closed conformation and interaction with MUNC18 results in Syt opening and SNARE complex formation.(66)
SNAP25	One of the components of the SNARE complex.
Synaptobrevin	One of the components of the SNARE complex.
RIM	Rab Interacting molecule plays role in AZ organization.
UNC13	An accessory protein that is important in SVs fusion.(67) Two isoforms UNC13A and UNC13B are placed 70 and 120 nm away from CaC via BRP and Syd-1 respectively, in <i>Drosophila</i> .(63)
a-Liprin	Liprin- α is important in anterograde transport including axonal transport of unc104.(68) Together with Syd-1 they assemble the first parts of AZ in <i>Drosophila</i> .(69)

2.6. Synaptopathies of Interest

Synaptopathy term is used to define any disease with synaptic abnormality. Abnormalities may be the outcome of direct synaptic dysfunction -mutations in neuroligin (70), NMDARs (71), mGluRs (72) lead to these group of diseases- or they may arise indirectly by any means that in the end changes synaptic signaling, as is the case for some forms of ASDs.(73, 74)

Rare metabolic diseases such as hyperekplexia (also known as Startle disease) (75, 76) and Angelman disease (77) are only some of the rare diseases that are classified as synaptopathies, indeed there is more than meets the eye since rare synaptopathic metabolic diseases increase exponentially in recent years.

Our group has identified several patients that can be classified in the synaptopathy subgroup, however, mostly there is no study exploring how knockdown of the gene products effect synapse morphology and synaptic protein levels. This study will focus on mutation harboring genes *UNC79* and *MBOAT7*- that are thought to be important players of synapse function.

2.6.1. *UNC79*

An affected child born to unaffected parents with distinctive craniofacial features, abnormal motor activity and tone, sleep disorder, autonomic instability, and developmental delay referred to our Metabolism Unit, Department of Pediatrics, Faculty of Medicine, Ankara, Turkey. For the genetic diagnosis of the patients, whole exome sequencing analyses were performed. A novel *de novo* variant (p.Thr1377Arg) in *UNC79* gene possibly linked to the pathogenicity of the patient was identified.

UNC79 is one of the accessory subunits of an orphan sodium leak channel known as *NALCN* which attracted attention recently upon its rediscovery by H.A. Nash in mutagenized flies.(7) Afterwards, the channel attracted attention for its sensitivity to volatile anesthetics, its role in rhythmic behaviors and circadian rhythm, and of course as a leak channel.(78-81) This channel is comprised of three subunits *NALCN* being the pore forming region and two accessory subunits renowned as *UNC79* and *UNC80* respectively.(82)

NALCN and its Interacting Partners

NALCN channel belongs to the 4x6TM ion channel family (83) and is comprised of three subunits: NALCN, UNC80, and UNC79 respectively.(80) It has diverged from voltage-gated channels and is mostly found as single copy in bilaterians and non-bilaterians except few organisms such as *C. elegans*.(84) Although, previous work showed that the major charge carrying ion at resting membrane potential is Na⁺ and thus the channel is a leak channel (80), hence its name, recent studies showed that NALCN channel also works in a voltage dependent manner.(85)

This channel shares many features of voltage gated Na⁺ channels, nevertheless, it digresses from these channels by its less positive S4 transmembrane segment (83) and by the unique motif present in its pore region: (EEKE), differing from both Na⁺ and Ca²⁺ channels.(80)

NALCN the pore component of NALCN channel is one of the core sleep regulating genes (86) and is known to modulate pacemaker activity.(87)

UNC79 and UNC80 are the two accessory subunits interacting with NALCN pore region and possess HEAT and armadillo repeats that interact with the pore of the complex via the intracellular II-III linker.(82, 88, 89) Both of the subunits are sizeable compared to common voltage gated Na⁺ channel subunits. On the contrary to their size, they do not have known functional domains or transmembrane domains, and are believed to play an important role in the localization and regulation of the NALCN channel complex in *Drosophila*.(90) Disease causing mutation in both *UNC80* (91) and *NALCN* (92-95) are associated with CLIFAHDD syndrome -congenital contractures of the limbs and face, abnormal tone, neonatal respiratory distress, developmental delay.(94, 96-101) No mutation, other than ours, that leads to CLIFAHDD in *UNC79* was identified so far. However, or patients pathophysiology closely resembles mutations in *NALCN* and *UNC80* that makes *UNC79* also a strong candidate.

NALCN channel is also shown to interact with two other molecules: The pore region binds to calmodulin (CaM) by its IQ like motif that lie in the C-terminal.(6, 82, 102-104) On the other side, binding to Nlf-1 (NCA localization factor 1) via NALCN's

extracellular loops is responsible for the localization of the channel and links the channel to molecular clock (105), besides, rhythmic expression of Nlf-1 results in low Na⁺ leak at night and high in the morning, thus changing the firing rates of *Drosophila* clock neurons.(78) Activation of this channel can be achieved via G protein coupled or G protein independent fashion (106): G protein-coupled channel activation depends on low extracellular Ca²⁺, whereas G protein-independent activation of the channel occurs via muscarinic acetylcholine receptors or substance P receptors.(107)

Literature Review

In this section we will especially focus on studies that are directly or indirectly related to neuronal function and NALCN channel:

In humans, NALCN is mostly expressed in neurons in the CNS and its expression pattern is in parallel with synaptophysin –a SV specific protein.(80) In *Drosophila*, NALCN is concentrated in neuropils indicating that it may again be an important player of synapse function in this organism.(7) Yet studies regarding this channel and its effects on synaptic function are limited.

- NALCN channel is mostly considered as a Na⁺ leak channel due to less positively charged S4 transmembrane segment that is believed to contribute to its voltage insensitivity; however Lu *et al.* expanded the function of this channel and found that this channel also functions as an extracellular calcium sensor, and regulates extracellular calcium dependent neuronal excitability (108), Chua *et al.* furthered this notion and proved that NALCN channel works in voltage dependent manner.(85)

- When one of the components of NALCN channel is mutated these animals displayed altered sensitivity to ethanol and volatile agents (VA) such as toluene and halothane.(81) Although some studies show variances for some of the VA's such as isoflurane (80), the general notion is true for all of them. On the other hand, it has long been known that volatile anesthetics and ethanol act on synapses and inhibit neurotransmitter release via an unknown mechanism. Apart from all these, one study conducted by Metz *et al.* showed that UNC13 is necessary for isoflurane sensitivity in

C. elegans.(109) However, there are no further studies available, and studies concerning the relationship between the trio –UNC79, volatile anesthetics, synapse function.

- UNC80 acts downstream of PIP2 (PIP2 is an important coupler of SV fusion to SV recycling), and PIP2 accumulation -no matter how- induces fainting phenotype in UNC80 mutant animals. Furthermore, UNC80 mutant *C. elegans* harbors reduced SVs.(110) Again, studies concerning UNC80's action on synaptic function is limited to this study.

- Last but not least, the function of this gene in circadian rhythm was illuminated just a couple of years ago. The channel is one of the known few channels that when mutated results in sleepless phenotype.(86) Furthermore, it oscillates in day/night intervals, being expressed higher in the mornings and lower at night. Interestingly, a core AZ component important in AZ maturation, BRP, shows cyclic expression in optic lamina (111), opening an open question of if there is a link between this channel and synaptic core BRP protein: A study conducted by Ghezzi and his colleagues' determined highly correlated gene expression profile for *brp* and *na* in *Drosophila*, strengthening this opinion (Figure 2.2).(8)

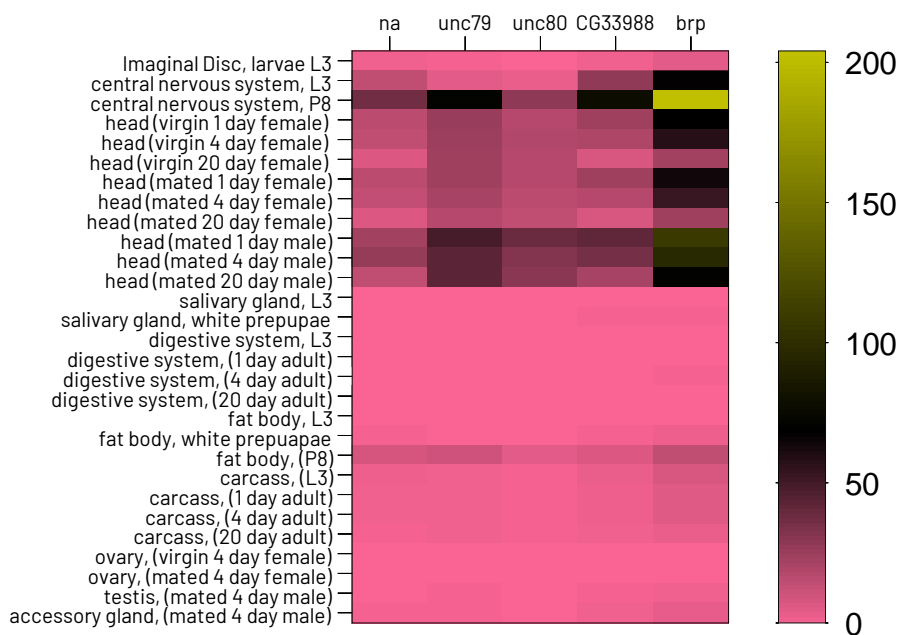


Figure 2.2. NALCN channel components are mostly expressed at central nervous system and head of *Drosophila*. (Modencode data) in parallel to BRP, synaptic AZ protein, suggesting that it may also have functions in synapse function (adapted from (8))

2.6.2. MBOAT7

The second gene of interest, MBOAT7, encodes an enzyme that preferentially attaches arachidonic acid to phosphoinositide tail. 12 Turkish patients harboring five different homozygous mutations (pArg87*, pGln376Lys, pTrp426*, pLeu227ProfsX65, and chr19:54.666.173-54.677.766/11594 bp del (112)) in MBOAT7 gene were identified via Sanger sequencing and whole exome sequencing.(4) MBOAT7 is an enzyme that sits in Lands cycle, also known as phospholipid remodeling pathway, hence mutations in the respective gene results in phospholipid remodeling disease with synaptopathic outcome. Clinical highlights of the disease are:

- Characteristic facial expressions: apathetic face, large ears, deep set eyes, short philtrum, broad forehead
- Global developmental delay
- Early onset seizures
- Speech and language impairments
- Intellectual disability
- Ataxic gait
- Neuroimaging Findings: Folium dysgenesis of the cerebellum with a particular appearance, cerebellar atrophy, enlarged perivascular areas.(4)

MBOAT7 is an O-acyltransferase enzyme responsible for specifically adding arachidonic acid to phosphoinositide's and are important players in phosphoinositide remodeling pathway -Lands cycle.(113)

To deeply understand MBOAT7 enzyme and its probable role in synaptic function, it is crucial to start from the very beginning, phospholipids, and build an understanding on top of it.

Phospholipids

Phospholipids (PLs), the main units of the cell membrane, are amphipathic molecules that consist of fatty acid chains at sn-1 and sn-2 and a phosphate group at sn-3 position (Figure 2.3). (114) PLs, based on their head groups, can be subdivided into seven groups, Phosphoinositides (PI), inositol bearing molecules, being one of them. (115) The inositol head group can be phosphorylated from three different positions -3,4, and/or 5th giving rise to seven possible PI species (Figure 2.4):

- Monophosphorylated PIs
 - $\text{PtdIns}3P$, $\text{PtdIns}4P$, and $\text{PtdIns}5P$
- Bisphosphorylated PIs
 - $\text{PtdIns}(3,5)P_2$, $\text{PtdIns}(4,5)P_2$, and $\text{PtdIns}(3,5)P_2$
- Triphosphorylated PIs
 - $\text{PtdIns}(3,4,5)P_3$

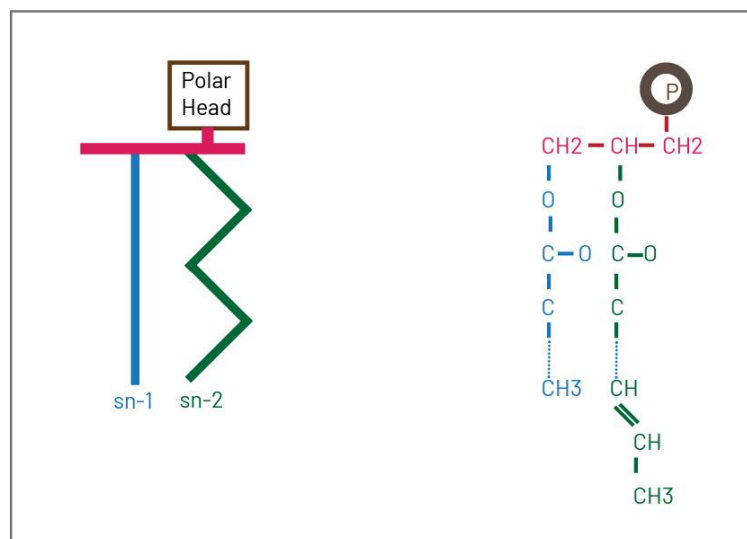


Figure 2.3. General representation of a phospholipid. Phospholipids are formed by a polar head group (brown) that is attached to a glycerol backbone (pink) at sn-3 position and two hydrocarbon tails that are esterified to the glycerol backbone at sn-1 and sn-2 positions (blue and green respectively).

Phosphorylation and dephosphorylation of the head group is achieved by specific kinases and phosphatases respectively and most of the processes are bidirectional. (116) PIs are known to be involved in modulation of important cellular processes -i.e. vesicular transport, endocytosis, exocytosis, regulation of ion

channels- by a phosphorylation and dephosphorylation cycle of the PI head group.(117, 118)

A unique feature of PI sub-species is their heterogeneous distribution among different sub-membranous compartments: For instance, PI4P are mostly found in golgi whereas PI(4,5)P₂ in the cell membrane to name a few (Figure 2.5).(119) Since different PIs can modulate different signaling cascades mostly via their negatively charged head groups this feature also becomes important in local modulation of signaling cascades.

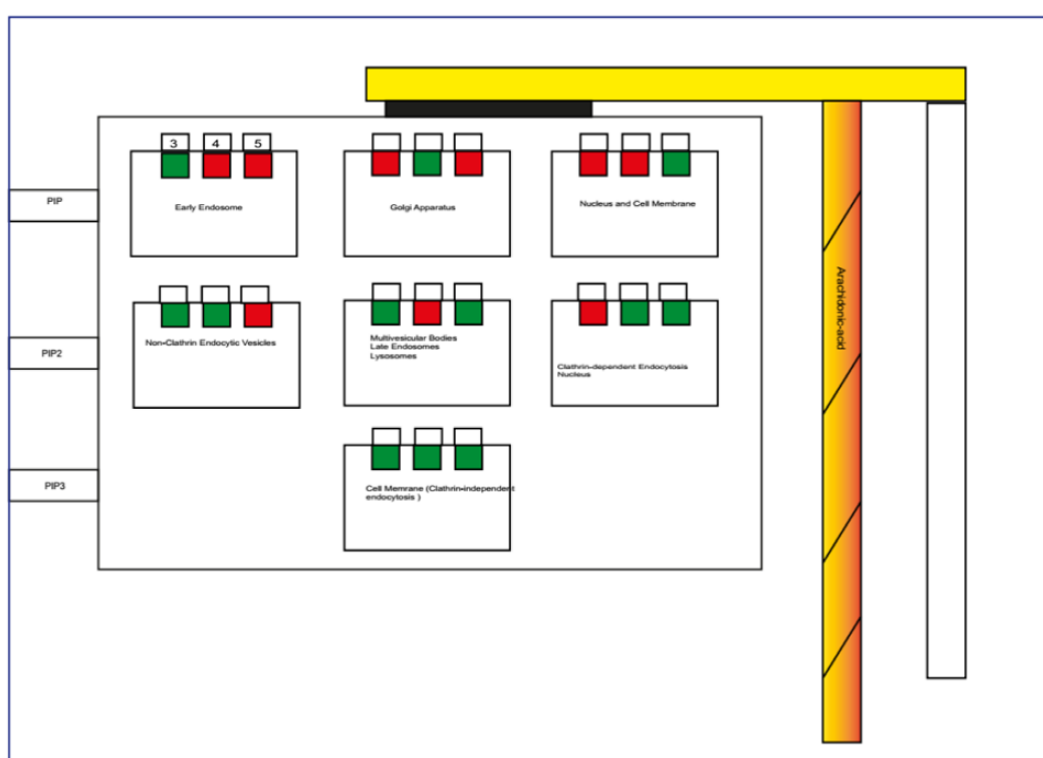


Figure 2.4. PI Acyl Species are heterogeneously distributed among different sub-membranous compartments. Phosphoinositide's can be phosphorylated from three different positions giving rise to monophosphorylated (PIP), biphosphorylated (PIP₂), trisphosphorylated (PIP₃) PIS: These PI species specifically dominate special membranes in mammalian tissues.(119)

PI head group phosphorylation and de-phosphorylation event is very dynamic and thus most of the research in this field is dedicated to PI subspecies with a focus on their head groups. However, in the invisible face of the iceberg lies: PIs acyl tail groups.

Phosphoinositide Acyl Tail

PI acyl tails, at first glance are mere hydrocarbon tails seemingly fulfilling only membrane attachment mission and are also considered as membrane fluidity regulators mostly due to their length and saturation status. However, when looked closely, their acyl tails, mostly one saturated and another unsaturated in positions sn-1 and sn-2 respectively (Figure 2.5), show a remarkable tissue-specific identity.(120) For instance, PIs in mammalian brains are mostly enriched in stearic acid ((C18:0) 18 carbons with no double bond) and arachidonic acid ((20:4) 20 Carbon chain with 4 double bonds in cis conformation) in its sn-1 and sn-2 position respectively.(9) On top of this, acyl compositions of PI, PIP, PIP₂ and PIP₃ are also very similar.(121) But how is this acyl chain specificity achieved?

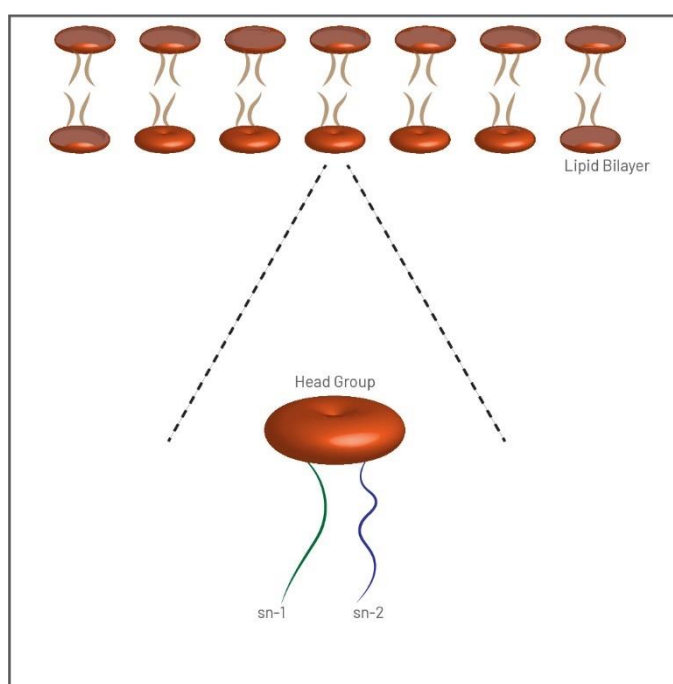


Figure 2.5. Phosphoinositide is a special type of phospholipid. It is composed of a polar head that can be phosphorylated from several sites and two polycarbon tails that are attached to sn-1 and sn-2 positions. The tail that is on sn-1 position is mostly unsaturated and is either palmitic acid (16:0) or stearic acid(18:0), whereas the tail on the sn-2 side is saturated and is mostly arachidonic acid (20:4, n-6) or decosahexaenoic acid (22:6n), omega6 and omega3 respectively.

Lipids are synthesized from glycerol-3-phosphate (G-3-P) in the so-called Kennedy pathway.(122, 123) This pathway ends up with fatty acids with

heterogeneous tail groups since Kennedy pathway is only concerned with degrading fatty acids but not with the tail group.(124)

Accordingly, degraded fatty acids bear asymmetrically distributed acyl chains, thus shows no tissue specific identity.(124)

Phospholipids has to undergo an acyl chain remodeling after Kennedy pathway via the only known phosphoinositide acyl chain remodeling pathway, Lands cycle.(125) Two main types of enzymes –Phospholipase and Lysophosphatidylinositol acyltransferase- play important roles in this pathway.(126) Phospholipase A1 and A2 play roles in the cleavage of acyl chains off phospholipids whereas lysophosphatidylinositol acyltransferases transfer acyl groups from acyl CoAs to the sn-2 position of lysophospholipids.(126)

Lands cycle, to the best knowledge only takes place in endoplasmic reticulum. The cycle ends with a *de novo* PI that has remodeled acyl chain.(125)

Acyl Chain Remodelling

Acyl chain remodeling can be achieved by either first removing sn-1 acyl chain or sn-2 acyl chain (Figure 2.6.).(121)

If the first scenario is the case:

- PhospholipaseA1 (PLA1) will remove the acyl chain in the sn-1 position
- AGPAT8 (2, Acyl LPI acyltransferase) adds stearic acid to sn-1 position
- This is followed by the removal of the acyl chain in the sn-2 position by phospholipaseA2 (PLA2) and arachidonic acid is attached by an enzyme called as MBOAT7 to the respective position.

If the second scenario is the case:

- First Phospholipase A2 (PLA2) will remove the acyl chain in the sn-2 position
- MBOAT7 will add arachidonic acid to the respective position
- phospholipaseA1 (PLA1) will remove the acyl chain in the sn-1 position
- AGPAT8 (2,Acyl LPI acyltransferase) adds stearic acid to sn-1 position

In either case the end product is the same: PI with stearic acid at sn-1 position and arachidonic acid at sn-2 position. In the end PIs are highly enriched with specific acyl chains. This composition is especially important in substrate specificity of the enzymes involved in PI cycle.

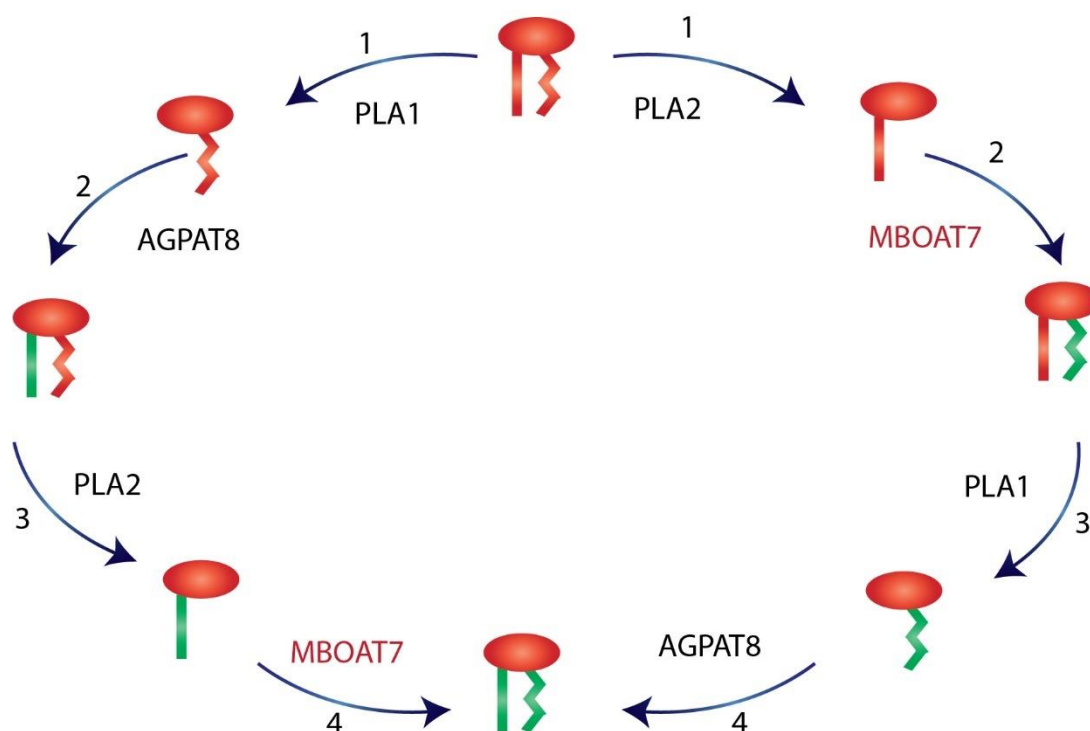


Figure 2.6. Acyl Chain Remodelling via Lands Cycle. Kickstarting Lands cycle is achieved either by removing sn-1 acyl chain or sn-2 acyl chain (1) and, in brains, ends up with PI with stearic acid at sn-1 (straight line) position and arachidonic acid at sn-2 position.

MBOAT7 *Drosophila* Ortholog Farjavit

Farjavit (*frj*), the *Drosophila* ortholog of MBOAT7 gene, shows 51% similarity and 33% identity with MBOAT7. *Drosophila* tissues lack arachidonic acid in their PIs, however when expressed in yeast, *frj* also preferentially attaches AA to PIs.

Although *frj* shows similarity to MBOAT7 whether it is also attaching arachidonic acid chains to phosphoinositide's, especially in brain, is not clear. The reason for this is arachidonic acid (20 carbon long) is absent in the brain tissue of *drosophila* heads (127) and *Drosophila* phospholipid acyl chains are no more than 20 carbon long.(128) On the other side, *frj* is present in the cell membrane in *Drosophila*

heads. On top of this, frj when expressed in yeast is shown to have a preference for arachidonic acid attachment to PI chains.(129) Considering, diet plays a big role in fatty acyl chains, and to our knowledge, there is no study concerning the effects of diet on fatty acid chain composition in *Drosophila*. On top of it, *Drosophila* can synthesize arachidonic acid from only special PUFAs i.e. docosahexaenoic acid (22:6n-3) being one of them.(128)

Synaptic Transmission vs MBOAT7

Arachidonic acid is a polyunsaturated fatty acid (PUFA). Hydrocarbon tails with unsaturated (double bond carbon atoms) results in loose distribution of cell membrane hence a more fluid and flexible membrane, and membrane fluidity is important in vesicle cycling and synapse function.(130) For instance, PUFA lacking *C. elegans* is known to harbor low numbers of SVs and shows mislocalization of synaptobrevin and synaptojanin proteins, interestingly, this phenotype can be rescued by not all PUFAs but a specific one: arachidonic acid.(131) Of note, PUFA rich diets only effect the expression of few genes most of them being vesicle cycle related, among them Munc18 is a well-studied vesicle fusion component.(132)

On the other hand Syx a protein important in vesicle fusion, is normally in closed state and can only bind in open state to Syt that is present on SVs.(133)

On top of these, MBOAT7 mutation in mice lowers the absolute levels of both arachidonic acid bearing phosphoinositide's and a special type of PI - PI(4,5)P₂- that is mostly present on the cell membrane and also dominated on synaptic terminals.(134)

2.7. *Drosophila Melanogaster* as a Model Organism

Drosophila melanogaster, better known as fruit fly, was first used as a model organism by T.H. Morgan in the beginning of 20th century and from that time on has been the chevalier for many scientific discoveries and Nobel prizes.(135-137) Due to the numerous research works conducted in *Drosophila*, fly library improved drastically by time, resulting in hundreds of driver lines that express Gal4

transcription factor in numerous temporal and spatial patterns. These lines ease tissue specific silencing of the gene of interest, and are also fast and cheap to perform research: For instance when silencing of the gene results in developmental delay and eventually lethal outcome (138) one can easily turn to tissue specific silencing of the gene. Furthermore, fruit fly, with its small size and short life span allows researcher to conduct and reproduce research in a very short time. On top of it, no ethical approval is needed and almost 70% of human genes are conserved.(139)

Drosophila, besides these advantages, share a stereotypical muscle pattern.(140) Since *Drosophila* larvae is opaque not only immunohistochemical studies but also *in vivo* imaging can be performed easily. On the other side, innumerable studies on molecular mechanism of synaptic transmission are conducted so far, thus previous knowledge eases understanding dysfunctions in synaptic level. Finally, *Drosophila* NMJs share functional and structural similarities to human synapses, making it an ideal organism to model diseases.(141)

2.8. GAL4-UAS System

GAL4-UAS system is used to silence or overexpress a gene of interest in a tissue specific manner: GAL4 Driver lines restrict expression of a gene to a desired tissue or time.(142)

GAL4 is a yeast based transcription factor and sits downstream of a tissue specific promoter, hence GAL4 is only expressed in the tissue of interest in which the promoter is activated. On the other side, in responder line, gene/RNAi of interest lies downstream of UAS (upstream activation sequence) sequence which can only be activated by GAL4 transcription factor.(143) When two lines, driver and responder lines are united, GAL4 will bind to UAS sequence in a tissue specific manner and thus drive the expression of gene/RNAi.(144) The ultimate result will be expression or knockdown of target gene in the desired tissue (Figure 2.2.).

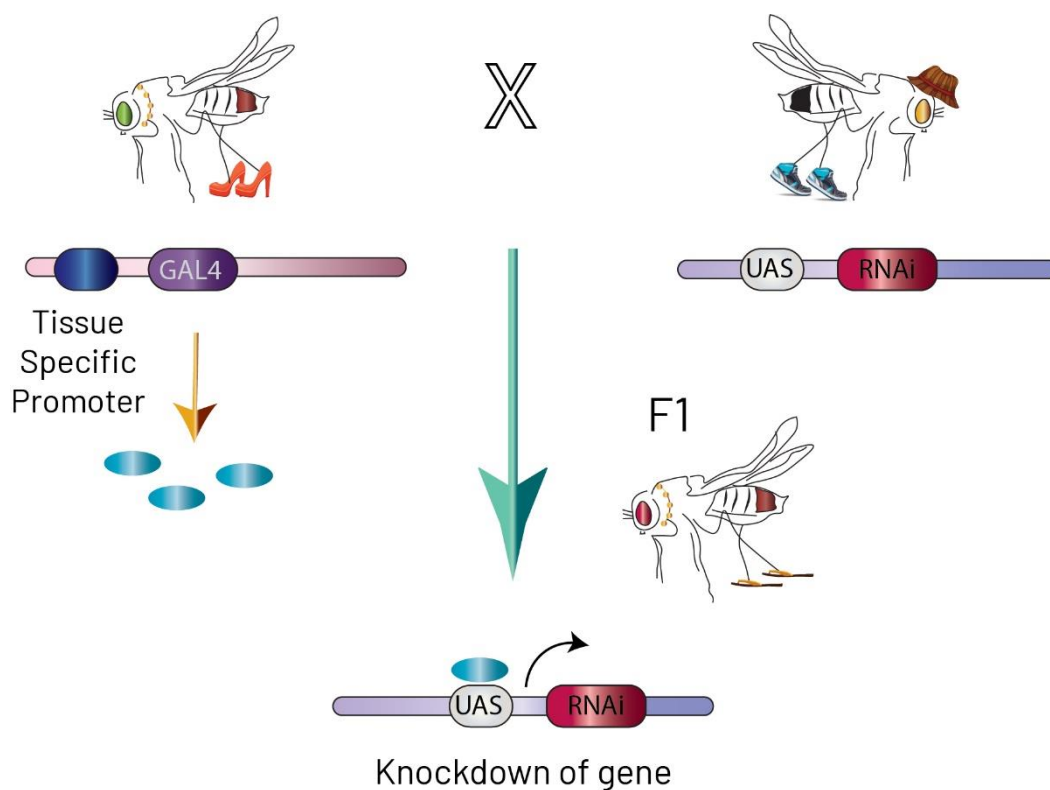


Figure 2.7. Depiction of Gal4-UAS System. Tissue specific silencing of the respective gene is achieved via combining UAS and GAL4 driver lines in the same tissue.

2.9. Problem Statement and Aim

AZ components and their interrelation with one another is well defined, however there is little study that highlights how synaptopathies affect conserved brp and glutamate receptor levels and morphology in *Drosophila* NMJs.

Considering the aforementioned information regarding synaptic function and gene of interests alongside with the pathophysiology of our patient we think that NALCN channel components and MBOAT7 enzyme has important roles in synaptic function and transmission. Hence, to gain understanding about how the gene effects synaptic morphologies and brp and glutamate receptor levels:

1. We knocked down NALCN channel components and frj in *Drosophila melanogaster* in a tissue specific manner (motoneuronally and pan-neuronally) and examined how brp and glutamate receptor levels changed relative to control groups via immunohistochemical staining and imaging.
2. Morphological parameters for active zones and postsynaptic side were analyzed upon frj and NALCN channel component silencing at NMJs protruding muscle4 of 3rd instar larvae.
3. BRP and glutamate receptor levels were measured in wild-type flies (w¹¹¹⁸) in a time-dependent fashion to understand if there is a circadian regulation.
4. We analyzed how environmental modulators i.e. diet changed brp and glutamate receptor levels and morphologies.
5. Finally we sought to understand how brp and glutamate receptor levels changed in a time-dependent manner upon motoneuronal silencing NALCN ortholog na.

3. MATERIALS METHODS

3.1. Fly Husbandry, Stocks, and Handling

Flies are raised in semi-defined Bloomington recipe or special food in 12 hour light-dark cycle (excluding one dissection at 29°C), at 25°C incubator and ~65% humidity or 29°C incubator. Food was changed three times a week. After crossing (8-14 virgin female and 8-12 male) flies were kept in the same incubator and food was changed in two-three day intervals. Lines and crosses used in this experiments are as follows:

UAS-na-RNAi/+ (VDRC #103754); UAS-na-RNAi/+ (VDRC #3306); UAS-unc79-RNAi/+ (VDRC #45780); UAS-unc79-RNAi/+ (VDRC #108132); UAS-unc80-RNAi/+ (VDRC #1309); UAS-unc80-RNAi/+ (VDRC #1310); UAS-unc80-RNAi/+ (VDRC #108934); UAS-frj-RNAi/+ (VDRC#51450); UAS-frj-RNAi/+ (VDRC#51451):

wild type: +/+ (*w¹¹¹⁸*); Ok6::+: Ok6-Gal4/+; elav::+: elav-Gal4/+; elav::na: elav-Gal4/+;;UAS-na-RNAi/+; Ok6::na: Ok6-Gal4/+;;UAS-na-RNAi/+; na::+: UAS-na-RNAi/+;;+/+; Ok6::+: Ok6-Gal4/+;; +/+; elav::+: elav-Gal4/+;; +/+; elav::unc79: elav-Gal4/+;;UAS-unc79-RNAi/+; Ok6::unc79: Ok6-Gal4/+;;UAS-unc79-RNAi/+; unc79::+: UAS-unc79-RNAi/+;;+/+; elav::unc80: elav-Gal4/+;;UAS-unc80-RNAi/+; Ok6:: unc80: Ok6-Gal4/+;;UAS-unc80-RNAi/+; unc80::+: UAS-unc80-RNAi/+;;+/+; elav::frj: elav-Gal4/+;;UAS-frj -RNAi/+; Ok6::frj: Ok6-Gal4/+;;UAS-frj-RNAi/+; frj::+: UAS-frj-RNAi/+;;+/+

Table 3.1. Genotypes of the 3rd instar larvae used in experiments

GENE	<i>Drosophila</i> Ortholog	Driver control	Construct Control	Silenced RNAi	Tissue silenced
NALCN	na	elav::w1118	na-RNAi::w1118	elav::na-RNAi	Brain
NALCN	na	Ok6::w1118	na-RNAi::w1118	Ok6::na-RNAi	Motor Neuron
UNC80	unc80	elav::w1118	unc80-RNAi::w1118	elav::unc80-RNAi	Brain
UNC80	unc80	Ok6::w1118	unc80-RNAi::w1118	Ok6::unc80-RNAi	Motor Neuron
UNC79	unc79	elav::w1118	unc79-RNAi::w1118	elav::unc79-RNAi	Brain
UNC79	unc79	Ok6::w1118	unc79-RNAi::w1118	Ok6::unc79-RNAi	Motor Neuron
MBOAT7	frj	elav::w1118	frj-RNAi::w1118	elav::frj-RNAi	Brain
MBOAT7	frj	Ok6::w1118	Ok6::frj-RNAi	Ok6::frj-RNAi	Motor Neuron

3.2. Immunostainings

Larvae dissections and staining were performed as described by Qin et. al (15): In short 3rd instar larvae were placed on a rubber pad; pinned from anterior and posterior ends, and covered with Ca⁺² free ice-cold hemolymph-like solution (70 mM NaCl, 5 mM KCl, 20 mM MgCl₂, 10 mM NaHCO₃, 5 mM trehalose, 115 mM sucrose, 5 mM HEPES, pH 7.2).(145) Afterwards, 3rd instar larvae were cut open from the midline and internal organs were removed, leaving the brain and muscles intact. Larvae were washed in HL-3 solution and fixed in methanol for 5 min with three times repetition of washing step. Immunostaining were performed in 0.05% PBT solution and larvae were blocked in 5% NGS (NGS, Sigma Aldrich). Larvae were incubated in the blocking solution for at least one hour and primary antibodies dissolved in 0.05% PBT and 5% NGS were added to larvae. Overnight incubation was held at 4°C. Afterwards, larvae were washed in %0.05 PBT solution for 3-5 times and incubated

for 4 hours in blocking solution with secondary antibodies. Larvae were washed in 0.05% PBT for one hour (room temperature) or overnight (4⁰C), mounted in Vectashield (Vector Laboratories, USA) and covered with coverslip (Carl Roth, Germany, H875).

The following primary and secondary antibodies were used: rabbit GluRIID (1:500 (15), mouse Nc82=anti-BRP C-term (1:150, Developmental Studies Hybridoma Bank, University of Iowa, Iowa City, IA, USA, AB Registry ID: AB_2314365); rabbit BRP Last200 (1:1000; (13), mouse GluRIIA (1:250, Developmental Studies Hybridoma Bank, University of Iowa, Iowa City, IA, USA), goat-anti-HRP-647 (1:500, Jackson ImmunoResearch, PA, USA, 123-605-021), goat anti-mouse Alexa-Fluor-488 (1:500, Life Technologies, CA, A11001), goat anti-rabbit-Cy3 (1:500, Jackson ImmunoResearch, PA, USA, 111-165-144)

3.3. Image Acquisition, Processing, and Analysis

Confocal images were acquired with Leica SP8 microscope (Leica Microsystems, Germany). *Drosophila* 3rd instar larvae muscle four 1b boutons (segments A3-A5) were imaged with a z step size of 0.25 μ m at room temperature with 63x objective.

Background of the image was subtracted via a custom written ImageJ script and a mask of the synaptic area was created as follows:

Synaptic area was defined by freehand selection tool on BRP channel and the selected region the Region of interest (ROI) was applied to the HRP channel (neuronal membrane marker) of the image to confine the mask to only to NMJ of interest. After clearing out the signals out of the NMJ a gaussian blur (1 pixel) was applied to the channel to blur the image and eventually binary HRP mask was created.

AZs and glutamate receptors falling into 1b NMJ were defined via an automated pipeline in Cell Profiler. In short two pipelines were created to define AZs and glutamate receptor spots respectively.

3.4. Image Processing in Cell Profiler

Images were grouped in cell profiler according to their names -one group constituted of BRP, glutamate receptor and HRP channels of the respective image. HRP mask was subtracted from BRP and glutamate receptor channels of the image to confine the analysis to the NMJ of interest. A gaussian blur of 1 (standard deviation of the kernel) was applied to the image of interest to blur brp and glutamate receptor spots respectively. To define each spot separately, different thresholding approaches -minimum cross entropy, robust background, and Otsu- were tested out and Otsu thresholding method was chosen to be the optimum among these methods for brp/glutamate receptor spot determination.

To define each brp/glutamate receptor spots separately, three class Otsu thresholding strategy was applied to each image and the middle peak was defined as background. This method works by minimizing the variance between background and foreground and separates spots accordingly.

Threshold smoothing scale of 1.0 was applied to the image to remove holes and jagged edges caused by noise in the acquired image and a threshold correction factor of 1.00 was applied to all of the images. Although for some of the images threshold correction factor 1.6 seems to work better and stringed the area to the AZ, due to the log-normal distribution of brp and glutamate receptor spot intensities, it also resulted in less calculated AZ, thus information loss. Hence, to be able to calculate most of the AZs, if not all, stringency factor of 1.6 was not applied to the images and no adjustment in threshold was made by leaving threshold correction factor 1.0. Upper and lower bonds of threshold were entered as 0.0 and 1.0 respectively.

To detect small areas of intense staining's, as it is also our case for brp and glutamate receptor spots, images were log-transformed before thresholding. Afterwards, clumped spots were separated according to intensity and dividing lines between clumped objects were drawn according to the lowest intensity measurements: We also tried to de-clump the objects according to shape however

not all brp's have the same shape, thus this approach mostly resulted in wrong declumping.

After defining the brp and glutamate receptor spots:

- Brp and glutamate receptor spot intensities were measured from whole image and also from each spot separately.
- Spot size, spot shape, zernike features, and additional statistics (i.e. object moments and inertia tensors were calculated for brp and glutamate receptor channels) and solidity were also measured for each spot.
- Afterwards, each brp and glutamate receptor spot was subdivided to 5 equally distributed rings. Magnitude and phase of intensity was calculated among these rings. This calculation is especially important to analyze the intensity in each ring of the brp/glutamate receptor spot. Mean intensity, and distribution of the intensity within each ring were calculated for future analysis. Since brp shape is dynamic and any shape change can also change synaptic plasticity these features are especially important.

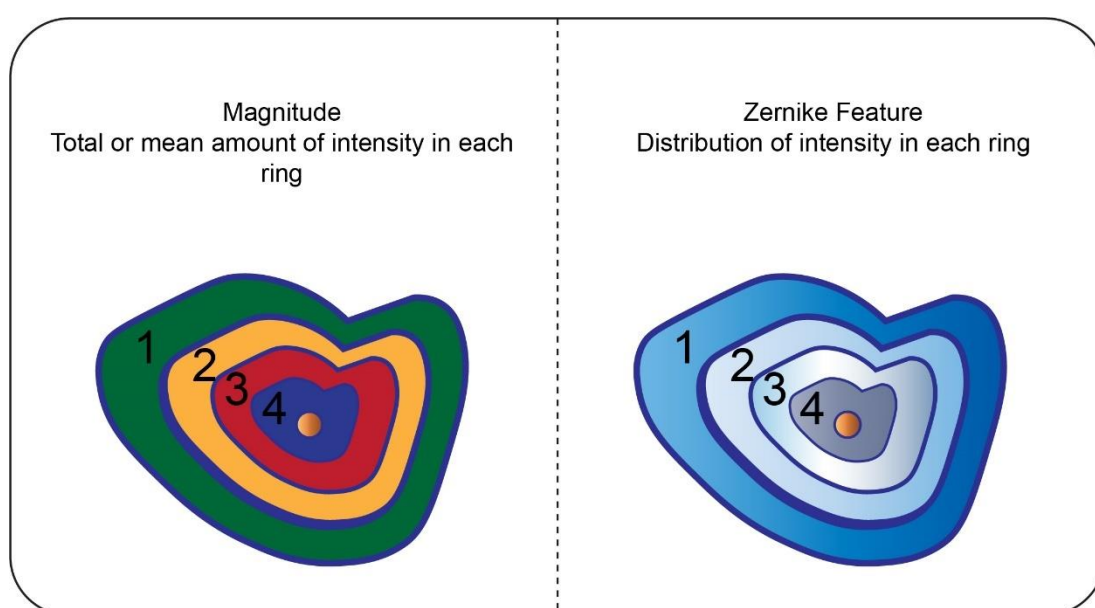


Figure 3.1. Representation of Magnitude and phase of intensity calculation from brp and glutamate receptor spots. Magnitude of the intensity only gives information for

intensity as a whole, namely, mean and integrated intensity is calculated from each ring without spatial information. Phase of intensity (Zernike features) gives also spatial information for the intensity in each ring (i.e. one side of the ring is darker than the other side).

These results were saved into dB folder. SQLite queries were executed to extract 'intensity and synapse morphology' information. These data were pasted to GraphPad Prism and statistical analysis and plotting of data were performed in this platform. Some of the data were plotted in '<https://rawgraphs.io>' an open-source website for graph plotting. Data visualization and infographic designs are performed in Adobe Illustrator.

3.5. Statistical Analysis

All data were analyzed and plotted in GraphPad prism (8.4.2.) (GraphPad, La Jolla, CA, USA). For illustration purposes some of the data were also plotted in a commercial website (<https://rawgraphs.io>) and infographic design was performed in Adobe Illustrator.

Two group analysis was performed with either non-parametric Mann-Whitney U-test or student's t-test. When analyzing more than two groups, first the distribution of data was determined with D'Agostino Pearson Normality test. Normally distributed data were analyzed with one-way ANOVA followed by a Tukey posthoc. Non-normally distributed data were analyzed with Kruskal-Wallis and followed by Dunn's test. Means and standard error of mean (SEM) are used to describe the variability within the sample (\pm SEM). p of 0.05 and below were considered significant *, P < 0.05; **, P < 0.01; ***, P < 0.001; n.s. (non-significant), p>0.05).

3.6. Solutions

Table 3.2. Solutions

SOLUTIONS		
Hemolyph-3	gr	mM
NaCl	4.090 g/l	70mM
KCL	0.372 g/l	5mM
MgCl	4.066 g/l	20mM
NaHCO ₃	0.840 g/l	10mM
Threalose	1.892 g/l	5mM
Sucrose	39.364 g/l	115mM
HEPES	1.192 g/l	5mM
Phosphate-buffered saline (PBS)	Amount to add (for 1× solution)	Final concentration (1×)
NaCl	8 g	137 mM
KCl	0.2 g	2.7 mM
Na ₂ HPO ₄ *2xH ₂ O	1.805 g	11.569 mM
KH ₂ PO ₄	0.24 g	1.8 mM
Phosphate buffered saline (PBS) containing 0.05% Triton X-100		
250 µl of Triton X-100 was added to 499,75 ml 1xPBS.		

Hemolyph-3 (HL3)

1lt of HL3 solution was prepared by adding NaCl, KCL, MgCl, NaHCO₃, Trehalose, Sucrose, HEPES in the amounts indicated in the table and pH was balanced by adding NaOH. Lastly, solution was filled up to 1liter.

Phosphate-buffered saline (PBS)

To get 1X PBS reagents were dissolved in 800 ml H₂O and pH was adjusted to 7.4 with HCL and solution was filled to 1lt with H₂O.

3.7. Reagents and Resources

Table 3.3. Reagent and Resources

REAGENT or RESOURCES	SOURCE	IDENTIFIER
Antibodies		
Mouse Monoclonal Nc82	Developmental Studies Hybridoma Bank	Cat# nc82, RRID: AB_2314865
Rabbit BRP^{last200}	Ullrich et al., 2015 (13)	N/A
Rabbit GluRIID	Qin et al, 2005 (15)	
GluRIIA	Developmental Studies Hybridoma Bank	8B4D2 (MH2B)
Goat anti-rabbit-Cy3	Jackson ImmunoResearch	Cat# 111-165-144, RRID: AB_2338006
Goat anti guinea-pig Alexa-488	Life Technologies	Cat# A11073, RRID: AB_2534117
goat anti-HRP-647	Jackson ImmunoResearch	Cat# 123-605-021 RRID: AB_2338967

Table 3.4. Software and Algorithms

SOFTWARE AND ALGORITHMS		
LAS X Software	Leica Microsystems	https://www.leica- microsystems.com/home/
LCS AF	Leica Microsystems	https://www.leica- microsystems.com/home/
ImageJ	NIH	Version 1.48q/1.50g; https://imagej.nih.gov/ij/
MATLAB	MathWorks	R2010b/R2016a
Cell Profiler	BSD 3-clause	4.2.1
DB Browser for SQLite (DB4S)		Version 3.12.2
Adobe Illustrator	Adobe Inc.	Version 24.0.1 (2020)
RawGraphs	OpenSource	https://www.rawgraphs.io
GraphPad Prism	GraphPad Software	Version 5.01/6.01
ffmpeg		Version4.3; ffmpeg.zeranoe.com
OTHER		
Leica SP8 Microscope	Leica Microsystems	https://www.leica- microsystems.com/home/

Table 3.5. Experimental Models: Organisms/Strains

EXPERIMENTAL MODELS: ORGANISMS/ STRAINS		
<i>D. melanogaster</i> : Wild type: w1118	Lab stock	N/A
<i>D. melanogaster</i> : Ok6-Gal4/II	Aberle et al., 2002	N/A
<i>D. melanogaster</i> : Elav-Gal4/I	Lin and Goodman, 1994	
<i>D. melanogaster</i> : UAS-na-RNAi/III	Bloomington #25808, FBgn0002917	https://flybase.org/reports/FBgn0002917
<i>D. melanogaster</i> : UAS-na-RNAi/II	VDRC #103754, FBgn0002917	http://flybase.org/reports/FBgn0002917
<i>D. melanogaster</i> : UAS-na-RNAi/III	VDRC #3306, FBgn0002917	http://flybase.org/reports/FBgn0002917
<i>D. melanogaster</i> : UAS-unc79-RNAi/II	VDRC #45780, FBgn0038693	http://flybase.org/reports/FBgn0038693
<i>D. melanogaster</i> : UAS-unc79-RNAi/II	VDRC #108132, FBgn0038693	http://flybase.org/reports/FBgn0038693
<i>D. melanogaster</i> : UAS-unc80-RNAi/III	VDRC #1309, FBgn0039536	http://flybase.org/reports/FBgn0039536
<i>D. melanogaster</i> : UAS-unc80-RNAi/II	VDRC #108934, FBgn0039536	http://flybase.org/reports/FBgn0039536
<i>D. melanogaster</i> : UAS-farjavit-RNAi/III	VDRC #51450, FBgn0031815	http://flybase.org/reports/FBgn0031815
<i>D. melanogaster</i> : UAS-farjavit-RNAi/III	VDRC #51451, FBgn0031815	http://flybase.org/reports/FBgn0031815

3.9 Fly Food Recipes

Table 3.6. Fly Food Ingredients

	BLOOMINGTON RECIPE	SPECIAL FOOD RECIPE
H2O	10lt	5lt
Agar	42gr	40gr
Rübersirup	183gr=126ml	
Malzin	666gr=500ml	
Yeast	75gr	400gr
Soja flour	83gr	
Mais flour	666gr	
Nipagin in Ethanol	13gr in 42ml	5gr in 50ml
Propionic acid	53ml	30ml
Yeast extract		100gr
Peptone		100gr
Grafschafhter sirup		450gr=307ml
MgSO₄x7H₂O		2.5gr
CaCl₂x2H₂O		2.5gr
Water	Water in pot: 4lt Water at the end: 2lt	Fill to 5lt

4. RESULTS

4.1. Motoneuronal and Pan-neuronal Silencing of NALCN Channel Components

In this study NALCN channel components; *na*, *unc79*, and *unc80* were silenced both moto-neuronally and pan-neuronally via Gal4-UAS system, larvae were stained against *brp* and glutamate receptor and imaging was performed via confocal microscope.

Three different groups were used in the study:

a. In the first group, RNAi line and Ok6-Gal4/II or *elav*-Gal4/I were brought together and thus motoneuronal silencing or pan-neuronal silencing of gene of interest was achieved.

b. Driver control (DC): Ok6-GAL4/II or *elav*-Gal4/I driver line was brought together with *w¹¹¹⁸* flies hence Gal4 without an upstream activator sequence (UAS) was prepared as driver control.

c. Construct control (CC): to understand if a leakage occurs in the absence of Gal4 driver line, RNAi line of interest were crossed with *w¹¹¹⁸* control flies.

Flies were kept at room temperature and crossed flies were placed to 25°C incubator. Afterwards, larvae were placed to 29°C incubator. And dissections were performed when all of the larvae reached 3rd instar stage.

During dissection, to restrain possible time-dependent variation in protein levels (*brp* and glutamate receptor), 2 CC, 2 DC, and 2 RNAi lines were taken out from the incubator and dissected at the same time, unless indicated otherwise. In total six larvae were dissected from each group, eventually 1b NMJs that innervate the 4th muscle between abdominal segments A3-A5 were scanned in confocal microscope.

After obtaining the images, all of the image processing steps were first performed in ImageJ. However, further analysis revealed that *brp* and glutamate receptor intensities were log-normally distributed (AZ intensities were gradually distributed) among NMJs (Figure 4.1), and examining each NMJs separately showed

that area and intensities in the same NMJ is linearly correlated with each other and neither area nor brp and glutamate receptor intensities are constant even in the same NMJ (Figure 4.2).

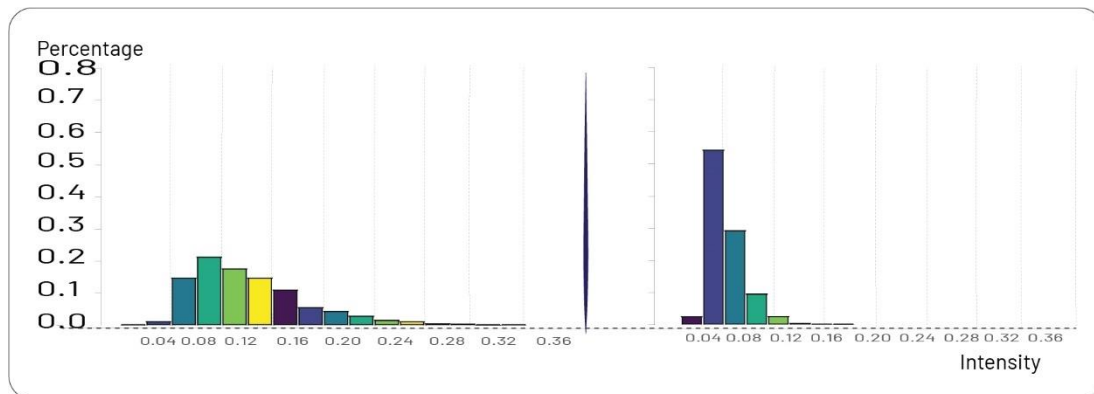


Figure 4.1. AZ intensities are lognormally distributed. Two separate experiments performed on w1118 flies resulted in two different lognormal distribution of brp intensities. A prominent change in skewness of the intensities among AZs draws attention (Column height represents the percentage of brp intensities in that range. Each column intensity is 0.02 apart from each other, dashed lines correspond to 0.04 intervals).

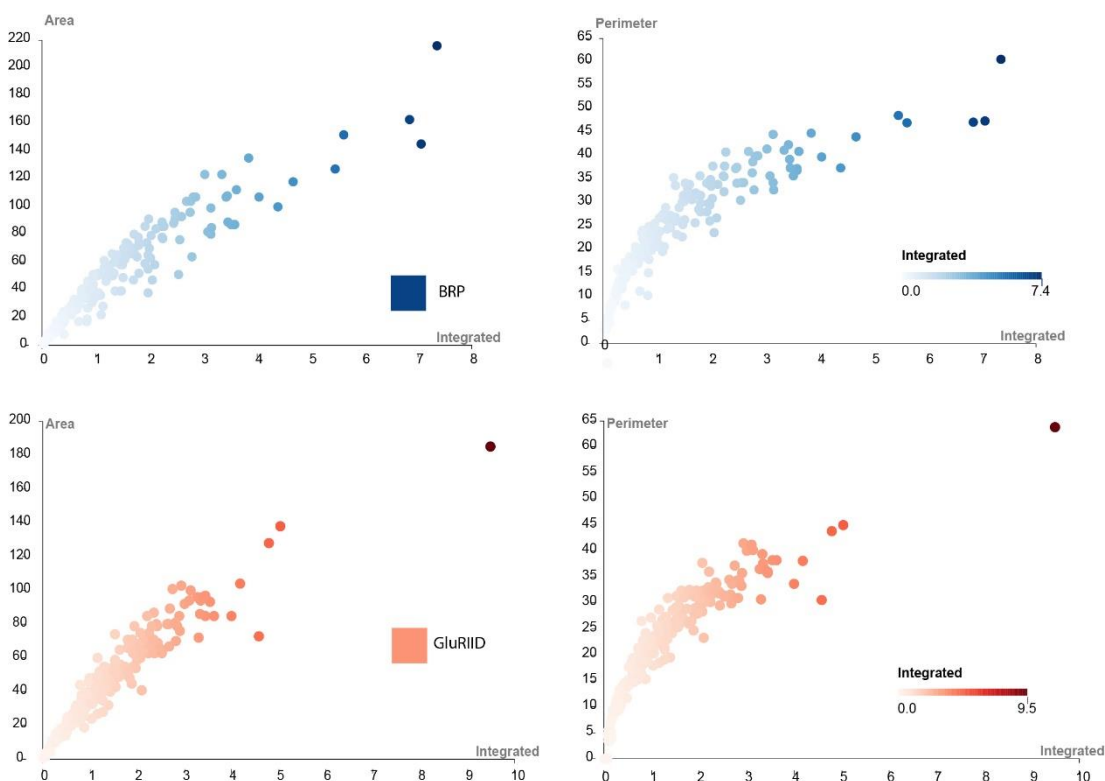


Figure 4.2. BRP and glutamate receptor spot areas and integrated intensity are directly proportional with each other.

Intensities in each brp and glutamate receptor spot were also heterogeneous (Figure 4.3, d), thus, to increase the sensitivity of thresholding and thus segmentation we first log-transformed the images by placing the log-value of intensities to each pixel and then segmented the images. Henceforward, we re-analyzed images in Cell Profiler.

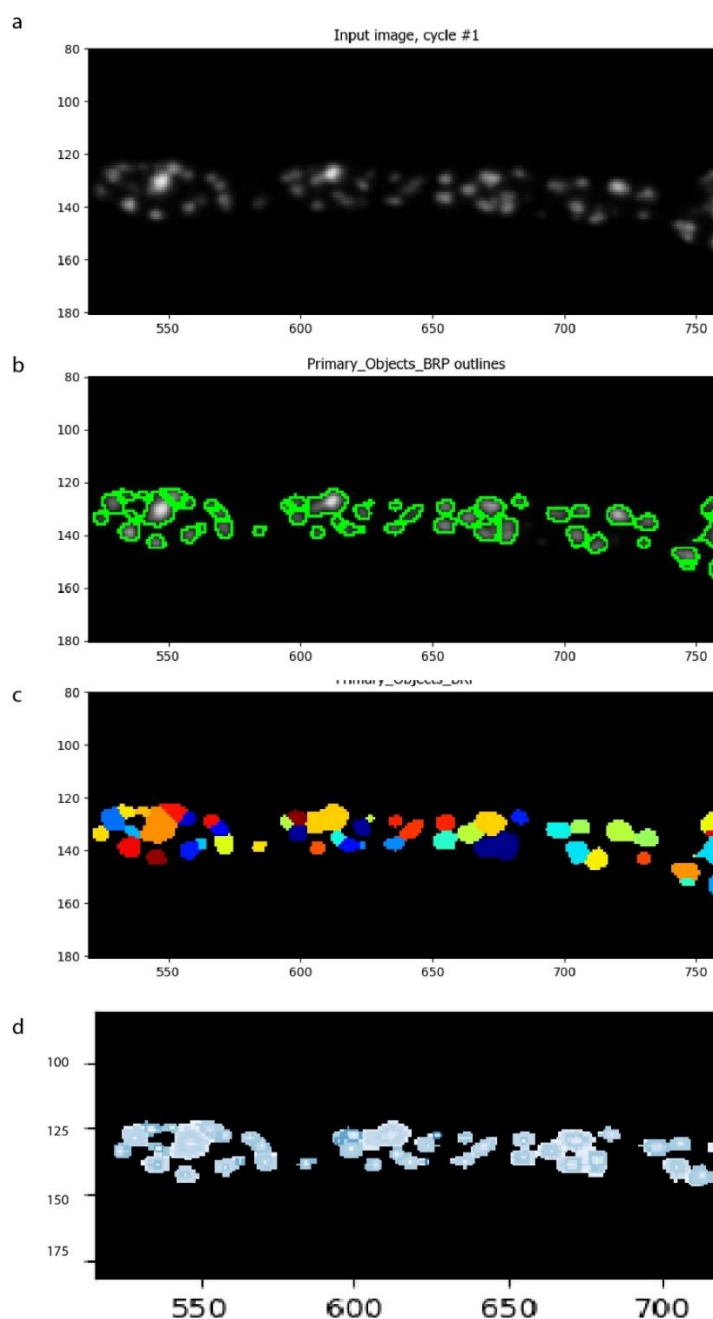


Figure 4.3. Input NMJs and segmented NMJs. Borders of AZs were defined by Otsu thresholding method (b) segmented AZs are shown with different colors(c). Each AZ were binned to 5 and intensity distribution in each ring are shown as heatmap (d).

AZs and glutamate receptor spots were defined with three class Otsu segmentation technique -middle peak was defined as background. BRP and glutamate receptor channels were segmented and analyzed separately. Furthering the analysis, we calculated brp and glutamate receptor intensities as mean⁴ and integrated values⁵.

Since brp is a very dynamic molecule with polarized elliptic shape (56), area⁶ and ellipticity (eccentricity)⁷ of AZs are most explanatory among measured morphological (perimeter, area, bbox area, compactness, Euler number, ferret diameters, and Zernike features) features. In this thesis, thus, we mostly present area and eccentricity measurements as a representation of synaptic morphological features. Lastly, the number of spots calculated is another feature that we presented throughout the thesis.

4.2. Motoneuronal and Pan-neuronal Silencing of NALCN Channel Components -Na, Unc79, and Unc80- Produced Discrepant Results

Silencing NALCN ortholog motoneuronally and staining larvae against brp and glutamate receptor, at first resulted in an increase in brp and glutamate receptor levels compared to control groups. This increase was accompanied by an area increase, but no significant change in brp and glutamate receptor eccentricity (roundness) were observed. On the other side, brp and glutamate receptor spot numbers remained constant (Figure 4.4).

Repeating the experiment one more time, opposed to the previous experiment, resulted in a decrease in both mean brp and glutamate receptor levels compared to control groups. On the other hand as it was the case with the previous

⁴ Mean BRP and glutamate receptor intensities were measured by first getting the intensity in each spot and dividing the value by the spot area.

⁵ BRP and glutamate receptor intensities in each spot were measured and an average of integrated brp and glutamate receptor intensities for each NMJ was calculated.

⁶ Area for each spot was calculated as arbitrary units (a.u) and average of these values for each NMJ was calculated.

⁷ Eccentricity value gives information about the roundness of the spots. It can take values between 0-1. When the value is closer to 1 the shape is more elliptic, whereas when it comes closer to zero the shape is more round.

experiment an increase in brp and glutamate receptor area was observed and no changes in neither eccentricity of the spots nor a change in spot number (Brp spot and glutamate receptor spot) were observed (Figure 4.4) (To ease the viewing, all replicated studies are shown in the same figure in two columns (indicated as 1 and 2)).

Motoneuronal silencing the accessory subunits, *unc79* and *unc80* resulted in similar outcomes: Performing the dissections several times resulted in altered brp and glutamate receptor intensities (Figure 4.6 & Figure 4.8) Morphology and eccentricity parameters also showed discrepancies between different dissections (Figure 4.6 & Figure 4.8)

In short, motoneuronal silencing of *na*, *unc79*, and *unc80* had no effect on AZ and glutamate receptor spot numbers (Figure 4.4, Figure 4.6 & Figure 4.8) On the other side, brp and glutamate receptor morphologies and intensities altered between different dissections compared to control groups.

Pan-neuronal silencing of gene of interest produced similar results, namely, AZ and glutamate receptor spot numbers did not change significantly among groups, whereas brp and glutamate receptor intensity and morphological data differed tremendously when the dissections were performed at different times compared to control groups (Please refer to Figure 4.5, Figure 4.7 & Figure 4.9 for detailed explanations).

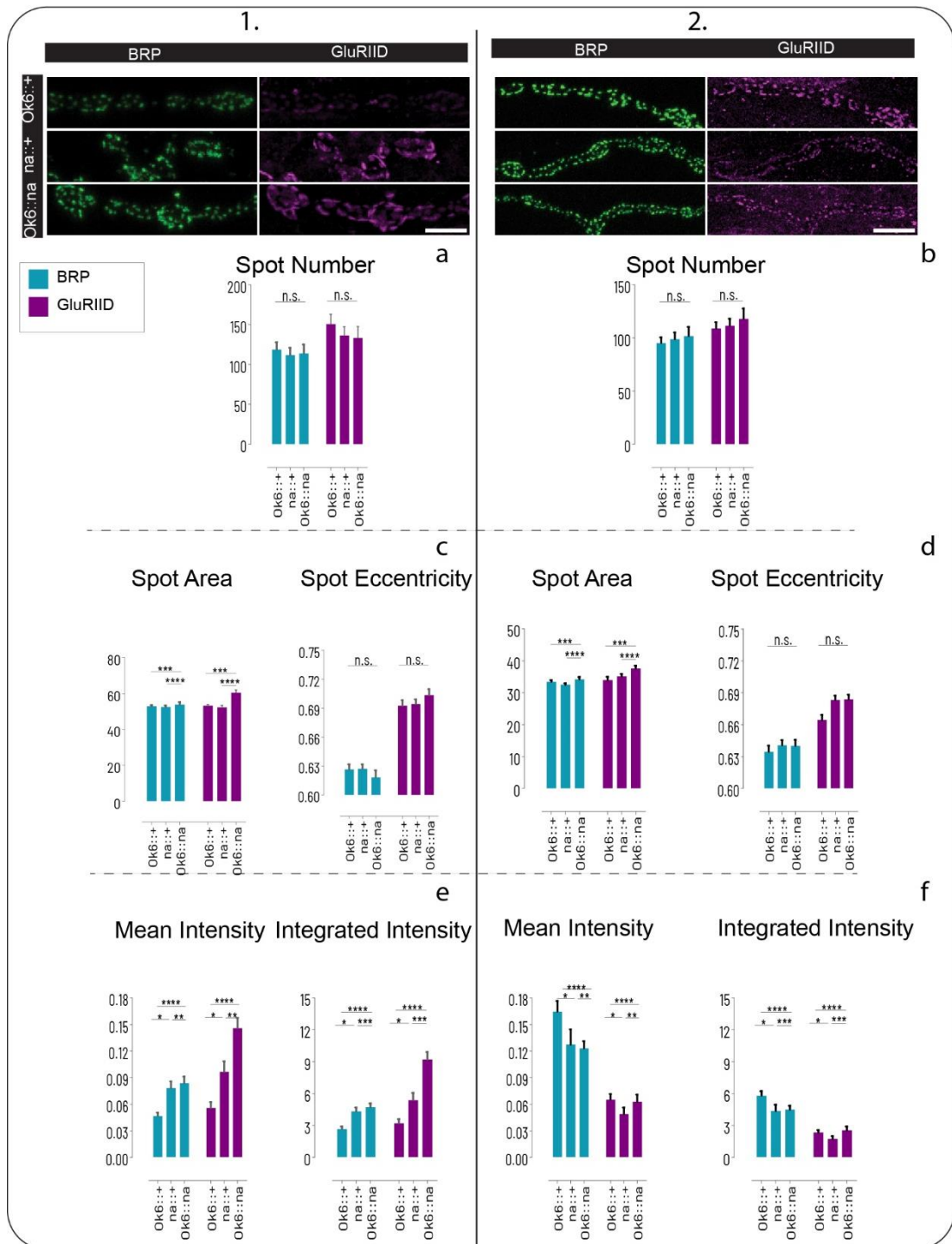


Figure 4.4. Motoneuronal silencing of na results in altered morphology and altered brp and glutamate receptor intensities. Results for two different dissections are shown in two columns as 1 and 2 respectively. BRP and glutamate receptor spot number did not change upon motoneuronal silencing of na (a, b). On the other side, morphology of the T-bars and glutamate receptor spots alongside with mean intensities showed discrepancies, namely when the experiment was replicated

results changed drastically compared to control group (c, d, e, and f). Motoneuronal silencing of na resulted in an increase in brp and glutamate receptor levels in one experiment, and brp and glutamate receptor levels decreased compared to control group when the experiment was replicated (e, f). Scale bars: 5 μ m.

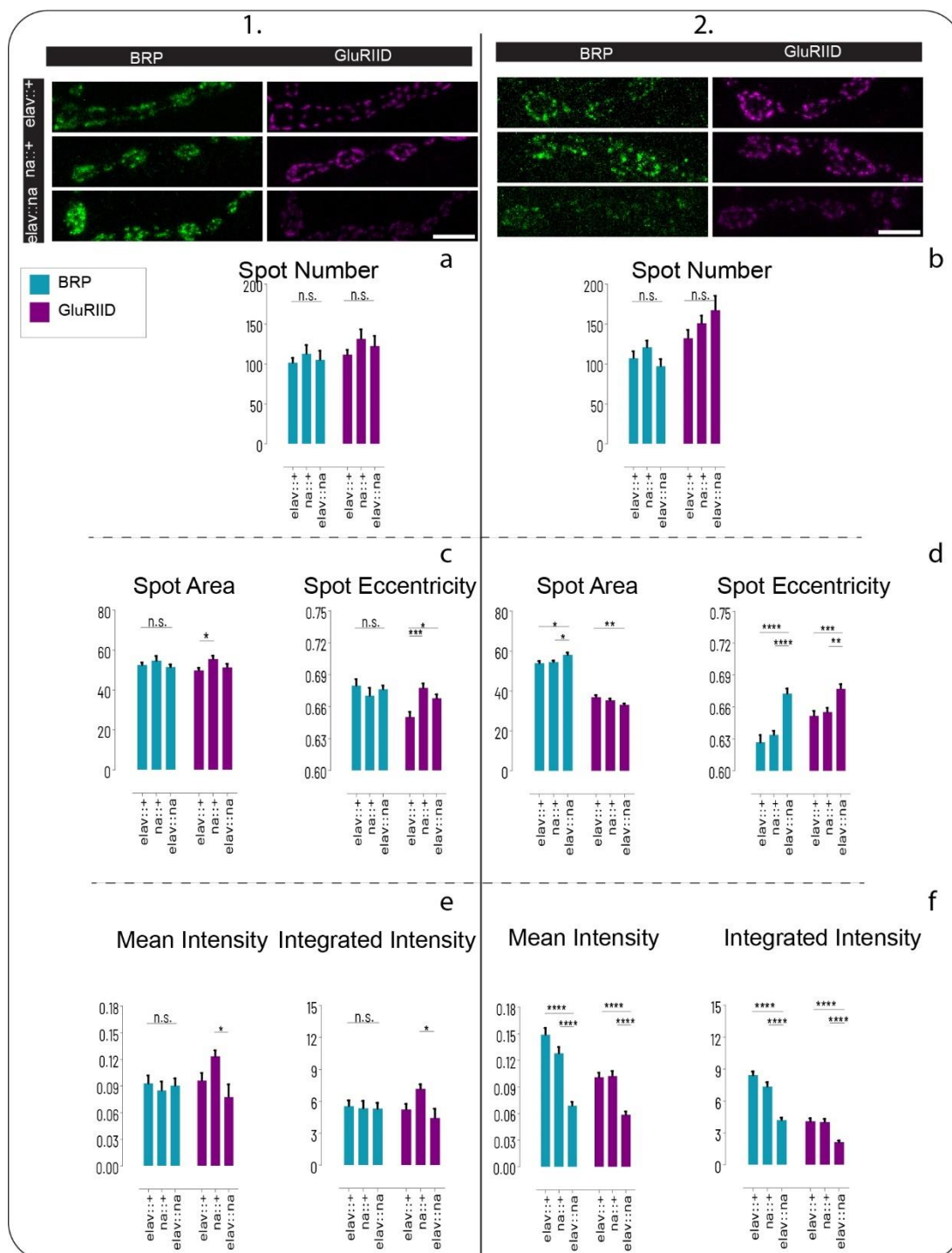


Figure 4.5. Pan-neuronal silencing of na results in altered morphology and intensity in both presynaptic and postsynaptic sides. Results for two different dissections are

shown in two columns as 1 and 2 respectively. BRP and glutamate receptor spot number did not change upon pan-neuronal silencing of na (a, b). On the other side, morphology of brp and glutamate receptor spots change drastically compared to control group (c, e). However, we could not observe the same changes when the experiment was replicated (d, f). The same was true for mean and integrated brp and glutamate receptor spot intensities (e, f). Scale bars: 5 μ m.

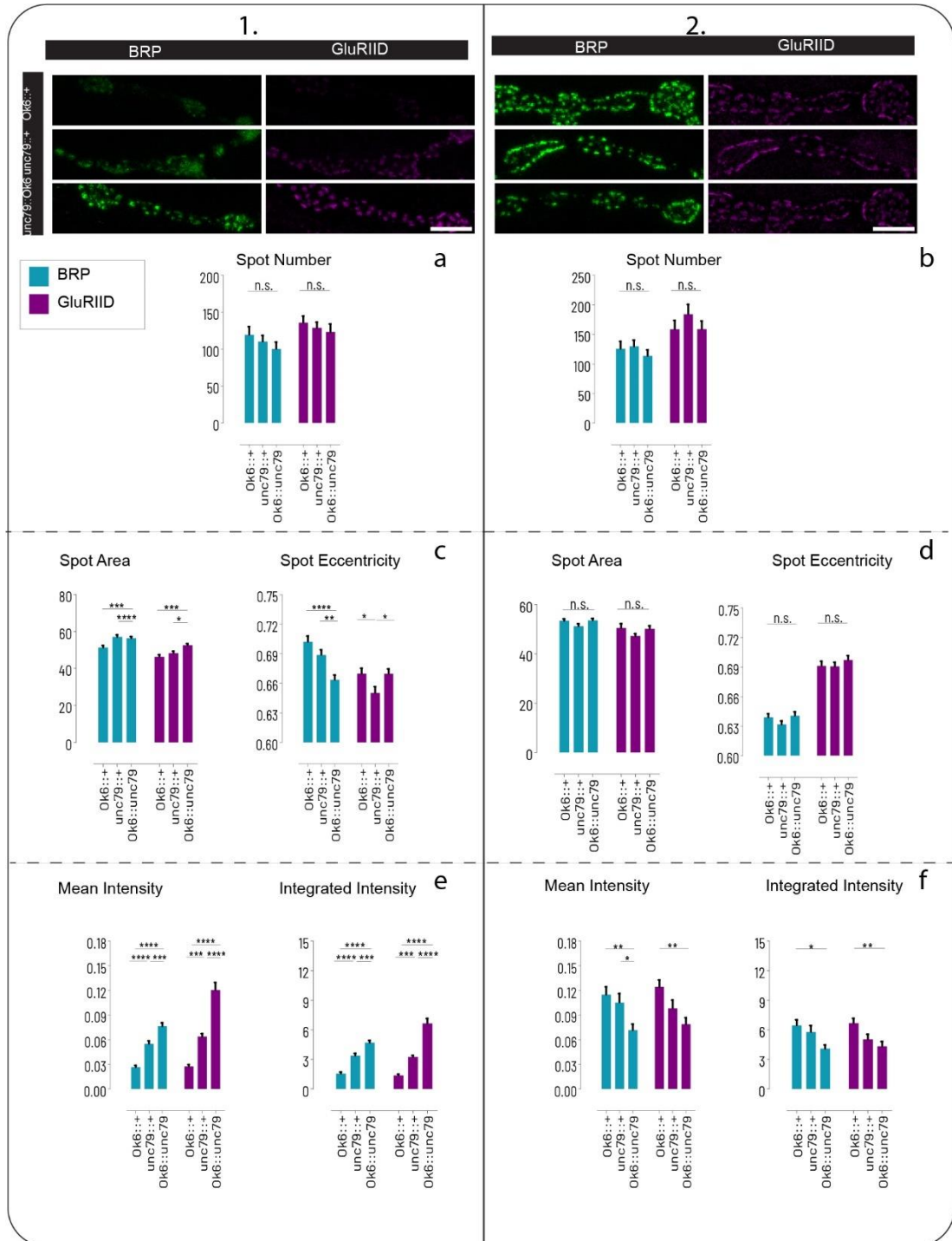


Figure 4.6. Motoneuronal silencing of the accessory subunit *unc79* results in altered morphology and intensity in both presynaptic and postsynaptic sides. Results for two different dissections are shown in two columns as 1 and 2 respectively. BRP and glutamate receptor spot number did not change upon pan-neuronal silencing of *unc79* (a, b). On the other side, morphology (area and eccentricity) of brp and glutamate receptor spots changed drastically when the experiment was conducted for the first time (c), however we could not see a difference in brp and glutamate receptor spot area, and eccentricity of the spots in both pre and post-synaptic sides when the experiment was replicated (d). On top of it, brp and glutamate receptor intensity was higher compared to control groups in the first experiment (e), but was lower compared to control groups when the experiment was replicated. Scale bars: 5 μ m.

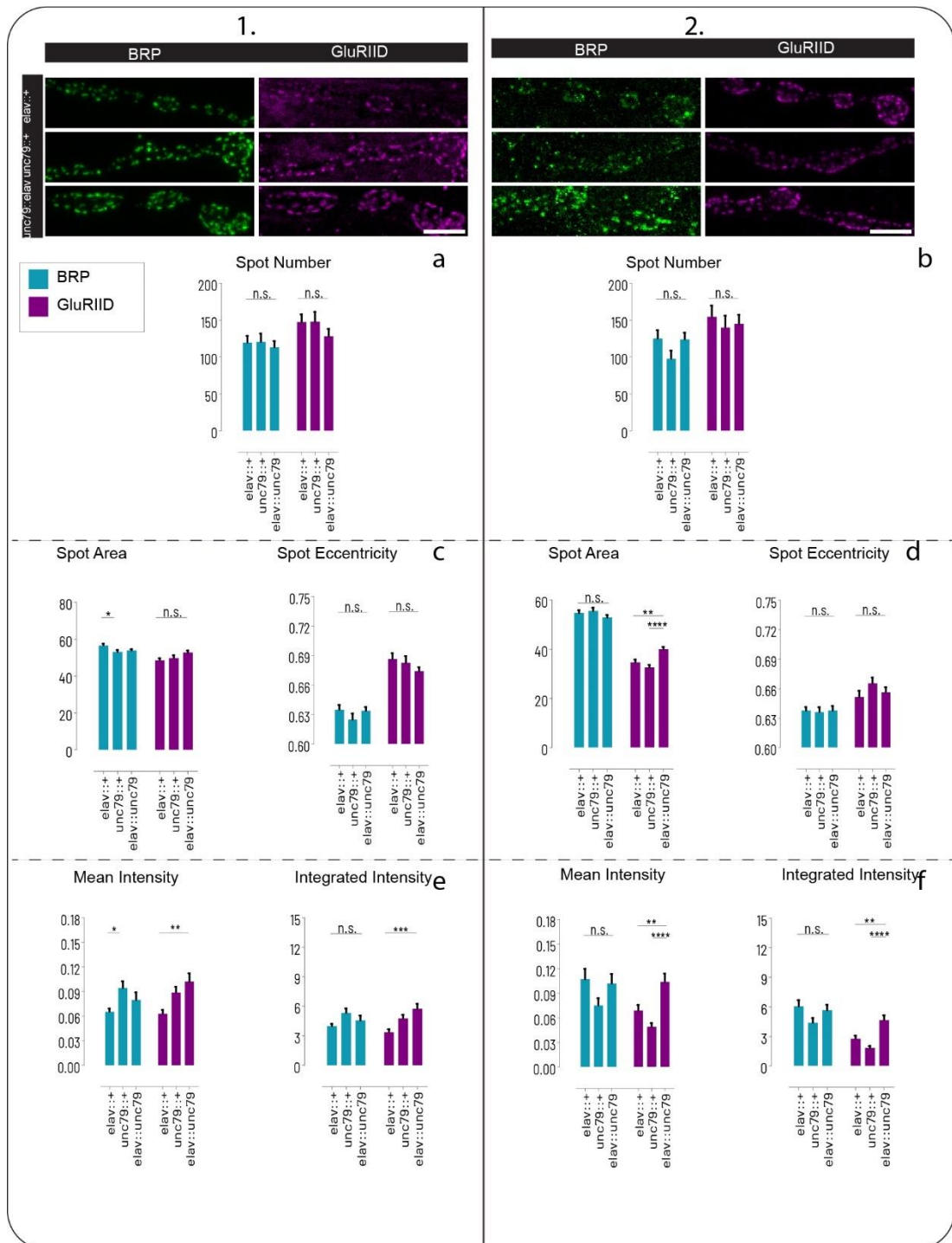


Figure 4.7. Pan-neuronal silencing of the accessory subunit *unc79* results in altered morphology and intensity in both presynaptic and postsynaptic sides. Results for two different dissections are shown in two columns 1 and 2 respectively. BRP and glutamate receptor spot number did not change upon pan-neuronal silencing of *unc79* (a, b). On top of it, morphology (area and eccentricity) of brp and glutamate receptor spots did not change in none of the groups except 1st experiment in which a significant decrease in brp spot area is observed between CC and DC (d, c). Mean

and integrated BRP and glutamate receptor intensities again showed inconsistent results (e, f). Scale bars: 5 μ m.

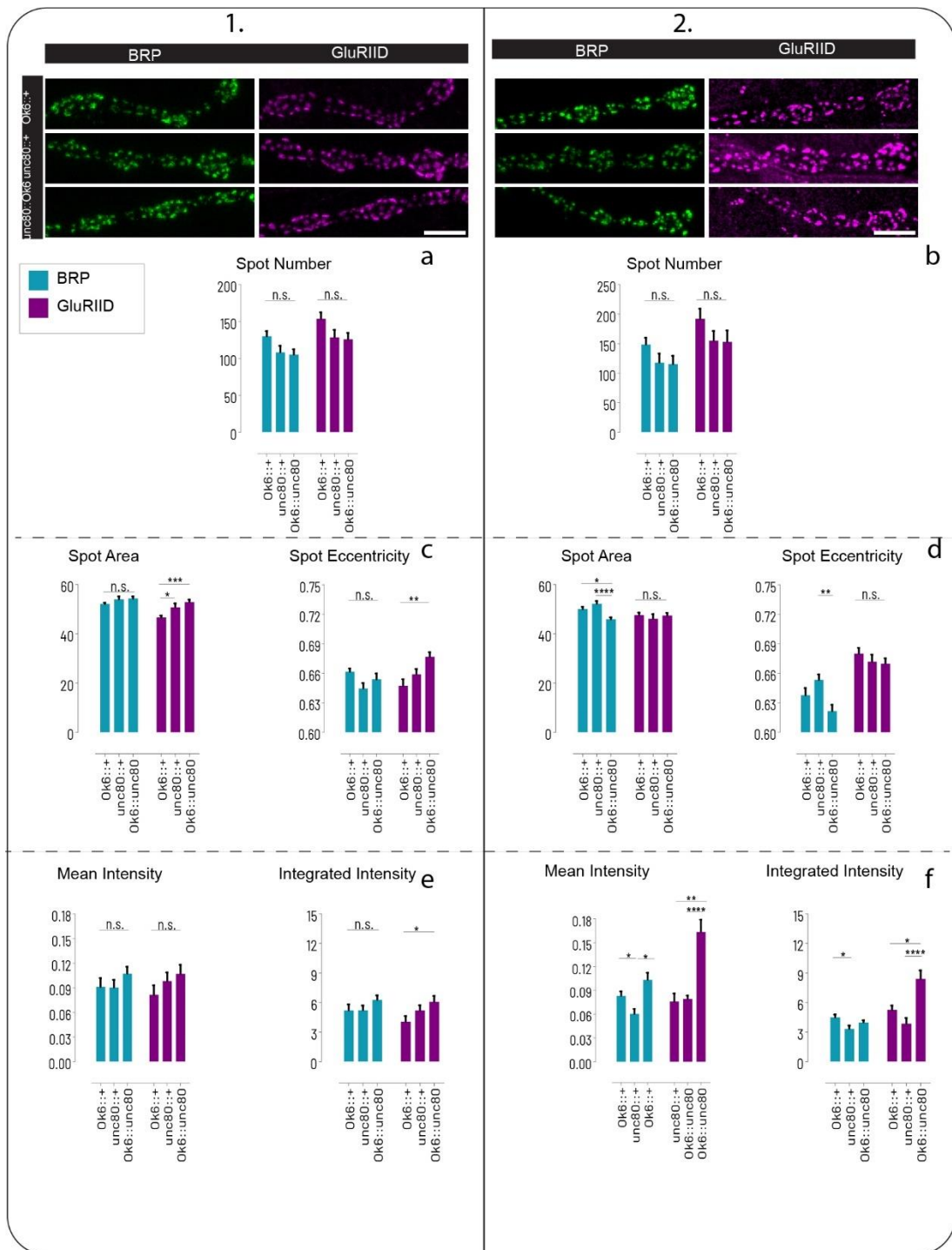


Figure 4.8. Motoneuronal silencing of the accessory subunit *unc80* resulted in inconsistent morphology and intensity. Results for two different dissections are shown in two columns 1 and 2 respectively. BRP and glutamate receptor spot number did not change upon pan-neuronal silencing of *unc80* (a, b). Morphology (area and eccentricity) of *brp* and glutamate receptor spots (c, d) and mean and integrated *brp*

and glutamate receptor intensities (e, f) showed discrepant results when dissections were replicated. Scale bars: 5 μ m.

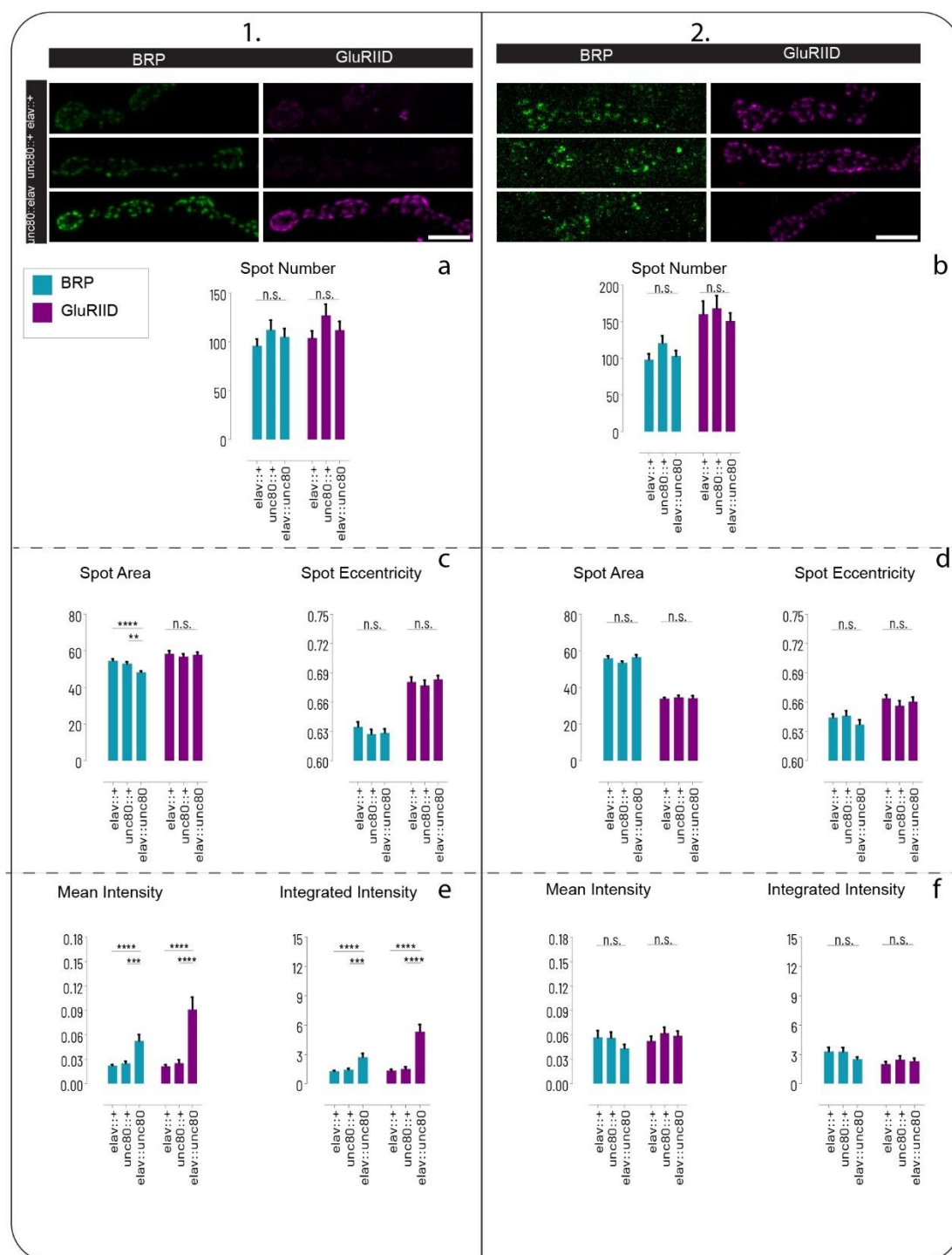


Figure 4.9. Pan-neuronal silencing of the accessory subunit *unc80* resulted in inconsistent morphology and intensity. Results for two different dissections are shown in two columns 1 and 2 respectively. BRP and glutamate receptor spot number did not change upon pan-neuronal silencing of *unc80* (a, b). On top of it, morphology (area and eccentricity) of brp and glutamate receptor spots (c, d) and mean and

integrated brp and glutamate receptor intensities (e, f) where not the same when the experiment was replicated. Scale bars: 5 μ m.

4.3. Motoneuronal Silencing of Farjavit

Since dissecting NALCN components resulted in discrepancies in both mean and integrated brp and glutamate receptor intensities, we further analyzed another synaptopathy related gene to find out if the outcome will be similar.

Farjavit (*frj*), *Drosophila* ortholog of MBOAT7 is an enzyme that stands in Lands cycle and preferentially attaches arachidonic acid to PIs. PIs are lipid molecules and important modulators of synaptic function.

Tissue specific silencing of *frj* with two different RNAi lines had different outcomes:

First dissection was performed by dissecting each group sequentially: Six larvae from one group was dissected and this dissection was preceded by another six larvae from another group (Figure 4.11.). In the second dissection, to restrain possible time-dependent variation in protein levels (brp and glutamate receptor), 2 CC, 2 DC, and 2 RNAi lines were taken out from the incubator and dissected at the same time (Figure 4.10.).

Motoneuronally down-regulating *frj* resulted in a decrease in brp levels compared to DC (*Ok6::+*), but not CC (*frj::+*), while BRP and glutamate receptor spot number did not change between groups. On the other side, brp spots were rounder whereas glutamate receptor spots were more elliptic compared to control groups (Figure 4.10).

Motoneuronal silencing performed with another RNAi line resulted in decrease in brp levels, but no significant change was observed in glutamate receptor levels (Figure 4.11). As a result, as it was the case with NALCN channel components, we could not observe the same alterations in intensities compared to control group.

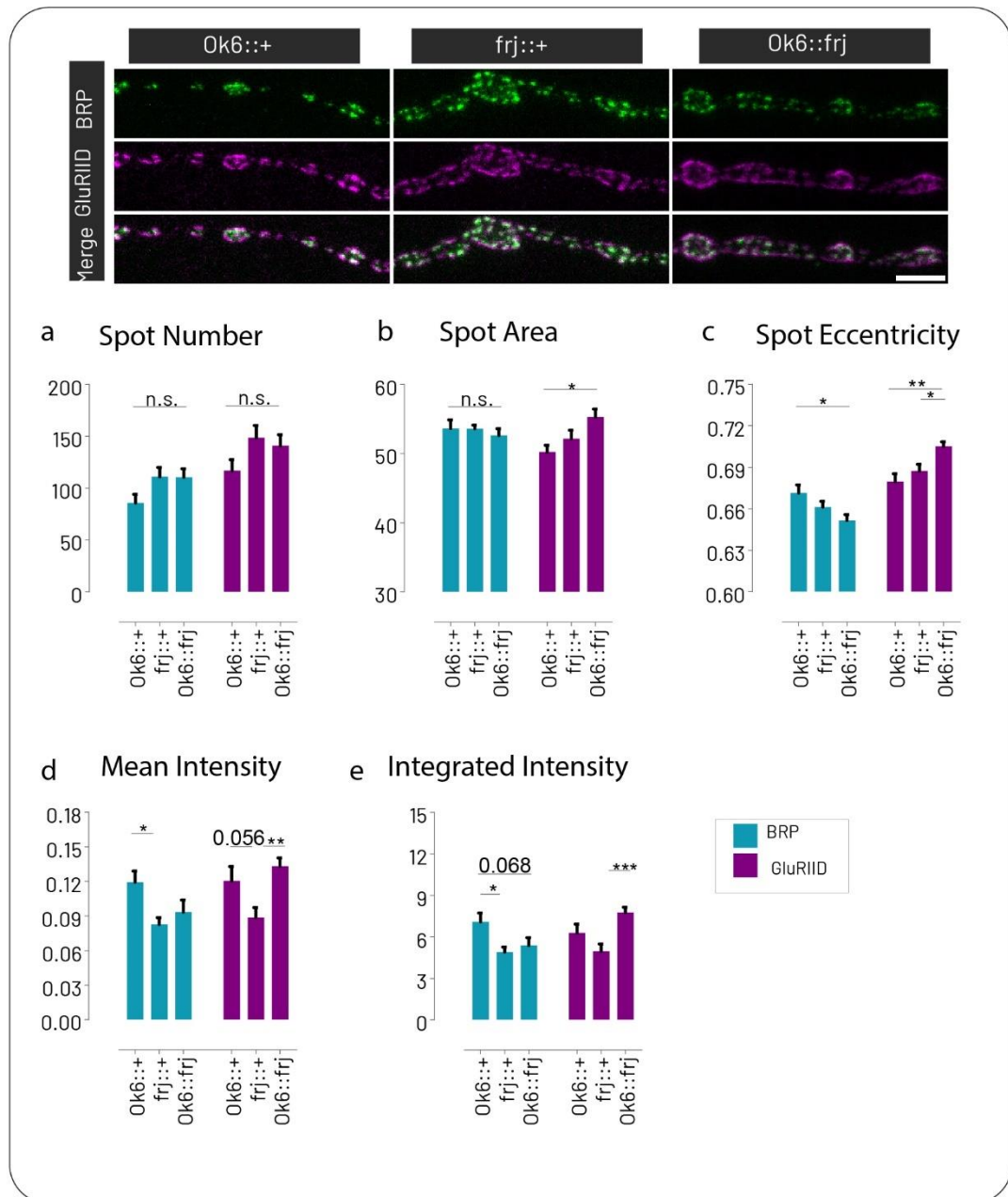


Figure 4.10. Motoneuronal silencing of *frj* results in altered morphology and intensity in both presynaptic and postsynaptic sides. BRP and glutamate receptor spot number did not change upon motoneuronal silencing of *frj* (a). On top of it, we observed changes in morphology of both brp and glutamate receptor spots, no change in brp area was observed compared to control group, whereas motoneuronally silenced *frj* has rounder brp spots(b,c). Mean and integrated brp and glutamate receptor intensities differed according to control group (d, e). Scale bars: 5 μ m.

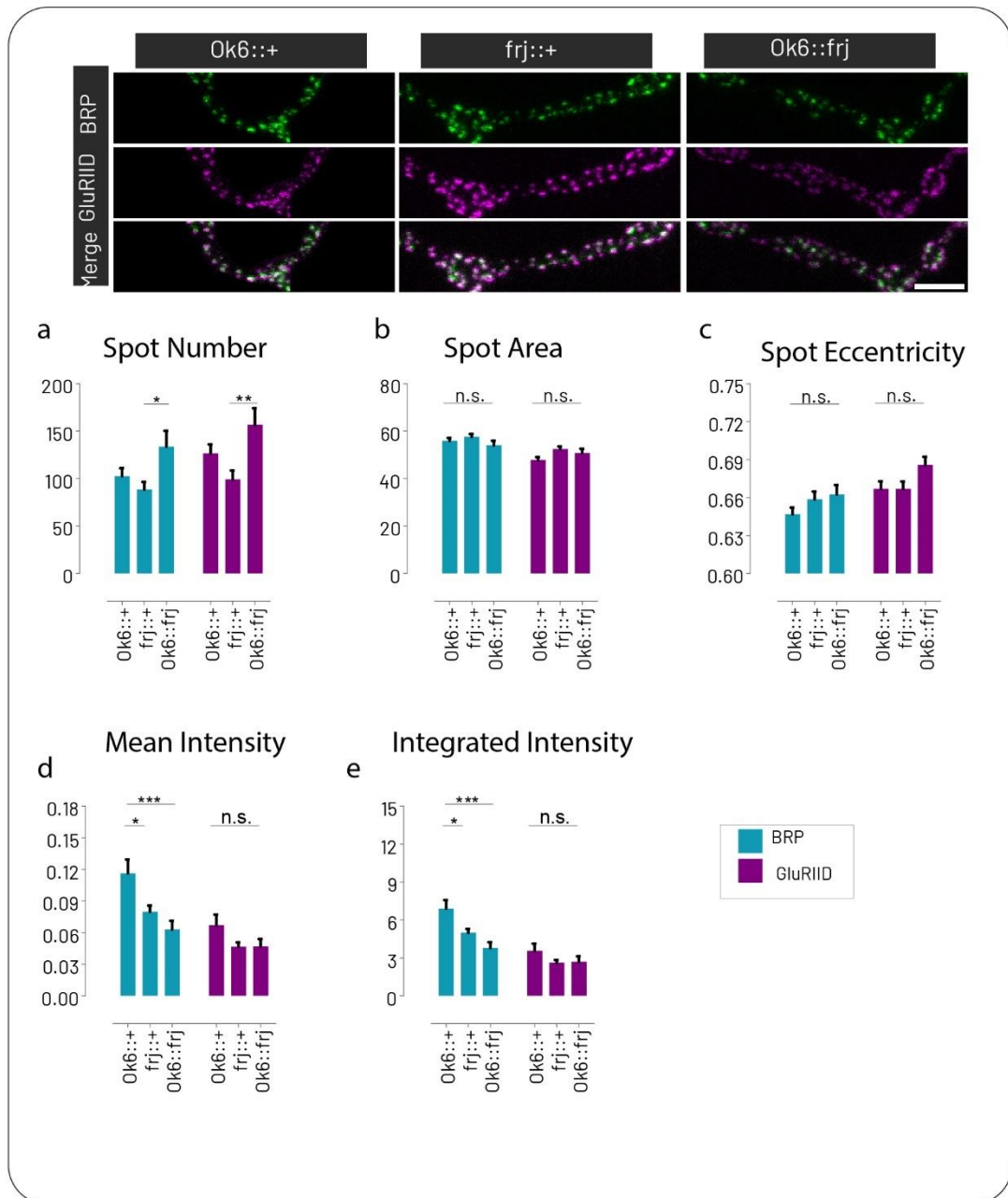


Figure 4.11. Motoneuronal silencing of *frj* results in altered morphology and intensity in both presynaptic and postsynaptic sides. BRP and glutamate receptor spot number differed between CC and motoneuronally silenced *frj* (a), whereas we could not observe a change in morphology of the spots both in presynaptic and postsynaptic sides (b,c). On top of it, *brp* intensities decreased upon motoneuronal *frj* silencing, but we could not observe a significant intensity change on postsynaptic side (d, e). Scale bars: 5 μ m.

4.4. Pan-Neuronal Silencing of Farjavit has no Effect on Brp and Glutamate Receptor Intensities

Pan-neuronal silencing of frj was followed by dissection of 3rd instar larvae and immunohistochemical staining. On the contrary, to the previous frj experiment, in which one dissection was performed sequentially, this time dissections were performed by using the same methodology that we used for dissecting NALCN channel components: We dissected larvae by taking two larvae from each group and dissected them at the same time.

Silencing frj pan-neuronally did not change brp and glutamate receptor levels compared to control groups (DC: elav::+, CC: frj::+) (Figure 4.12). Replicating the experiment in gender dependent manner again resulted in no change in brp and glutamate receptor intensities compared to control groups. On the other hand, morphology features (area, eccentricity) did not change in brp channel in the first experiment (Figure 4.12), whereas we observed a slight decrease in brp eccentricity in females compared to construct control in the second dissection (Figure 4.13), other than this morphologies were very similar. Besides, glutamate receptor spot area and eccentricities increased and decreased respectively compared to control group (Figure 4.12 b and c). Gender dependent dissection eliminated glutamate receptor morphology discrepancies and we observed and no significant change neither in area nor eccentricity of the glutamate receptor spots (Figure 4.13).

In short, no intensity changes were observed in both brp and glutamate receptor channels when compared to control groups. On top of it, no gender dependent intensity changes in both brp and glutamate receptor levels were observed. On the other hand, we observed a slight change in spot number between control groups in first dissection. Whereas morphological changes were mostly eliminated especially in glutamate receptor spots when dissections were performed in a gender-dependent manner (Figure 4.12). Still, we observed eccentricity differences in brp channel even when the dissections were performed in a gender-dependent fashion (Figure 4.13).

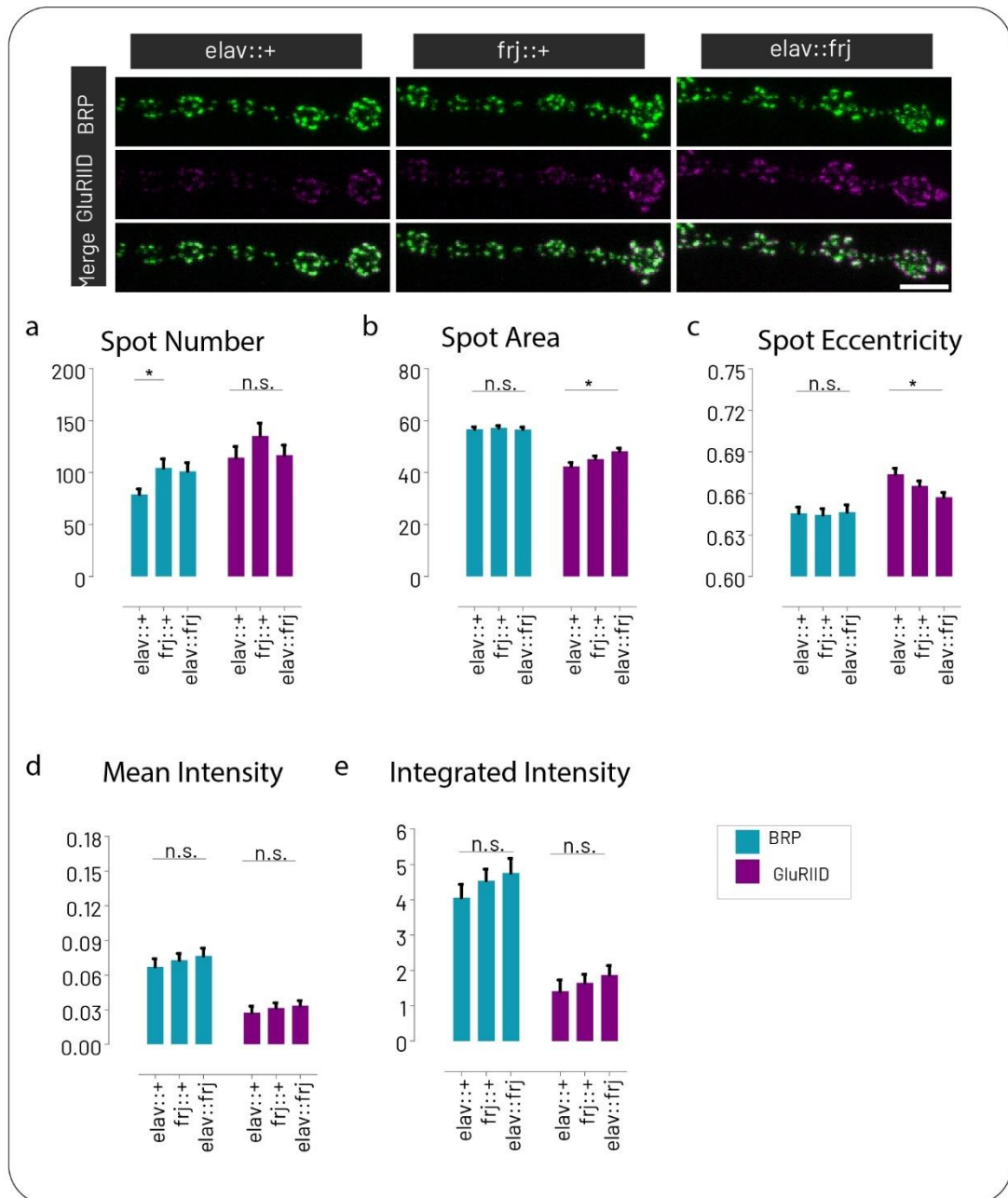


Figure 4.12. Pan-neuronal silencing of *frj* results in no change in *brp* and glutamate receptor intensities. BRP spot number was higher in pan-neuronally silenced *frj* group (a). On top of it, we observed slight change in both area and eccentricity of glutamate receptor spots whereas *brp* morphology was the same in all of the groups (b, c). Mean and integrated *brp* and glutamate receptor intensities, on the other hand, were constant (d, e). Scale bars: 5 μ m.

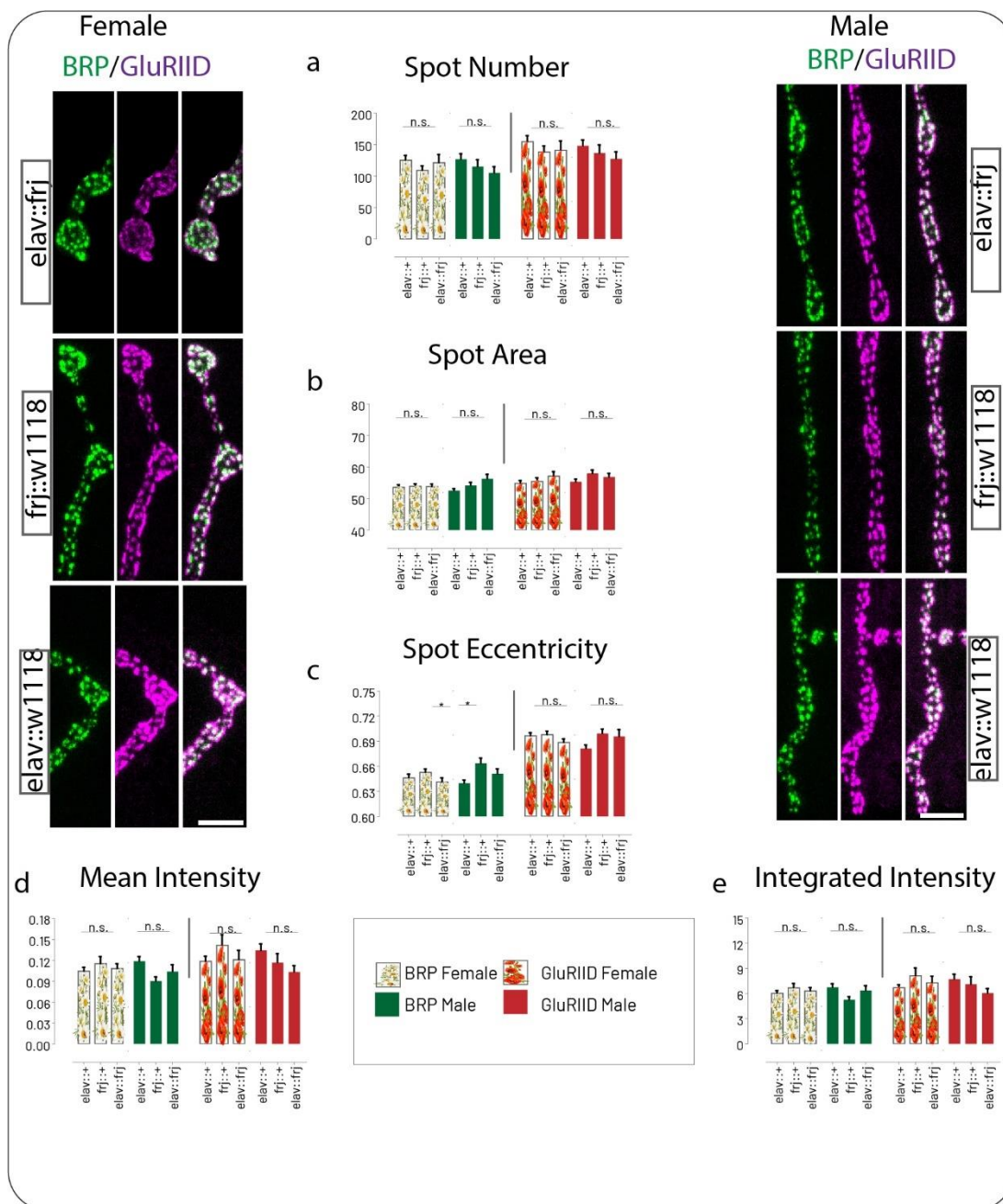


Figure 4.13. Gender dependent pan-neuronal silencing of *frj* has no effect on *brp* and glutamate receptor intensities. *BRP* and glutamate receptor spot number and spot area did not change upon neither pan-neuronal silencing of *frj* nor in a gender dependent manner (a, b). Slight changes in spot eccentricity at *brp* spots in both females and males were observed, but no gender dependent change in the roundness of glutamate receptor spots were observed (c). Mean and integrated *brp* and glutamate receptor intensities also did not change in a gender dependent fashion (d, e). Scale bars: 5 μ m.

4.5. BRP and Glutamate Receptor Levels are not Constant in Wild-Type (w1118) *Drosophila melanogaster* at 29 °C

As mentioned, motoneuronal and pan-neuronal silencing of NALCN channel components resulted in altered intensities and altered morphological features in presynaptic and postsynaptic brp and glutamate receptor respectively.

Due to the discrepancies especially in the intensities in both brp and glutamate receptor channels we stepped back and wondered how brp and glutamate receptor levels changed at different times in wild type (w1118) fly larvae at motoneuronal NMJs. It has been reported that brp levels oscillate in photoreceptors of flies thus we concluded that it may be also the case for NMJs of *Drosophila* 3rd instar larvae.(111, 146)

Flies were reared in semi-defined Bloomington recipe at RT and crosses were kept in 29C incubator. Namely, flies that were raised in RT were exposed to day-light (On dissection date, day light was between 4.43 and 21.30 →3.53-4.43 and 21.30-22.20 were civil twilights) and larvae were placed in 29^oC incubator (lights were on between 07:00-20:00) (Figure 4.14). 3rd instar larvae were dissected at random time points and mean brp and glutamate receptor spot intensities were analyzed at the specified time points (Figure 4.14). Approximately 5 fold change in brp intensity and almost 7 fold change in glutamate receptor intensity was observed between max and min mean intensities (min-max): 0.008- 0.053 (Glutamate receptor); 0.02-0.10) (BRP) (Figure 4.14). Hence, immunohistochemical analysis showed that BRP and glutamate receptor levels are not constant during day in wild type 3rd instar larvae NMJs. Two peaks close to lights-on and lights-off and a nadir at 15:00 p.m. was observed. The minimum intensity was close to the second peak (2h apart from each other), showing that brp and glutamate receptor levels can increase steeply (Figure 4.14 (Time:15.00 and 17.00). Moreover, brp and glutamate receptor levels did not change significantly between the first peak and first nadir. In other words, when peak and nadir time points were excluded, there was no significant change in neither brp nor glutamate receptor levels at other time points (5 time points: Hours: 9, 11, 13, 19,21) (Figure 4.14).

Of note, in incubator light behavior is totally different from sun: At room temperature (RT), flies were exposed to natural light, consequently, light levels increased gradually and so did the temperature, on the other hand in the incubator light had an on-off state while temperature was constant.

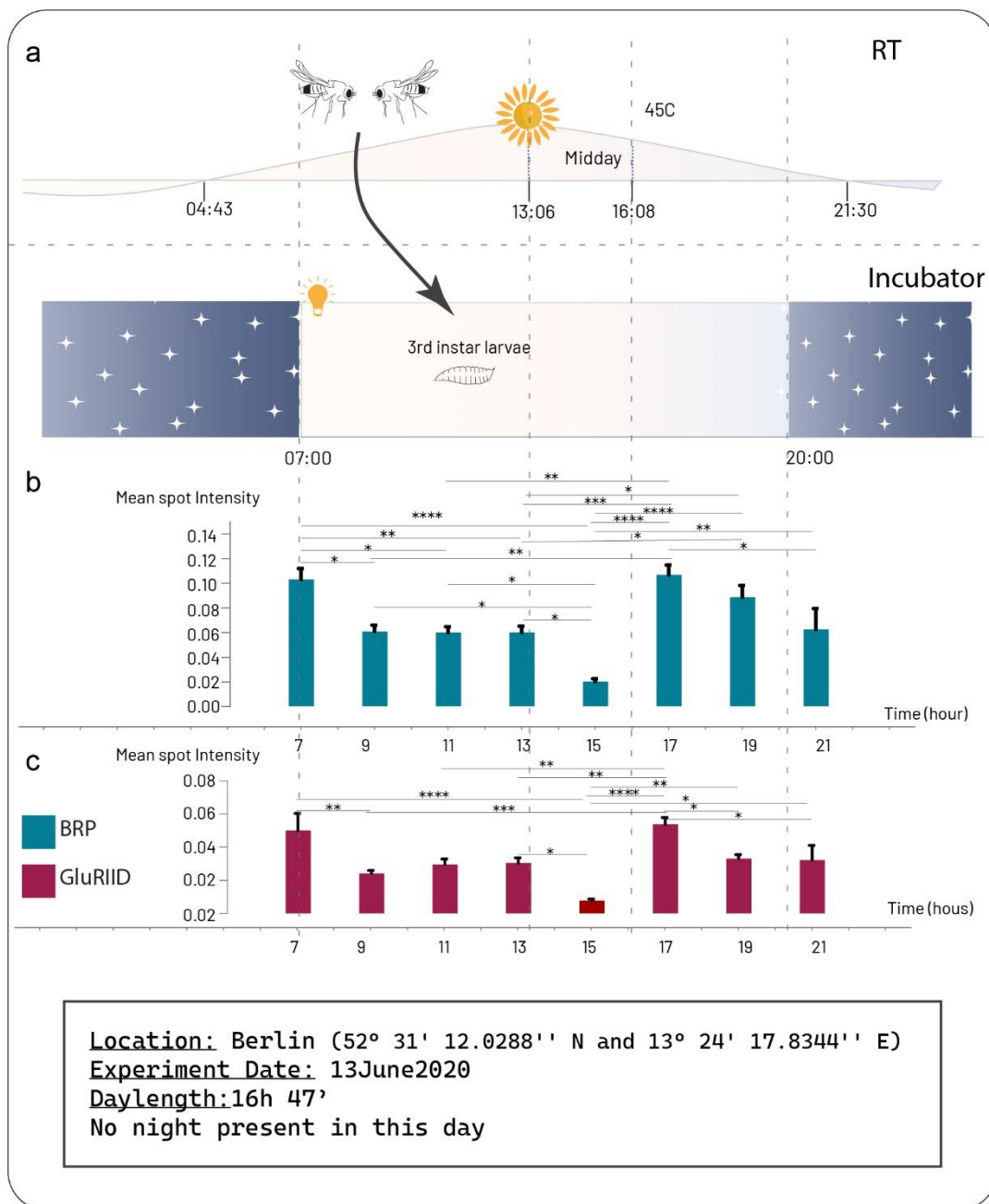


Figure 4.14. BRP and glutamate receptor levels are not constant in 3rd instar larvae. Flies were kept at RT under day light and larvae were placed in 29°C incubator (a). Mean BRP intensities at AZs at different time points (b). Two peaks in mean brp (b) and mean glutamate receptor intensities (c) were observed at 7.00 and 17.00

respectively and a the lowest intensity was observed very close to the second peak in both brp and glutamate receptor channels (b, c).

4.6. BRP and Glutamate Receptor Levels are not Constant in Wild-Type (W1118) *Drosophila Melanogaster* at 25 °C

Next, we sought to understand if we could observe brp and glutamate receptor intensity change when larvae and flies were placed under more controlled environment, namely:

Flies and larvae were kept in the same incubator at 25°C and a couple of experiments were performed with slightly different conditions (Table 4.1):

1. Same number of female and male w1118 flies were crossed and placed to two separate vials (Figure 4.15 a, fly color), placed into the incubator, were treated in the same way from the beginning until dissection. However, in the incubator lights on phase was not beginning at 8:00, it was shifted by an unknown hour (not more than three hours) (Figure 4.15 a, arrows on top of the clock) and humidity was also fluctuating. Yet, two vials were kept in the same environment and the conditions were the same for both of the larvae. In this experiment our aim was to understand if we can see the same oscillatory pattern in both of the vials (Figure 4.15 a)

2. Flies were raised in semi-defined Bloomington recipe and crosses were kept in 25°C incubator. Dissections were performed for two consecutive days by using larvae from the same vial. Only one dissection (ZT22) was performed approximately 40 min earlier than the other dissection (Figure 4.15 b). With this experimental design we wondered if we could see the same oscillatory pattern in the same vial in two consecutive days.

3. Same number of female and male w1118 flies that were kept at 25°C incubator were crossed and larvae were kept in the same incubator under 12h light/dark environment (50% light amount), 65% humidity, and 50% circulating air. 3rd instar w¹¹¹⁸ larvae from two different vials were dissected at specified time points (Figure 4.15 c). The experiment is the same experiment as experiment 1 with only a more controlled environment.

Table 4.1. Description of the environmental cues for w1118 dissections.

	1st Experiment (Figure 8a)	2nd Experiment (Figure 8b)	3rd Experiment (Figure 8c)
Flies	25°C incubator	25°C incubator	25°C incubator
Larvae	25°C incubator Same number of female and male flies were raised at different vials.	25°C incubator Only one vial of crossing was prepared.	25°C incubator Same number of female and male flies were raised in two different vials.
Environment	12h light dark cycle (lights-on-off shifted)	12h light-dark cycle	12h light-dark cycle
Humidity	Fluctuated between 60-95%	60-65% Humidity	65% Humidity
Circulating air	n.a.	n.a.	50%
Light amount	n.a.	n.a.	50%
Incubator Condition	Incubator used by others too (door opens and closes at different times)	No-one used the incubator.	No-one used the incubator.

We observed the same oscillatory pattern when the dissections were replicated, though in the second experiment at time point ZT22 (Figure 4.15 b) dissection time differed for 40 min between the two dissections in which we saw a difference between brp and glutamate receptor intensities when two dissections

were compared to each other. Other than the aforementioned time, intensities were very similar in a time dependent fashion: Amplitude of brp and glutamate receptor differed slightly for some time points but this difference did not affect the overall shape of the oscillatory pattern (i.e. Figure 4.15 a (ZT23); Figure 4.15 c (ZT0)). On top of it, we observed at least two fold change in mean brp/glutamate receptor levels between nadir and peak points, and up to 4 fold change in mean brp levels, and up to 5 fold change in mean glutamate receptor levels (Figure 4.16).

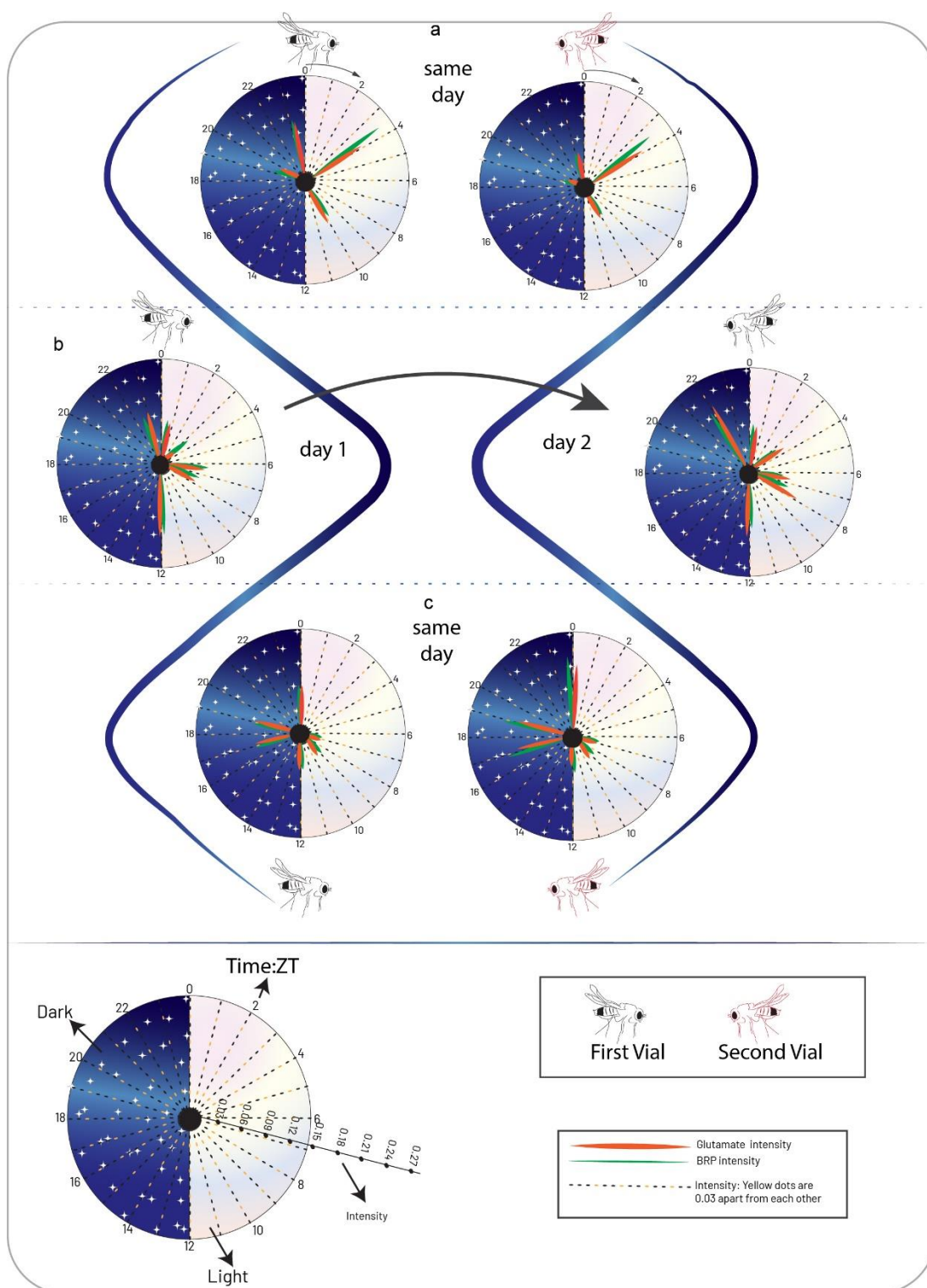


Figure 4.15. BRP and glutamate receptor oscillate with the same pattern. First set of experiments were performed at 25°C, but the exact time when lights were on was missing -though it was known that lights were on after 8.00 and was open for 12h. Mean brp and glutamate receptor intensities oscillated with the same oscillatory

pattern in the two experiments. On the other hand, amplitude of mean brp and mean glutamate receptor levels differed at some time points (ZT10 and ZT23) between the two groups (a). Mean brp and glutamate receptor oscillatory pattern was the same when the experiment was conducted in two consecutive days. The only difference in mean brp/glutamate receptor intensity was observed at ZT22, in which dissection was not performed at the same time (40 min difference between starting points) (b) The same experimental design as in (a) was performed in another incubator with constant light, humidity, and constant air circulation (c). Same oscillatory pattern were observed when two experiments with same conditions were run in parallel. The only difference was the amplitude of mean brp and glutamate receptor levels at some time points (i.e. ZT0) (c).

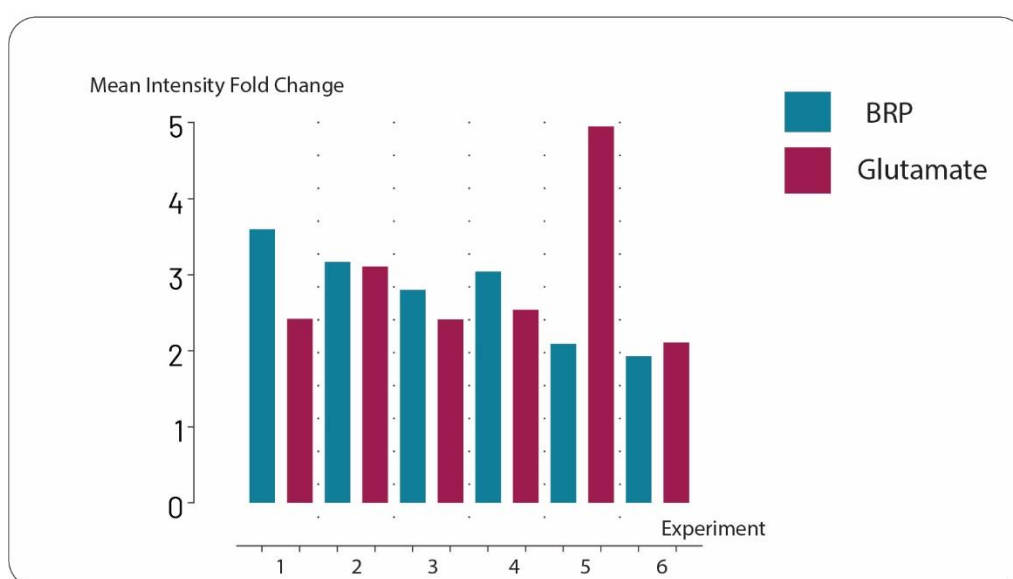


Figure 4.16. Mean BRP and glutamate receptor changes at least two fold. Six separate experiments were analyzed and at least two fold change in both brp and glutamate receptor levels were observed between max and min brp and glutamate receptor mean intensities.

4.6.1. BRP and Glutamate Receptor Levels Fluctuate in a Time-Dependent Manner

We would like to further expand the results for second experimental design (Figure 4.15 b).

We observed significant change in both brp and glutamate receptor levels between ZT11 and all five time points, but though brp levels were lowest in the middle of the day (time point:3 →ZT3.5) we could not observe a significant difference

compared to other time points. Looking from glutamate receptor side, however, we did observe significant change between this time point (3: ZT:3.3) and most of the time points (Figure 4.17 a). Performing the dissections on the consecutive day with the larvae that were reared in the same vial also gave close results: Time dependent brp and glutamate receptor change of brp draws attention since it results in close oscillatory patterns (Figure 4.17 a&b)

However, as it was the case for the first experiment conducted at 29⁰C (Figure 4.14) when lowest and highest intensity time points were excluded from the analysis we could not see any significant change between other three time points. Replicating the experiment on the following day resulted in an upside down bell curve shape (Figure 4.17 b&d). The highest two intensities were observed close to lights-on and off respectively with a more prominent difference in glutamate receptor side (Figure 4.17 c&d). The lowest intensity was observed at the same time, yet it was not as prominent as in previous day (Figure 4.15 c&d).

On the other hand, when AZ morphologies were analyzed we could not see a relationship between AZ morphology and time (Figure 4.17 e)

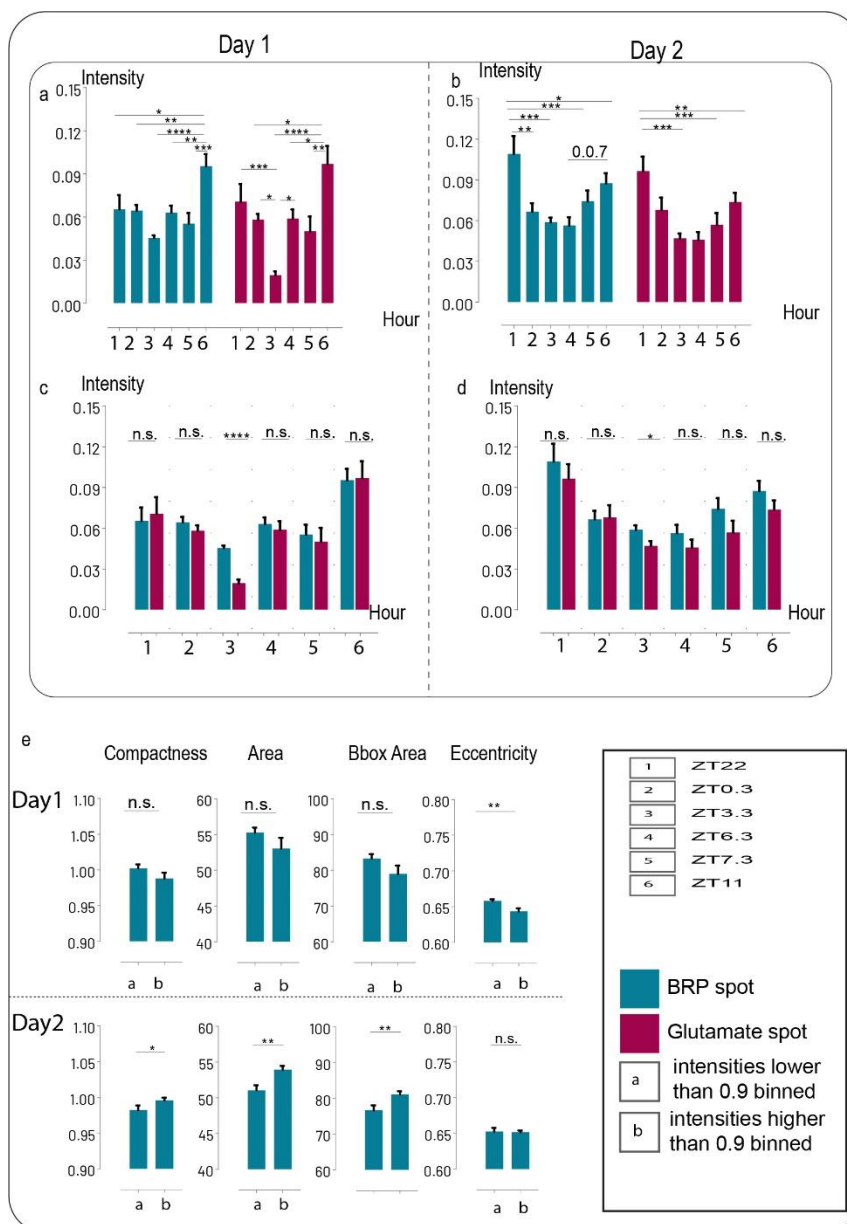


Figure 4.17. Dissecting larvae in two consecutive days resulted in approximately the same mean intensities at same time points.

Then we compared mean brp and glutamate receptor levels in a time dependent fashion: We reanalyzed the samples, to see if brp and glutamate receptor levels are same at in a time-dependent fashion (Figure 4.18). We observed significant difference in both brp and glutamate receptor levels at ZT3.3 and a significant change in brp levels at ZT22 (Figure 4.18). Of note these time points are close to the activity peaks and siesta phases observed in previous studies in *Drosophila*.

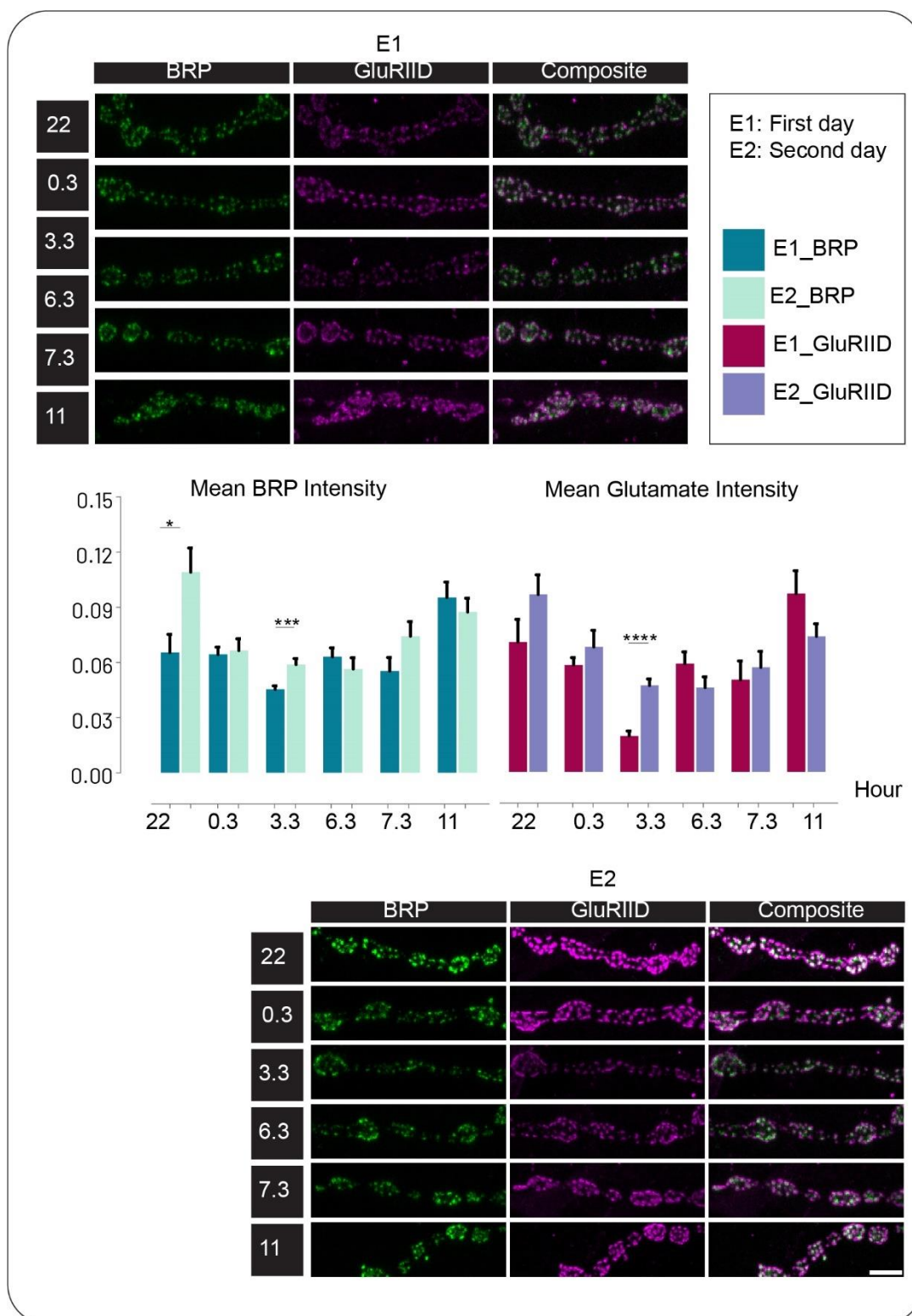


Figure 4.18. Mean BRP and mean glutamate receptor intensities showed upside down shaped bell curve on both days. Significant change in brp levels (day 1 and 2) were observed at ZT 22, however at this time point dissections were performed with

a slight shift in time. At ZT3.5 we observed a significant change between brp and glutamate receptor levels. Lowest brp values were also obtained at this time point. Scale bars: 5 μ m.

4.7. Shifting Dissection Time for Only One-Two Hours Results in Non-Significant Change in Intensities

In the previous experiments we showed that BRP and glutamate receptor levels were not the same at all time points and brp and glutamate receptor levels oscillated with the same pattern. However, when the experiment was replicated, for very few time points -especially at min and max intensities- we could not observe the same increase/decrease:

We postulated that:

- An acute increase in brp/glutamate receptor levels and/or
- Slight change in the timing of the peaks (i.e. due to environmental homeostatic reasons)

may be the reason for this observation.

Thus, we dissected the larvae by slightly changing the dissection time points (time points in which peaks and nadirs were observed were omitted):

We dissected larvae by shifting the lowest brp/glutamate receptor observed time point (ZT3 and ZT15) and also by switching shifting brp/glutamate receptor observed time points (ZT21 and ZT9) by only one-two hours and also included another time point in which we did not observe neither lowest nor highest brp/glutamate receptor levels in any of the previous experiments (ZT17.30).

On the other side, apart from the previous experiment we also changed the diet to see if diet will affect brp and glutamate receptor intensities at different times. Thus, we changed the food (normal food (Bloomington recipe) and special food) and run two dissections in parallel using the aforementioned time points (Detailed experimental conditions are stated in Table 4.2)

No significant change between neither mean nor integrated brp levels were observed in normal food treated and special food treated group (Figure 4.19 a, b)).

On top of it, as it was the case in previous experiments, AZ number also did not change significantly at different time points in normal food and special food treated groups (Figure 4.17 c). Although brp levels were not significantly different from each other; lowest total brp levels were observed at ZT3 and ZT15 (Figure 4.19 b), two time points close to nadirs that were observed in previous experiments. Highest mean brp level was observed at ZT9 in normal food treated group (close to peak point that was observed in previous experiment) (Figure 4.15 c&d).

We observed a more obvious oscillatory behavior when diet was changed to special food, though again mean and integrated intensities were not significantly different between different time points.

In short, the oscillatory pattern was similar to the previous dissections in which brp and glutamate receptor levels changed drastically (Figure 4.15). However, no significant change in brp levels were observed.

Table 4.2. Experimental Conditions for normal food and special food vials.

	Normal Food	Special Food
Flies	25°C incubator	25°C incubator
Larvae	25°C incubator Same number of female and male flies were raised at different vials.	25°C incubator Same number of female and male flies were raised at different vials.
Food	Bloomington Recipe	Special Food
Environment	12h light-dark cycle	12h light-dark cycle
Humidity	65% Humidity	65% Humidity
Circulating air	50%	50%
Light amount	50%	50%
Incubator Condition	No one used the incubator. No outside sound	No one used the incubator. No outside sound

On the other side, we observed tremendous change in brp/glutamate receptor spot morphology and intensity when we changed the diet. Mean and integrated BRP intensities were always higher in normal food fed larvae (Figure 4.19) and binning the results obtained from all time points resulted in a significant increase in mean brp intensity compared to normal food fed larvae (Figure 4.19).

On the other hand, AZ area was always smaller and AZs were rounder (lower eccentricity) in special food reared larvae (Figure 4.19).

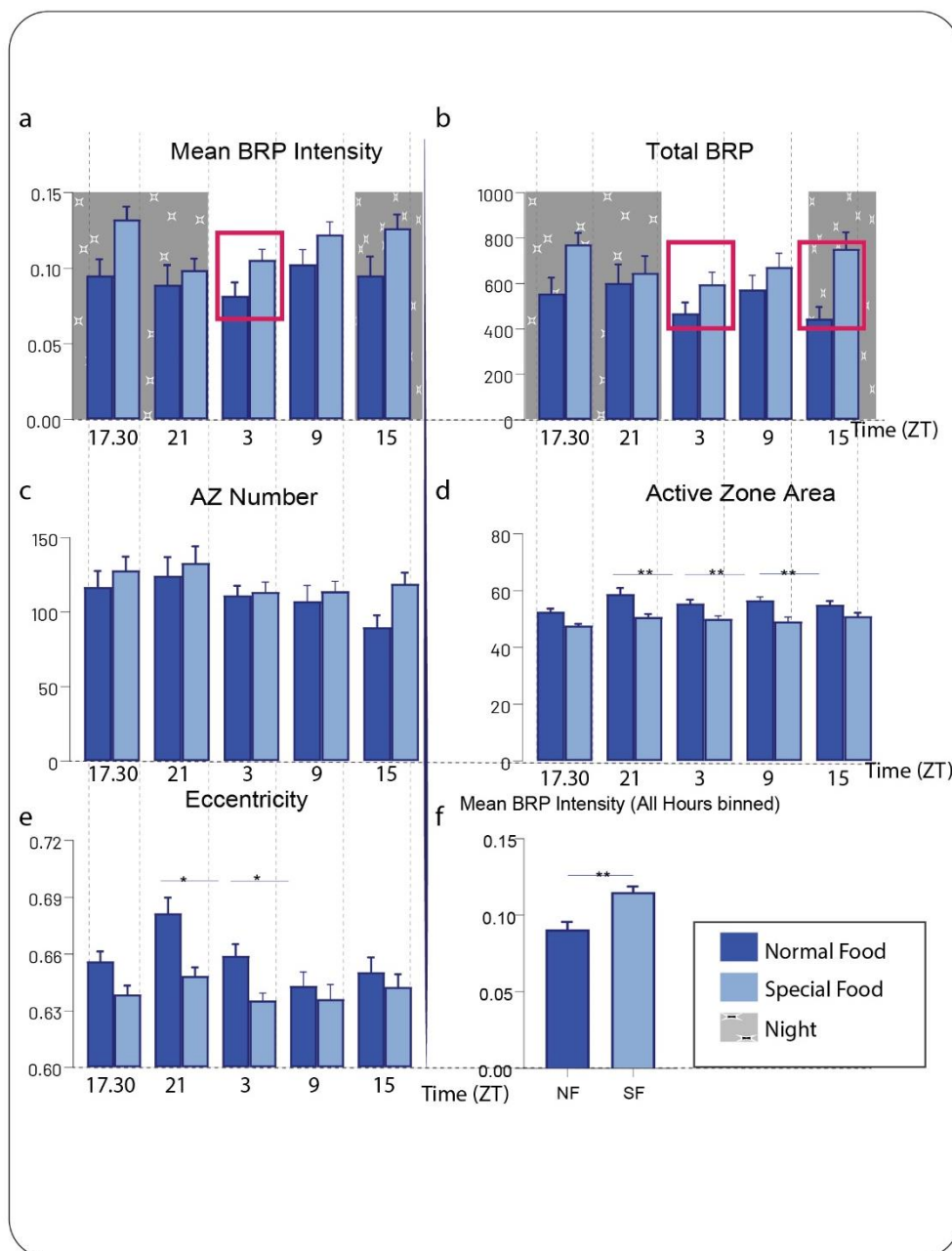


Figure 4.19. Changing diet has an impact on AZ shape and intensity. Mean (a) and integrated BRP (b) intensities are higher in special food reared larvae. AZ number is higher (c), whereas AZ area is lower (d) in special food fed group. AZs appear more round in special fed group (e).

Afterwards, we binned all time points: AZ number and glutamate receptor spot number were close to each other in normal food and special food treated group. Though, spot area, bbox area, perimeter, and compactness lowered drastically in special food fed larvae. Lastly brp and glutamate receptor spots appeared rounder

and mean and integrated intensity of brp/glutamate receptor increased in special food fed group (Figure 4.20)

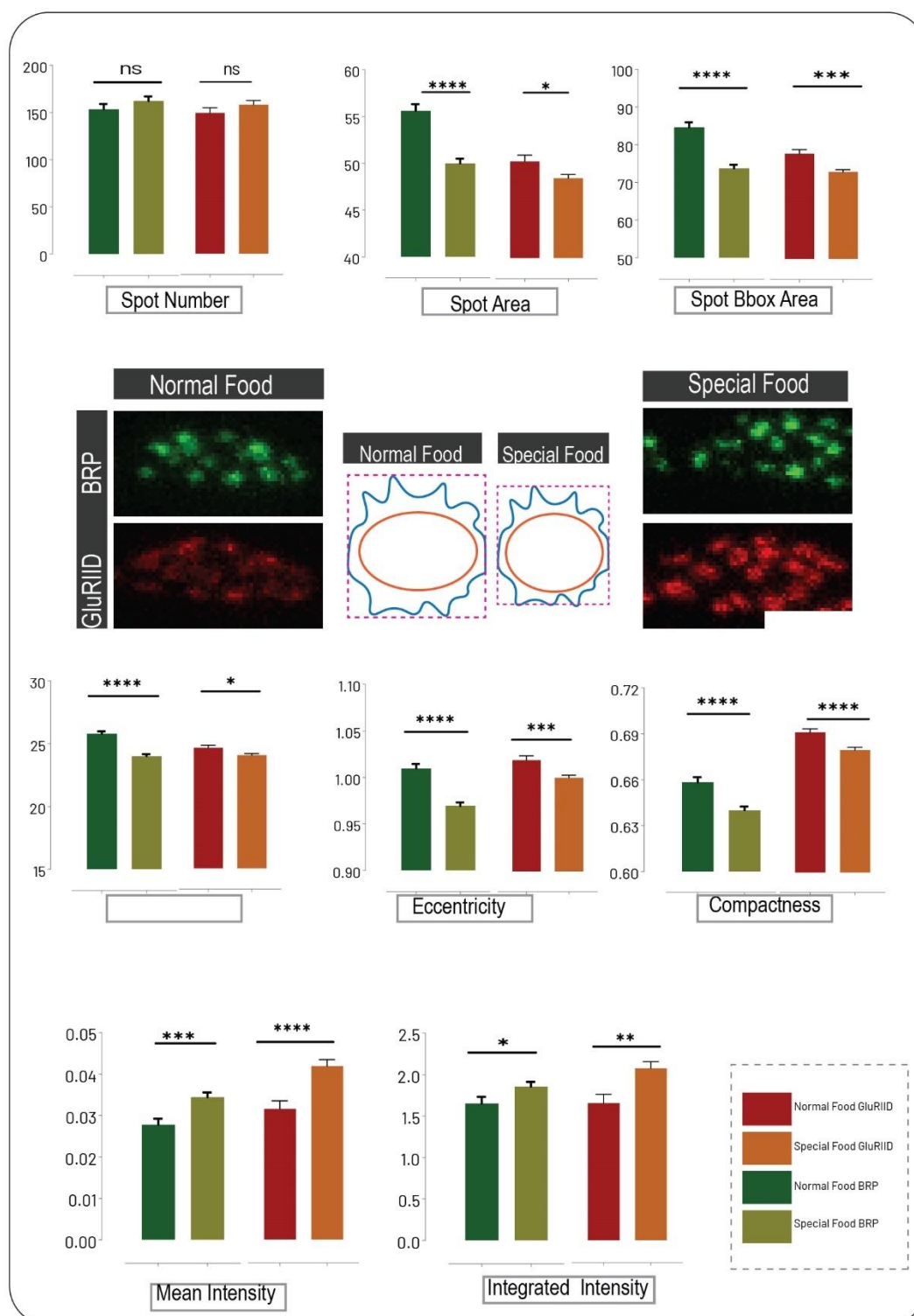


Figure 4.20. Tremendous changes in both spot shape of brp/glutamate receptor and intensity changes in brp/glutamate receptor were observed. BRP and glutamate

receptor spot number did not change between normal food and special food treated group (a). Spot morphologies: Area (b), bbox area (c), perimeter (d), compactness (e), and eccentricity (f) were lower in special food fed larvae, whereas mean (g) and integrated (h) brp and glutamate receptor spot intensities were higher compared to normal food fed larvae. (scale bar 2,5 μ m)

4.8. Dissecting Larvae by Taking Sequential Time Points Results in Gradual Change in BRP and Glutamate Receptor Levels

Until now we always performed analysis by taking separate time points. Then we wondered what would happen if we spanned sequential time points. We started dissecting the animals at 17:40 and finished at 22:20 (20:00 is the time point in which lights turn off). When performing dissections we binned time points and dissected approximately 6 larvae for each time point (Figure 4.21), we did not take larvae one by one (Previous experience showed that intruding with animal behavior and environment factors causes a change in brp/glutamate receptor levels (Data not shown). Thus we tried to behave as gentle as possible). When dissection of 6 larvae finished we took another set of larvae and dissected them. As a result, mean and integrated intensity increased gradually during this time period. On the other hand, spot number, spot perimeter, and spot area did not change significantly. Interestingly brp and glutamate receptor spot shape changed significantly and became rounder when intensity increased (Figure 4.21).

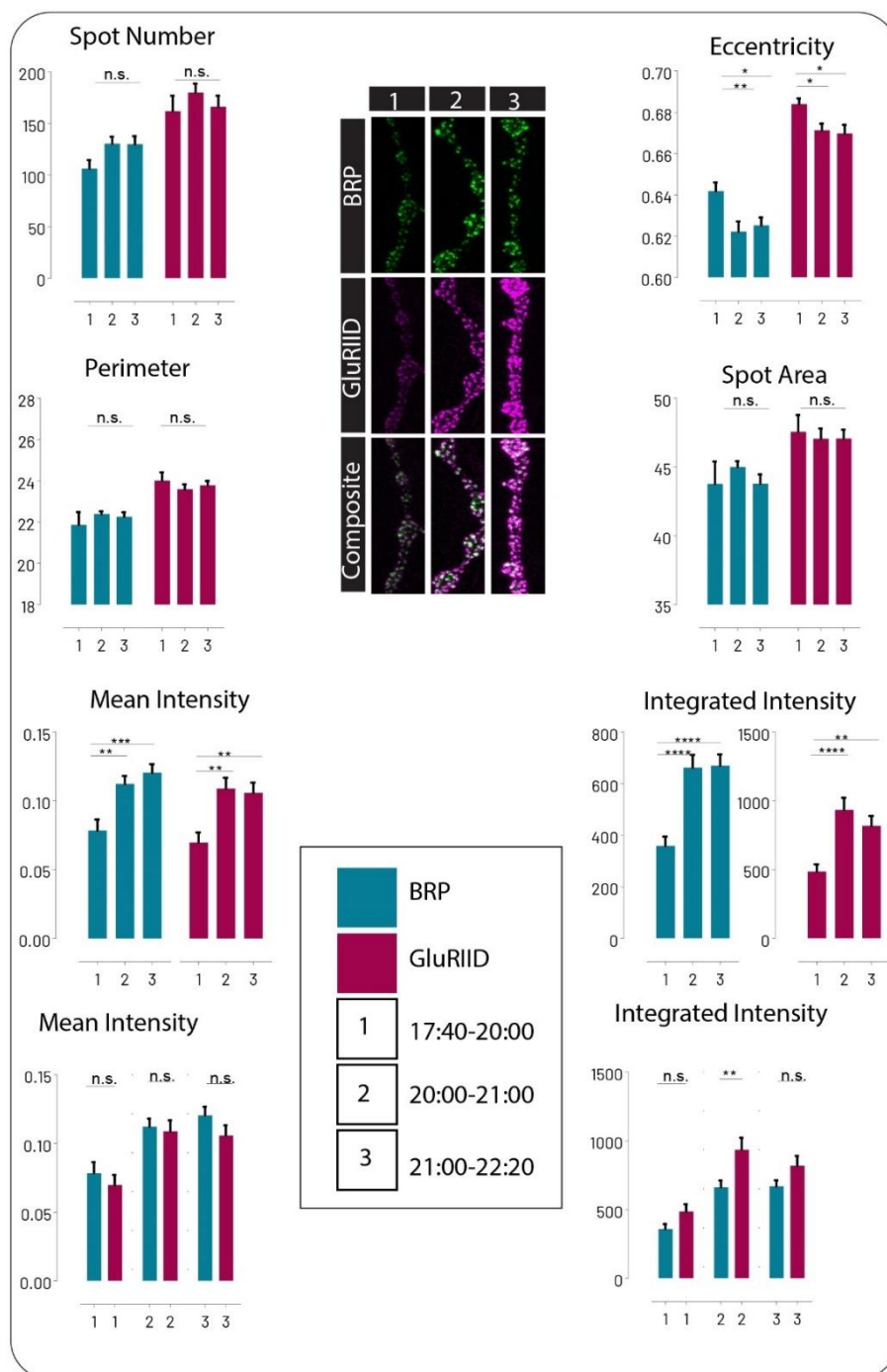


Figure 4.21. Dissecting larvae by taking consecutive times results in gradual brp and glutamate receptor intensity increase and a change in brp and glutamate receptor morphologies. Mean and integrated BRP and glutamate receptor spot intensities increased gradually by time. No change in brp and glutamate receptor spot number was observed during this time period. Spot morphologies -area and perimeter- did not change whereas spots become rounder when brp and glutamate receptor intensities increased.

4.9. Motoneuronally Silencing *na* Produces Phase Shift in BRP/Glutamate Receptor Levels

In the end, we turned to the very beginning and asked if we could see a difference when we dissected *nalcn* components with the same approach, namely dissecting larvae by taking sequential time points. We started dissection at 21.44 and finished at 1.33. The starting time point were specifically chosen to include time point that was used in previous experiment (Figure 4.19) to see if we could observe close mean *brp*/glutamate receptor values at this time point on another day with totally different larvae.

On the other side, of note, this dissection was performed at night and we took utmost precautions to not intrude with larval sleep/locomotor behavior:

1. We used dimmer outside light especially during opening the incubator
2. Took a set of larvae at the same time to lower the intrusion of especially remaining larvae.
3. No-one used the incubator during these days.
4. No sound was made in the environment.

In short:

In driver control *brp* and glutamate receptor spot intensities decreased gradually by time, whereas silencing *NALCN* in motor neurons resulted in an increase in *brp* and glutamate receptor levels (Figure 4.20 c).

Mean *brp* and glutamate receptor intensity at time point 1 (Figure 4.20 c) was very close to the mean values obtained from another experiment that was performed previously spanning approximately the same time (Figure 4.19, time point 3).

If each time point was treated as a separate dissection we lost gradual decrease increase information (Figure 4.20 d), binning all of intensities also resulted in a non-significant change among groups (Figure 4.20 e) explaining the discrepancies observed in previous experiments.

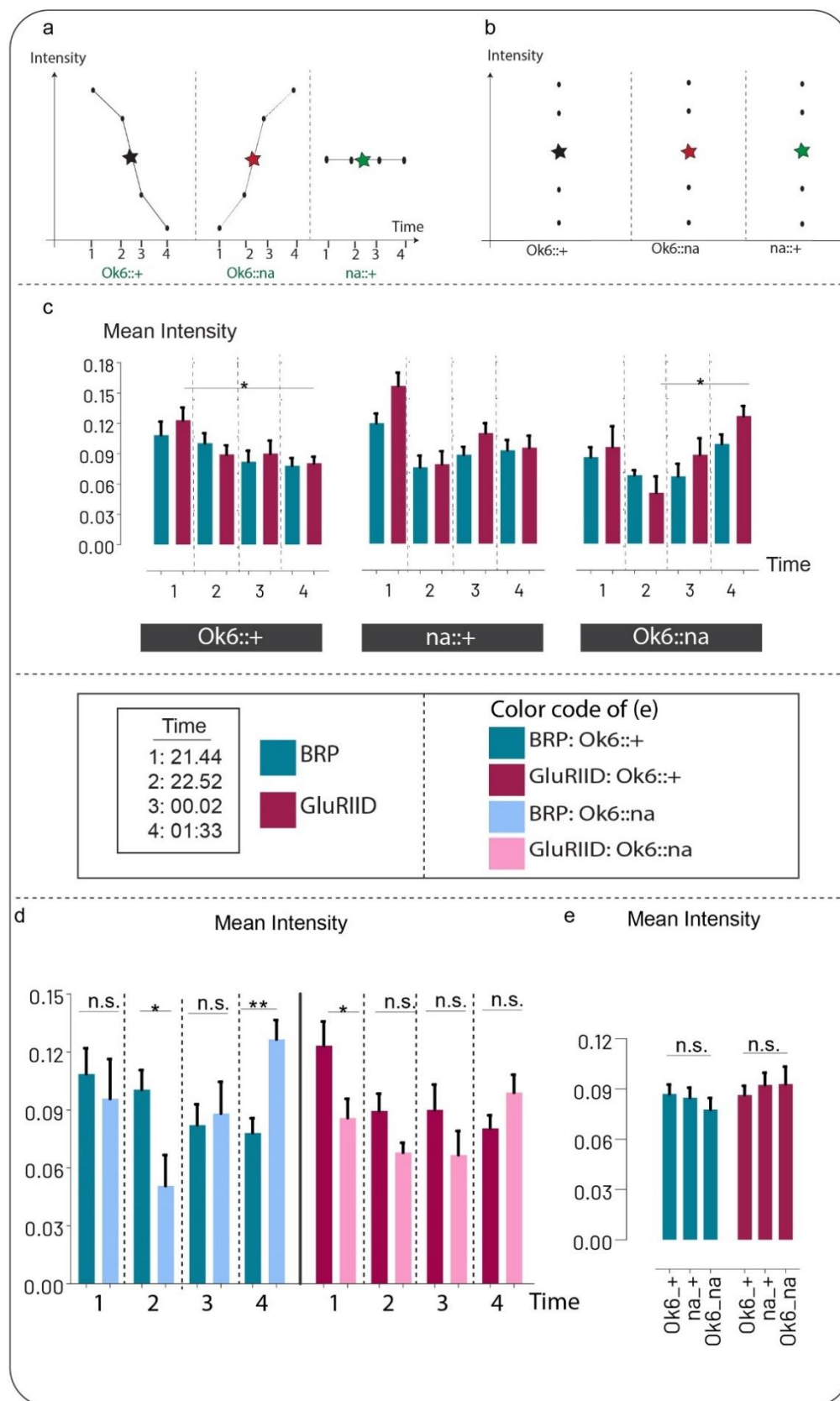


Figure 4.22. BRP/Glutamate Receptor Intensities that are dissected in a time-dependent fashion.

5. DISCUSSION

5.1. Silencing NALCN Channel Components Produced Discrepant Results

This study is the first time in which NALCN channel components and frj were motoneuronally and pan-neuronally silenced and the effects were analyzed at AZ level with the aid of immunofluorescent labeling and confocal microscopy.

BRP and glutamate receptor were used as pre and post-synaptic markers respectively: BRP, marks AZs and is widely used to determine the shape of AZs. It is a coiled-coil molecule that forms T-shaped meshwork, adopts an elongated shape, and is located vis-a-vis glutamate receptors in *Drosophila* NMJs. Staining brp C-terminal (Nc82) and glutamate receptor (GluRIID) provides information regarding the presynaptic morphology and its relation with postsynaptic glutamate receptor thus synaptic and postsynaptic morphology and function.

In this study, confocal scanning were performed from 1b glutamatergic NMJs that protrude the 4th muscle of abdominal segments in 3rd instar larvae. Afterwards, confocal stacks of the images from brp and glutamate receptor channels were segmented with a custom written pipeline and analysis of brp and glutamate receptor channels were performed separately.

UNC79 is the accessory subunit of *NALCN* channel that is comprised of two accessory and one pore forming unit. Until now, several infants harboring mutations in *NALCN* and *UNC80* were reported: Mutations in infants mostly are associated with sleep (100, 147, 148) and respiratory disturbances(101, 148-151), reversed sleep wake cycles(149), and altered anesthetic sensitivity.(149) Other prominent dysfunctions are movement disorders accompanying developmental delay and seizures with severe intellectual disability.(98, 147, 148) No mutations in *UNC79* were reported so far, yet our patient that harbors a probable pathogenic mutation on *UNC79* shows the same pathophysiological features of *NALCN* and *UNC80* mutant infants.

Previous studies of NALCN channel components on animal models, on the other hand, are associated with volatile anesthetic sensitivity (80, 152-159),

dreamless mutants (86), circadian (30, 87, 90, 160-162) and locomotor activity alterations in *Drosophila* (7, 157, 162) and *C. elegans*.(163)

NALCN channel subunits are expressed in the whole brain of *Drosophila*, and as the aforementioned information indicates, anesthetic sensitivity, locomotor activity alterations, circadian rhythm disturbances phenocopy pathogenicity of NALCN and UNC80 mutant infants, hence *Drosophila* is an attractive candidate for studying the effects of knockdown of the respective genes on synapse function: Moto-neuronally silencing the pore region ortholog, *na*, resulted in an increase in both *brp* and glutamate receptor levels, however, redoing the dissection ended up with a totally different outcome, namely a decrease in both *brp* and glutamate receptor levels compared to control groups. AZ area and roundness also changed compared to control groups, but due to the discrepancies in both intensity and shape no relationship could be drawn.

Performing the very same dissection on pan-neuronally silenced 3rd instar larvae also ended up with same discrepancies. What is more, Motoneuronal and pan-neuronal silencing of NALCN channel accessory subunits, *unc79* and *unc80*, resulted with the same outcome: Performing dissections several times at random times resulted in an increase, decrease and constant *brp* and glutamate receptor levels relative to control groups (CC and DC), so did the morphology of pre- and postsynaptic side. These results cannot be linked to solely RNAi lines that may exhibit leakage, since replicating the dissection with different RNAi lines did not change the results.

Previous studies on NALCN channel component *na* has revealed discrepancies on anesthetic sensitivity too: *Drosophila* mutants harboring hypomorphic *na* were both reported as resistant (157, 158, 164, 165) and hypersensitive (81, 159) to halothane. Anesthetics are well known targets that alter synaptic signaling and plasticity.(166, 167) Our study and previous studies on anesthetic sensitivity shows that the results cannot be explained with hit-or-miss or RNAi line used, but most probably has a common reason behind. Not to mention, anesthetics function through

synapses and thus synapse function and anesthetic sensitivity is closely correlated.(167)

On top of this, previous research that looked to locomotor pattern and circadian rhythm upon silencing NALCN channel components reported that silencing *na* alters locomotor pattern and circadian rhythm.(7, 30, 87, 90, 157, 160-162) These results provide both a probable explanation for the results and insight for future experimental design: In our experimental design, dissections were performed at random times and a third dimension -time- was not considered when dissecting. Previous anesthetic sensitivity studies were also performed without considering time. Hence, the results might suggest that another dimension, time, has to be considered when performing dissections.

5.2. Not Pan-Neuronally but Motoneuronally Silencing MBOAT7 Ortholog *frj* Produced Discrepant Results

On the other side, MBOAT7 ortholog of *frj*, were silenced in parallel to NALCN channel components. MBOAT7 is known to preferentially add arachidonic acid to PIs thus is important in PI remodeling.(4) PIs have several important synaptic functions one of them being formation of open Syx via the help of arachidonic acid that is placed mostly to sn-2 positions of PIs in the brain, while open Syx facilitates SNARE formation and eventually vesicle fusion.(168)

frj is expressed in *Drosophila* brain yet *Drosophila* brain PIs lack arachidonic acid on their sn-2 position leaving its function in *Drosophila* a conundrum.(127)

Pan-neuronally silencing *frj* ended up with viable progeny and no intensity change in neither brp and nor glutamate receptor relative to control groups were observed. Next, we sought to understand if we could observe gender-dependent changes in brp and glutamate receptor levels, since female *Drosophila* possess high numbers of polyunsaturated phospholipids compared to male *Drosophila*.(169) Performing gender-dependent dissections in pan-neuronally silenced larvae also resulted in no alterations in both brp and glutamate receptor intensities. Though, we observed changes in synaptic morphologies no conclusion could be drawn with the

information in hand due to discrepancies in morphology data among different dissections.

Of note, we performed the work with only one RNAi line and hence at least one other RNAi line is needed to verify the result. The reason lying behind this is, even a small leakage in the respective gene product is mostly enough to circumvent the pathogenicity in metabolic disease related genes.

When the respective gene was silenced motoneuronally with two different RNAi lines, we again observed discrepant results compared to control groups. A drastic change in brp and glutamate receptor levels compared to control groups in one of the dissections were observed. This dissection, however, opposed to the previous dissections (NALCN and pan-neuronally silenced MBOAT7) were performed by dissecting each group sequentially, resulting in time difference between dissected groups. This change may be the result of the time difference, hence, brp and glutamate receptor levels in wild-type flies has to be measured first in a time-dependent fashion to draw an exact conclusion.

5.3. BRP Oscillates at *Drosophila* Neuromuscular Junctions

A possible explanation for discrepant results observed in the studies may be due to a time-dependent change in brp and glutamate receptor levels in control flies. Indeed a handful of papers state that brp levels change (170-173) in a time-dependent fashion in some of the tissues of *Drosophila*, but recently, opposed to the previous observations, one group stated that brp levels do not change in *Drosophila* brain.(174)

Oscillations observed in the previous studies are mostly regarded as tissue specific. And there is no consensus even in the papers claiming that brp oscillates in a daily basis: For some of them brp and synapse number is high at night (170) whereas for others it is high at day-time, and yet another group claims that brp changes with locomotor activity (111) whereas, for one other group - intensity change in brp is correlated with sleep need. (172) On top of all, most of the studies are performed in adult flies and few studies concerning *Drosophila* larvae are present.

Thus we first sought to understand if brp and glutamate receptor levels oscillate at 3rd instar larvae NMJs of wild-type (*w¹¹¹⁸*) flies by performing immunohistochemical staining in a time-dependent fashion.

Immunohistochemical staining of presynaptic and postsynaptic sides at random time points against brp and glutamate receptor showed that not only brp but also glutamate receptor levels fluctuate in 3rd instar 1b NMJs. At least two fold and up to 5 fold change in glutamate receptor levels and up to four fold change in brp levels were observed. Not to mention, spot area and shape was also changing at differing times, to the contrary brp and glutamate receptor spot numbers were constant in nearly all of the dissections performed so far (At least 200 separate experiments were taken into consideration), if not all.

Of note, the reason for observing significant change in AZ and glutamate receptor spot number in very few experiments (2-3) might be due to the segmentation step: All of the NMJs were scanned with the same settings to be able to compare the result with each other. Due to the immense intensity differences among AZ staining, intensities lying in the lower band were too dim to count and segment, giving a possible explanation for the spot number difference in the few experiments. In short, due to the immense number of studies in which number of AZs were close to each other, we can conclude that there are fix amount of AZs in NMJs. This study is in line with previous studies which indicate that AZ numbers are predefined.(175, 176)

Apart from that, dissecting larvae at different time points in both day-time and night showed that brp/glutamate receptor levels are not constant neither at night nor day. Thus timing of the dissections is the main determinant of the results. These result gives a plausible explanation why some groups were claiming that brp is high at night (170) and others not, namely, the discrepancies among whether brp is high at night or day in previous research is most probably not related to the tissue in which dissection is performed, but solely to the dissection times. For instance Ruiz et al, opposed to other studies, states that brp staining is higher at night. However, the group took two time points ZT19 and ZT7 as night and day respectively. Performing

the study with the same time points gave the same results in our studies. However taking another time point at night and day had the opposite outcome. Besides, of note, in previous research day/night and activity/sleep are, at some instances, used interchangeably, but *Drosophila* are crepuscular, meaning that they are not sleeping whole night (are active before lights-on phase and are also active after lights-off phase) and show a siesta phase in the middle of the day when the lights are on. In most of the previous studies this information was not taken into account -especially in the timing of immunohistochemical staining- and findings were discussed by excluding this information. Indeed, in the aforementioned study, daytime (ZT7) is close to the middle of the day in which flies may undergo a siesta phase and time point taken as night (ZT19) on the other hand is after midnight in which an increase in brp and glutamate receptor levels were observed is close to the dawn perception that is observed as acute locomotor activity increase in *Drosophila*.

Afterwards, we proceeded by comparing brp/glutamate receptor intensities of 3rd instar larvae in a time-dependent manner. We observed that BRP and glutamate receptor intensities are close to each other in a time dependent fashion, excluding times that are close to acute locomotor activity (before lights-on lights-off) and acute locomotor inactivity (siesta phase in the middle of the day):

Performing the experiment by dissecting larvae at random time points in two consecutive days produced nearly the same mean intensities in a time dependent fashion. On the other side, performing the very same experiment, with two different vials of w¹¹¹⁸ flies that were reared under same environmental conditions but with different flies, produced very close mean brp and glutamate receptor intensities in a time-dependent fashion, indicating that the timing of the events is regulated by circadian rhythm. Hence the results clearly show that timing is one of the main determinants of brp/glutamate receptor intensities.

Highest brp and glutamate receptor intensities were observed close to light on-off phase, and the lowest brp intensity was observed in the middle of the day or close to midnight. Looking from AZ level, all of the AZ intensities and AZ areas in NMJs were gradually distributed yet, despite the lognormal distribution, the highest mean

intensities observed in different dissections were mostly very close to each other, indicating that it is a result of most probably a well-defined time-dependent distribution of active zone intensities. In short, time is one of the most important determinants for brp/glutamate receptor intensities.

However, we must add-up that at some instances, we could not observe the peaks at the specified times when the experiment was performed at another day: It is well documented that locomotor activity changes are acute and the observed results may be related to slight shifts in onset time of acute locomotor activity. Since these dissections were performed at specified times without spanning a time period, missing the peak time points is probable with our experimental design.

Yet another issue, in very few dissections we did not observe oscillations in brp and glutamate receptor levels (data not shown) which is also reported in one study.⁽¹⁷⁴⁾ We hypothesized that the underlying reason for non-significant increase might be the timing of the dissections or environmental factors. Hence, to test the first phenomenon we dissected the larvae by shifting the dissection time for only one-two hours, in other words, shifting the time points in which we observed significant change in brp and glutamate receptor levels in previous dissections. Interestingly, now we did not observe any significant change in brp levels. However we saw the same oscillatory pattern with a lower amplitude, giving explanation for the non-significant levels of brp and glutamate receptor levels that was observed by our group and one other group.

We also postulated that another reasoning for not seeing significant changes in brp and glutamate receptor levels at different times could be due to environmental factors that may change the amplitude and/or variance of brp/glutamate receptor intensities:

To test this hypothesis, we used food as an environmental factor. Flies that were reared in special food, showed an increase in both mean and integrated brp and glutamate receptor intensities, namely an amplitude change in brp and glutamate receptor levels compared to flies that were reared in semi-defined Bloomington recipe indicating that amplitude of brp levels is internally and externally regulated.

Brp and glutamate receptor spot areas were smaller in special food reared *w¹¹¹⁸* group, and the spots were more round compared to control group at all time points indicating that morphology of active zones are drastically effected by diet.

Temperature was another factor that draw our attention, larvae raised at 29°C showed 5 fold and 7 fold increase in brp and glutamate receptor levels respectively, which is much higher compared to the increase observed at 25°C, yet, of note, the humidity was not the same in all of the incubators, hence a more controlled dissection is needed to unquestioningly drive such a conclusion.

Until this time, all dissections were performed by taking separate time-points. We thus tried to understand how brp and glutamate receptor levels change when larvae were dissected by taking sequential time points: In *w¹¹¹⁸* 3rd instar larvae we saw a gradual increase in brp and glutamate receptor levels when a period close to lights-off phase were spanned (approximately between ZT10-ZT14.30 -lights-off phase starts at ZT12). This notion is in parallel with the locomotor peak time observed in *w¹¹¹⁸* flies close to lights-off phase. (90)

With all of these information in hand, we turned to the very beginning and dissected motoneuronally silenced *na* larvae in a time-dependent fashion by taking sequential time points. We observed a phase shift in brp and glutamate receptor levels compared to control group, namely while brp and glutamate receptor levels decreased in driver control (*Ok6::+*) in a time-dependent fashion as midnight approached (between ZT14(22.00)-ZT17.30(01.30)), the opposite was true for motoneuronally silenced *na* larvae. These alterations closely fit circadian and locomotor alterations that are observed when silencing NALCN channel components in *Drosophila*.(7, 90, 162)

NALCN is one of the core sleep regulating genes.(86) Furthermore, recent studies showed that brp and locomotor activity/locomotor inactivity(sleep) are closely correlated in *Drosophila*.(172) Hence, reversed sleep wake cycles, and sleep disturbances observed in some of the infants fits brp and glutamate receptor level alterations. However, we cannot conclude that brp/glutamate receptor level changes are the sole reason for sleep disturbances, because synaptic protein levels are

interconnected with each other, and synaptic protein circuitry defines the overall result. Thus it seems more probable that the relative levels of synaptic proteins at the specified times may define locomotor pattern. Hence, before drawing a clear conclusion, proteins that alter by time should be identified meticulously to eliminate possible confounding results.

Our study does not give real-time information regarding how locomotor data changes in larvae upon brp and glutamate receptor intensity change. The reason behind this is, we could not find an optimum method in which we can collect data without intruding with larvae locomotor activity due to:

1. Any small intrusion in even fly vial (i.e. due to collecting larvae at one time point) and changing the environmental conditions resulted in brp level alterations (recording larvae movement and dissecting them at the same time resulted in totally different brp intensities (data not shown)) and thus a possible locomotor change in larvae.
2. Locomotor patterns could only be recorded in RT (to reduce the opening and closing rate of incubator) in water (for easing analyzing), hence environment and lighting also changed during video shooting.

6. CONCLUSION

Synaptopathies take up a lot of room in rare metabolic diseases, yet we mostly do not know if the mutation harboring gene has an effect on synapse morphology and synaptic function which hinders reasoning the pathophysiology.

NALCN channel is formed by three domains: NALCN the pore region, unc79 and unc80 accessory subunits; the channel is known to interact with Mid-1 that is known to form a bridge between circadian rhythm and NALCN channel. Mutations in channel components NALCN and UNC80 are associated with alterations in circadian rhythm, locomotor behavior, anesthetic sensitivity in both humans and model organisms. The aforementioned pathophysiologies are closely linked to synapse function, however, to our knowledge there is no study concerning how downregulation of channel components alters synaptic function.

On the other side, MBOAT7 an enzyme that lies in Lands lipid remodeling pathway is known to prudentially add AA to PIs. Most brain PIs in mammals are enriched in AA, and PIs and AAs are known regulators of synapse function.

In this study, with the means of *Drosophila* model organism and Gal4-UAS system we downregulated the aforementioned genes in a tissue specific manner in *Drosophila* motoneurons and the whole CNS. Brp was used to mark AZs and glutamate receptor was used as a postsynaptic marker.

Downregulating NALCN channel components in motoneurons and the whole CNS resulted in discrepant brp and glutamate receptor levels compared to control groups. On the other side, downregulating another synaptopathy related gene, frj, pan-neuronally had no effect on brp and glutamate receptor levels, however motoneuronal silencing, resulted in discrepancies compared to control groups.

Dissecting 3rd instar larvae in a time-dependent fashion showed that brp and glutamate receptor levels are not constant in neuromuscular junctions of *Drosophila* and show rhythmic intensity changes. The rhythm matches locomotor activity pattern of *Drosophila* that is mentioned in literature.

Changing the environmental factors also had an impact on brp and glutamate receptor morphologies and intensities showing that synapses are extremely dynamic structures and oscillations are regulated via circadian and environmental factors.

Lastly motoneuronally downregulating na and dissecting 3rd instar larvae in a time-dependent manner resulted in a phase shift in the oscillation pattern of brp and glutamate receptor explaining the discrepancies observed in the previous works.

With this work for the first time:

- NALCN channel components and MBOAT7 orthologs were silenced in *Drosophila* in a tissue dependent manner and brp and glutamate receptor levels and morphologies were measured.
- BRP and glutamate receptor levels were shown to oscillate in a time dependent fashion in *Drosophila* NMJs.
- Environmental factors i.e. food, temperature add up to the oscillatory behavior of brp and glutamate receptor intensities and diet has a big impact on synapse morphology.
- The discrepancies in brp and glutamate receptor levels is a result of phase shift of brp and glutamate receptor oscillations.

Lastly motoneuronally downregulating na in a time dependent manner resulted in a phase shift in the oscillation pattern of brp and glutamate receptor explaining the discrepancies observed in the previous works.

7. REFERENCES

1. Fernandes J, Saudubray J-M, Van den Berghe G, Walter JH. Inborn metabolic diseases: diagnosis and treatment: Springer Science & Business Media; 2006.
2. Saudubray J-M, Garcia-Cazorla A. An overview of inborn errors of metabolism affecting the brain: from neurodevelopment to neurodegenerative disorders. *Dialogues in clinical neuroscience*. 2022.
3. Akizu N, Cantagrel V, Zaki MS, Al-Gazali L, Wang X, Rosti RO, et al. Biallelic mutations in SNX14 cause a syndromic form of cerebellar atrophy and lysosome-autophagosome dysfunction. *Nature genetics*. 2015;47(5):528-34.
4. Dursun A, Yalnızođlu D, Özgöl RK, Karlı Ođuz K, Yücel-Yılmaz D. Clinical highlights of a very rare phospholipid remodeling disease due to MBOAT7 gene defect. *American Journal of Medical Genetics Part B: Neuropsychiatric Genetics*. 2020;183(1):3-4.
5. Yücel-Yılmaz D, Yücesan E, Yalnızođlu D, Ođuz KK, Sađırođlu MŞ, Özbek U, et al. Clinical phenotype of hereditary spastic paraplegia due to KIF1C gene mutations across life span. *Brain and Development*. 2018;40(6):458-64.
6. Chua HC, Kschonsak M, Weidling C, Chakouri N, Noland CL, Schott K, et al. Structure and function of the human NALCN-UNC79-UNC80-FAM155A-CaM complex. *Biophysical Journal*. 2022;121(3):96a.
7. Nash HA, Scott RL, Lear BC, Allada R. An unusual cation channel mediates photic control of locomotion in *Drosophila*. *Current biology*. 2002;12(24):2152-8.
8. Ghezzi A, Liebeskind BJ, Thompson A, Atkinson NS, Zakon HH. Ancient association between cation leak channels and Mid1 proteins is conserved in fungi and animals. *Frontiers in molecular neuroscience*. 2014;7:15.
9. Blunsom NJ, and Shamshad Cockcroft. Phosphatidylinositol synthesis at the endoplasmic reticulum. *Biochimica Et Biophysica Acta (BBA)-Molecular and Cell Biology of Lipids* 2020;1865(158471).
10. Stein S, Bogard E, Boice N, Fernandez V, Field T, Gilstrap A, et al. Principles for interactions with biopharmaceutical companies: the development of guidelines for patient advocacy organizations in the field of rare diseases. *Orphanet Journal of Rare Diseases*. 2018;13(1):1-10.
11. Bellettato CM, Hubert L, Scarpa M, Wangler MF. Inborn errors of metabolism involving complex molecules: lysosomal and peroxisomal storage diseases. *Pediatric Clinics*. 2018;65(2):353-73.
12. Walter AM, Groffen AJ, Sørensen JB, Verhage M. Multiple Ca²⁺ sensors in secretion: teammates, competitors or autocrats? *Trends in neurosciences*. 2011;34(9):487-97.
13. Ullrich A, Böhme MA, Schöneberg J, Depner H, Sigrist SJ, Noé F. Dynamical organization of syntaxin-1A at the presynaptic active zone. *PLoS computational biology*. 2015;11(9):e1004407.

14. Bellen RGZaHJ. The Architecture of the Active Zone in the Presynaptic Nerve Terminal. *Physiology*. 2004:262–70.
15. Qin G, Schwarz T, Kittel RJ, Schmid A, Rasse TM, Kappei D, et al. Four different subunits are essential for expressing the synaptic glutamate receptor at neuromuscular junctions of *Drosophila*. *Journal of neuroscience*. 2005;25(12):3209-18.
16. Südhof TC. Calcium control of neurotransmitter release. *Cold Spring Harbor perspectives in biology*. 2012;4(1):a011353.
17. Menon KP, Carrillo RA, Zinn K. Development and plasticity of the *Drosophila* larval neuromuscular junction. *Wiley Interdisciplinary Reviews: Developmental Biology*. 2013;2(5):647-70.
18. Johansen J, Halpern ME, Johansen KM, Keshishian H. Stereotypic morphology of glutamatergic synapses on identified muscle cells of *Drosophila* larvae. *Journal of Neuroscience*. 1989;9(2):710-25.
19. Landgraf M, Thor S, editors. *Development of Drosophila motoneurons: specification and morphology*. *Seminars in cell & developmental biology*; 2006: Elsevier.
20. Beckett K, Baylies MK. The development of the *Drosophila* larval body wall muscles. *International review of neurobiology*. 2006;75:55-70.
21. Sink H. *Muscle development in drosophila*: Springer; 2006.
22. Slater C. *Neuromuscular junction (NMJ): mammalian development*. 2009.
23. Gowda S, Salim S, Mohammad F. Anatomy and neural pathways modulating distinct locomotor behaviors in *Drosophila* larva. *Biology*. 2021;10(2):90.
24. Fox LE, Soll DR, Wu C-F. Coordination and modulation of locomotion pattern generators in *Drosophila* larvae: effects of altered biogenic amine levels by the tyramine β hydroxylase mutation. *Journal of Neuroscience*. 2006;26(5):1486-98.
25. Jha SK, Jha VM. *Sleep, Memory and Synaptic Plasticity*: Springer; 2019.
26. Vanin S, Bhutani S, Montelli S, Menegazzi P, Green EW, Pegoraro M, et al. Unexpected features of *Drosophila* circadian behavioural rhythms under natural conditions. *Nature*. 2012;484(7394):371-5.
27. Menegazzi P, Beer K, Grebler V, Schlichting M, Schubert FK, Helfrich-Förster C. A functional clock within the main morning and evening neurons of *D. melanogaster* is not sufficient for wild-type locomotor activity under changing day length. *Frontiers in Physiology*. 2020;11:229.
28. Grima B, Chélot E, Xia R, Rouyer F. Morning and evening peaks of activity rely on different clock neurons of the *Drosophila* brain. *Nature*. 2004;431(7010):869-73.
29. Yoshii T, Funada Y, Ibuki-Ishibashi T, Matsumoto A, Tanimura T, Tomioka K. *Drosophila* cryb mutation reveals two circadian clocks that drive locomotor rhythm

and have different responsiveness to light. *Journal of insect physiology*. 2004;50(6):479-88.

30. Zhang L, Chung BY, Lear BC, Kilman VL, Liu Y, Mahesh G, et al. DN1p circadian neurons coordinate acute light and PDF inputs to produce robust daily behavior in *Drosophila*. *Current Biology*. 2010;20(7):591-9.

31. Picot M, Cusumano P, Klarsfeld A, Ueda R, Rouyer F. Light activates output from evening neurons and inhibits output from morning neurons in the *Drosophila* circadian clock. *PLoS biology*. 2007;5(11):e315.

32. Zhang Y, Liu Y, Bilodeau-Wentworth D, Hardin PE, Emery P. Light and temperature control the contribution of specific DN1 neurons to *Drosophila* circadian behavior. *Current Biology*. 2010;20(7):600-5.

33. Artiushin G, Sehgal A. The *Drosophila* circuitry of sleep–wake regulation. *Current opinion in neurobiology*. 2017;44:243-50.

34. Huber R, Hill SL, Holladay C, Biesiadecki M, Tononi G, Cirelli C. Sleep homeostasis in *Drosophila melanogaster*. *Sleep*. 2004;27(4):628-39.

35. Hendricks JC, Finn SM, Panckeri KA, Chavkin J, Williams JA, Sehgal A, et al. Rest in *Drosophila* is a sleep-like state. *Neuron*. 2000;25(1):129-38.

36. Malpel S, Klarsfeld A, Rouyer F. Larval optic nerve and adult extra-retinal photoreceptors sequentially associate with clock neurons during *Drosophila* brain development. 2002.

37. Nitabach MN, Blau J, Holmes TC. Electrical silencing of *Drosophila* pacemaker neurons stops the free-running circadian clock. *Cell*. 2002;109(4):485-95.

38. Blau J, Young MW. Cycling *vrille* expression is required for a functional *Drosophila* clock. *Cell*. 1999;99(6):661-71.

39. Mazzoni EO, Desplan C, Blau J. Circadian pacemaker neurons transmit and modulate visual information to control a rapid behavioral response. *Neuron*. 2005;45(2):293-300.

40. Sprecher SG, Desplan C. Switch of rhodopsin expression in terminally differentiated *Drosophila* sensory neurons. *Nature*. 2008;454(7203):533-7.

41. Kilo L, Stürner T, Tavosanis G, Ziegler AB. *Drosophila* Dendritic Arborisation Neurons: Fantastic Actin Dynamics and Where to Find Them. *Cells*. 2021;10(10):2777.

42. Grueber WB, Jan LY, Jan YN. Tiling of the *Drosophila* epidermis by multidendritic sensory neurons. 2002.

43. Terada S-I, Matsubara D, Onodera K, Matsuzaki M, Uemura T, Usui T. Neuronal processing of noxious thermal stimuli mediated by dendritic Ca²⁺ influx in *Drosophila* somatosensory neurons. *Elife*. 2016;5:e12959.

44. Xiang Y, Yuan Q, Vogt N, Looger LL, Jan LY, Jan YN. Light-avoidance-mediating photoreceptors tile the *Drosophila* larval body wall. *Nature*. 2010;468(7326):921-6.

45. Fioravante D, Regehr WG. Short-term forms of presynaptic plasticity. *Current opinion in neurobiology*. 2011;21(2):269-74.
46. Ho VM, Lee J-A, Martin KC. The cell biology of synaptic plasticity. *Science*. 2011;334(6056):623-8.
47. Kennedy MB. Synaptic signaling in learning and memory. *Cold Spring Harbor perspectives in biology*. 2016;8(2):a016824.
48. Abbott LF, Nelson SB. Synaptic plasticity: taming the beast. *Nature neuroscience*. 2000;3(11):1178-83.
49. Malenka RC, Siegelbaum SA. Synaptic plasticity. *Synapses*. 2001:393-453.
50. Zucker RS, Regehr WG. Short-term synaptic plasticity. *Annual review of physiology*. 2002;64(1):355-405.
51. Cajigas IJ, Will T, Schuman EM. Protein homeostasis and synaptic plasticity. *The EMBO journal*. 2010;29(16):2746-52.
52. Pfeiffer BE, Huber KM. Current advances in local protein synthesis and synaptic plasticity. *Journal of Neuroscience*. 2006;26(27):7147-50.
53. Sutton MA, Schuman EM. Dendritic protein synthesis, synaptic plasticity, and memory. *Cell*. 2006;127(1):49-58.
54. Fouquet W, Oswald D, Wichmann C, Mertel S, Depner H, Dyba M, et al. Maturation of active zone assembly by *Drosophila* Bruchpilot. *Journal of Cell Biology*. 2009;186(1):129-45.
55. Marrone DF, Petit TL. The role of synaptic morphology in neural plasticity: structural interactions underlying synaptic power. *Brain research reviews*. 2002;38(3):291-308.
56. Ehmann N, Van De Linde S, Alon A, Ljaschenko D, Keung XZ, Holm T, et al. Quantitative super-resolution imaging of Bruchpilot distinguishes active zone states. *Nature communications*. 2014;5(1):1-12.
57. Podufall J, Tian R, Knoche E, Puchkov D, Walter AM, Rosa S, et al. A presynaptic role for the cytomatrix protein GIT in synaptic vesicle recycling. *Cell reports*. 2014;7(5):1417-25.
58. Schoch S, Gundelfinger ED. Molecular organization of the presynaptic active zone. *Cell and tissue research*. 2006;326(2):379-91.
59. Südhof TC. The presynaptic active zone. *Neuron*. 2012;75(1):11-25.
60. Rein K, Zöckler M, Heisenberg M. A quantitative three-dimensional model of the *Drosophila* optic lobes. *Current Biology*. 1999;9(2):93-S2.
61. Hallermann S, Kittel RJ, Wichmann C, Weyhersmüller A, Fouquet W, Mertel S, et al. Naked dense bodies provoke depression. *Journal of Neuroscience*. 2010;30(43):14340-5.

62. Kittel RJ, Wichmann C, Rasse TM, Fouquet W, Schmidt M, Schmid A, et al. Bruchpilot promotes active zone assembly, Ca²⁺ channel clustering, and vesicle release. *Science*. 2006;312(5776):1051-4.
63. Böhme MA, Beis C, Reddy-Alla S, Reynolds E, Mampell MM, Grasskamp AT, et al. Active zone scaffolds differentially accumulate Unc13 isoforms to tune Ca²⁺ channel-vesicle coupling. *Nature neuroscience*. 2016;19(10):1311-20.
64. Acuna C, Liu X, Südhof TC. How to make an active zone: unexpected universal functional redundancy between RIMs and RIM-BPs. *Neuron*. 2016;91(4):792-807.
65. Liu-Yesucevitz L, Bassell GJ, Gitler AD, Hart AC, Klann E, Richter JD, et al. Local RNA translation at the synapse and in disease. *Journal of Neuroscience*. 2011;31(45):16086-93.
66. Südhof TC. A molecular machine for neurotransmitter release: synaptotagmin and beyond. *Nature medicine*. 2013;19(10):1227-31.
67. Richmond JE, Davis WS, Jorgensen EM. UNC-13 is required for synaptic vesicle fusion in *C. elegans*. *Nature neuroscience*. 1999;2(11):959-64.
68. Holbrook S, Finley JK, Lyons EL, Herman TG. Loss of *syd-1* from R7 neurons disrupts two distinct phases of presynaptic development. *Journal of Neuroscience*. 2012;32(50):18101-11.
69. Oswald D, Khorramshahi O, Gupta VK, Banovic D, Depner H, Fouquet W, et al. Cooperation of *Syd-1* with Neurexin synchronizes pre- with postsynaptic assembly. *Nature neuroscience*. 2012;15(9):1219-26.
70. Babaev O, Botta P, Meyer E, Müller C, Ehrenreich H, Brose N, et al. Neuroligin 2 deletion alters inhibitory synapse function and anxiety-associated neuronal activation in the amygdala. *Neuropharmacology*. 2016;100:56-65.
71. Chefdeville A. NMDAR Encephalitis, a model of synaptopathy: Université de Lyon; 2017.
72. D'Antoni S, Spatuzza M, Bonaccorso CM, Musumeci SA, Ciranna L, Nicoletti F, et al. Dysregulation of group-I metabotropic glutamate (mGlu) receptor mediated signalling in disorders associated with Intellectual Disability and Autism. *Neuroscience & Biobehavioral Reviews*. 2014;46:228-41.
73. Rosti RO, Sadek AA, Vaux KK, Gleeson JG. The genetic landscape of autism spectrum disorders. *Developmental Medicine & Child Neurology*. 2014;56(1):12-8.
74. Huguet G, Ey E, Bourgeron T. The genetic landscapes of autism spectrum disorders. *Annual review of genomics and human genetics*. 2013;14:191-213.
75. Shiang R, Ryan SG, Zhu Y-Z, Hahn AF, O'Connell P, Wasmuth JJ. Mutations in the $\alpha 1$ subunit of the inhibitory glycine receptor cause the dominant neurologic disorder, hyperekplexia. *Nature genetics*. 1993;5(4):351-8.
76. Zhan F-x, Wang S-G, Cao L. Advances in hyperekplexia and other startle syndromes. *Neurological Sciences*. 2021;42(10):4095-107.

77. Musi C. JNKS AS THERAPEUTIC TARGETS TO TACKLE SYNAPTIC DYSFUNCTION IN NEURODEVELOPMENTAL AND NEURODEGENERATIVE DISEASES. 2022.
78. Flourakis M, Kula-Eversole E, Hutchison AL, Han TH, Aranda K, Moose DL, et al. A conserved bicycle model for circadian clock control of membrane excitability. *Cell*. 2015;162(4):836-48.
79. Lu B, Su Y, Das S, Liu J, Xia J, Ren D. The neuronal channel NALCN contributes resting sodium permeability and is required for normal respiratory rhythm. *Cell*. 2007;129(2):371-83.
80. Cochet-Bissuel M, Lory P, Monteil A. The sodium leak channel, NALCN, in health and disease. *Frontiers in cellular neuroscience*. 2014;8:132.
81. Humphrey JA, Hamming KS, Thacker CM, Scott RL, Sedensky MM, Snutch TP, et al. A putative cation channel and its novel regulator: cross-species conservation of effects on general anesthesia. *Current Biology*. 2007;17(7):624-9.
82. Zhou L, Liu H, Zhao Q, Wu J, Yan Z. Architecture of the human NALCN channelosome. *Cell Discovery*. 2022;8(1):1-11.
83. Gilon P, Rorsman P. NALCN: a regulated leak channel. *EMBO reports*. 2009;10(9):963-4.
84. Liebeskind BJ, Hillis DM, Zakon HH. Phylogeny unites animal sodium leak channels with fungal calcium channels in an ancient, voltage-insensitive clade. *Molecular biology and evolution*. 2012;29(12):3613-6.
85. Chua HC, Wulf M, Weidling C, Rasmussen LP, Pless SA. The NALCN channel complex is voltage sensitive and directly modulated by extracellular calcium. *Science advances*. 2020;6(17):eaaz3154.
86. Funato H, Miyoshi C, Fujiyama T, Kanda T, Sato M, Wang Z, et al. Forward-genetics analysis of sleep in randomly mutagenized mice. *Nature*. 2016;539(7629):378-83.
87. Lu TZ, Feng Z-P. NALCN: a regulator of pacemaker activity. *Molecular neurobiology*. 2012;45(3):415-23.
88. Kschonsak M, Chua HC, Weidling C, Chakouri N, Noland CL, Schott K, et al. Structural architecture of the human NALCN channelosome. *Nature*. 2022;603(7899):180-6.
89. Kschonsak M, Chua HC, Noland CL, Weidling C, Clairfeuille T, Bahlke OØ, et al. Structure of the human sodium leak channel NALCN. *Nature*. 2020;587(7833):313-8.
90. Lear BC, Darrah EJ, Aldrich BT, Gebre S, Scott RL, Nash HA, et al. UNC79 and UNC80, putative auxiliary subunits of the NARROW ABDOMEN ion channel, are indispensable for robust circadian locomotor rhythms in *Drosophila*. *PloS one*. 2013;8(11):e78147.
91. Shamseldin HE, Faqeih E, Alasmari A, Zaki MS, Gleeson JG, Alkuraya FS. Mutations in UNC80, encoding part of the UNC79-UNC80-NALCN channel complex,

cause autosomal-recessive severe infantile encephalopathy. *The American Journal of Human Genetics*. 2016;98(1):210-5.

92. Aoyagi K, Rossignol E, Hamdan FF, Mulcahy B, Xie L, Nagamatsu S, et al. A gain-of-function mutation in NALCN in a child with intellectual disability, ataxia, and arthrogryposis. *Human Mutation*. 2015;36(8):753-7.

93. Bramswig NC, Bertoli-Avella AM, Albrecht B, Al Aqeel AI, Alhashem A, Al-Sannaa N, et al. Genetic variants in components of the NALCN–UNC80–UNC79 ion channel complex cause a broad clinical phenotype (NALCN channelopathies). *Human genetics*. 2018;137(9):753-68.

94. Bourque DK, Dymont DA, MacLusky I, Kernohan KD, McMillan HJ. Periodic breathing in patients with NALCN mutations. *Journal of human genetics*. 2018;63(10):1093-6.

95. Bouasse M, Impheng H, Servant Z, Lory P, Monteil A. Functional expression of CLIFAHDD and IHPRF pathogenic variants of the NALCN channel in neuronal cells reveals both gain-and loss-of-function properties. *Scientific Reports*. 2019;9(1):1-14.

96. Köroğlu Ç, Seven M, Tolun A. Recessive truncating NALCN mutation in infantile neuroaxonal dystrophy with facial dysmorphism. *Journal of medical genetics*. 2013;50(8):515-20.

97. Fukai R, Saitsu H, Okamoto N, Sakai Y, Fattal-Valevski A, Masaaki S, et al. De novo missense mutations in NALCN cause developmental and intellectual impairment with hypotonia. *Journal of human genetics*. 2016;61(5):451-5.

98. Bend EG, Si Y, Stevenson DA, Bayrak-Toydemir P, Newcomb TM, Jorgensen EM, et al. NALCN channelopathies: Distinguishing gain-of-function and loss-of-function mutations. *Neurology*. 2016;87(11):1131-9.

99. Perez Y, Kadir R, Volodarsky M, Noyman I, Flusser H, Shorer Z, et al. UNC80 mutation causes a syndrome of hypotonia, severe intellectual disability, dyskinesia and dysmorphism, similar to that caused by mutations in its interacting cation channel NALCN. *Journal of medical genetics*. 2016;53(6):397-402.

100. Takenouchi T, Inaba M, Uehara T, Takahashi T, Kosaki K, Mizuno S. Biallelic mutations in NALCN: expanding the genotypic and phenotypic spectra of IHPRF1. *American journal of medical genetics Part A*. 2018;176(2):431-7.

101. Campbell J, FitzPatrick DR, Azam T, Gibson NA, Somerville L, Joss SK, et al. NALCN dysfunction as a cause of disordered respiratory rhythm with central apnea. *Pediatrics*. 2018;141(Supplement_5):S485-S90.

102. Lunni Z, Liu H, Zhao Q, Wu J, Yan Z. Architecture of the human NALCN channelosome. *Cell Discovery*. 2022;8(1).

103. Liu Y, Bezanilla F. Hydrophobic residues in S6 segments of nav contribute to the fast inactivation gate. *Biophysical Journal*. 2022;121(3):96a.

104. Yang X-R, Poulin H, Pouliot V, Plumereau Q, Appendino JP, Au PYB, et al. Biophysical characterization of SCN1A and SCN2A variants related to epilepsy. *Biophysical Journal*. 2022;121(3):96a.
105. Xie L, Gao S, Alcaire SM, Aoyagi K, Wang Y, Griffin JK, et al. NLF-1 delivers a sodium leak channel to regulate neuronal excitability and modulate rhythmic locomotion. *Neuron*. 2013;77(6):1069-82.
106. Topalidou I, Chen P-A, Cooper K, Watanabe S, Jorgensen EM, Ailion M. The NCA-1 and NCA-2 ion channels function downstream of Gq and Rho to regulate locomotion in *Caenorhabditis elegans*. *Genetics*. 2017;206(1):265-82.
107. Lu B, Su Y, Das S, Wang H, Wang Y, Liu J, et al. Peptide neurotransmitters activate a cation channel complex of NALCN and UNC-80. *Nature*. 2009;457(7230):741-4.
108. Lu B, Zhang Q, Wang H, Wang Y, Nakayama M, Ren D. Extracellular calcium controls background current and neuronal excitability via an UNC79-UNC80-NALCN cation channel complex. *Neuron*. 2010;68(3):488-99.
109. Metz LB, Dasgupta N, Liu C, Hunt SJ, Crowder CM. An evolutionarily conserved presynaptic protein is required for isoflurane sensitivity in *Caenorhabditis elegans*. *The Journal of the American Society of Anesthesiologists*. 2007;107(6):971-82.
110. Jospin M, Watanabe S, Joshi D, Young S, Hamming K, Thacker C, et al. UNC-80 and the NCA ion channels contribute to endocytosis defects in synaptojanin mutants. *Current Biology*. 2007;17(18):1595-600.
111. Górska-Andrzejak J, Makuch R, Stefan J, Görlich A, Semik D, Pyza E. Circadian expression of the presynaptic active zone protein Bruchpilot in the lamina of *Drosophila melanogaster*. *Developmental Neurobiology*. 2013;73(1):14-26.
112. Yalnızoğlu D, Özgül RK, Oğuz KK, Özer B, Yücel-Yılmaz D, Gürbüz B, et al. Expanding the phenotype of phospholipid remodelling disease due to MBOAT7 gene defect. *Journal of Inherited Metabolic Disease*. 2019;42(2):381-8.
113. Lee H-C, Inoue T, Imae R, Kono N, Shirae S, Matsuda S, et al. *Caenorhabditis elegans* mboa-7, a member of the MBOAT family, is required for selective incorporation of polyunsaturated fatty acids into phosphatidylinositol. *Molecular biology of the cell*. 2008;19(3):1174-84.
114. Drescher S, van Hoogevest P. The phospholipid research center: current research in phospholipids and their use in drug delivery. *Pharmaceutics*. 2020;12(12):1235.
115. Aktas M, Danne L, Möller P, Narberhaus F. Membrane lipids in *Agrobacterium tumefaciens*: biosynthetic pathways and importance for pathogenesis. *Frontiers in plant science*. 2014;5:109.
116. Raghu P, Joseph A, Krishnan H, Singh P, Saha S. Phosphoinositides: regulators of nervous system function in health and disease. *Frontiers in molecular neuroscience*. 2019;12:208.

117. Balla T, Szentpetery Z, Kim YJ. Phosphoinositide signaling: new tools and insights. *Physiology*. 2009.
118. Mayinger P. Phosphoinositides and vesicular membrane traffic. *Biochimica et Biophysica Acta (BBA)-Molecular and Cell Biology of Lipids*. 2012;1821(8):1104-13.
119. Phan TK, Williams SA, Bindra GK, Lay FT, Poon IK, Hulett MD. Phosphoinositides: multipurpose cellular lipids with emerging roles in cell death. *Cell Death & Differentiation*. 2019;26(5):781-93.
120. Shindou H, Hishikawa D, Harayama T, Yuki K, Shimizu T. Recent progress on acyl CoA: lysophospholipid acyltransferase research. *Journal of lipid research*. 2009;50:S46-S51.
121. Barneda D, Cosulich S, Stephens L, Hawkins P. How is the acyl chain composition of phosphoinositides created and does it matter? *Biochemical Society Transactions*. 2019;47(5):1291-305.
122. Kennedy EP, Weiss SB. The function of cytidine coenzymes in the biosynthesis of phospholipides. *Journal of Biological Chemistry*. 1956;222(1):193-214.
123. Gibellini F, Smith TK. The Kennedy pathway—de novo synthesis of phosphatidylethanolamine and phosphatidylcholine. *IUBMB life*. 2010;62(6):414-28.
124. Yamashita A, Hayashi Y, Matsumoto N, Nemoto-Sasaki Y, Oka S, Tanikawa T, et al. Glycerophosphate/Acylglycerophosphate Acyltransferases. *Biology*. 2014;3(4):801.
125. Lands WE. Metabolism of glycerolipides: a comparison of lecithin and triglyceride synthesis. *Journal of Biological chemistry*. 1958;231(2):883-8.
126. D'Souza K, and Richard M. Epan. Enrichment of phosphatidylinositols with specific acyl chains. *Biochimica et Biophysica Acta (BBA)-Biomembranes*. 2014;1838.6:1501-8.
127. YOSHIOKA T, INOUE H, KASAMA T, SEYAMA Y, NAKASHIMA S, NOZAWA Y, et al. Evidence that arachidonic acid is deficient in phosphatidylinositol of *Drosophila* heads. *The Journal of Biochemistry*. 1985;98(3):657-62.
128. Shen LR, Lai CQ, Feng X, Parnell LD, Wan JB, Wang JD, et al. *Drosophila* lacks C20 and C22 PUFAs. *Journal of lipid research*. 2010;51(10):2985-92.
129. Steinhauer J, Gijón MA, Riekhof WR, Voelker DR, Murphy RC, Treisman JE. *Drosophila* lysophospholipid acyltransferases are specifically required for germ cell development. *Molecular biology of the cell*. 2009;20(24):5224-35.
130. Ziegler AB, Ménagé C, Grégoire S, Garcia T, Ferveur J-F, Bretillon L, et al. Lack of dietary polyunsaturated fatty acids causes synapse dysfunction in the *drosophila* visual system. *PLoS One*. 2015;10(8):e0135353.
131. Marza E, Long T, Saiardi A, Sumakovic M, Eimer S, Hall DH, et al. Polyunsaturated fatty acids influence synaptojanin localization to regulate synaptic vesicle recycling. *Molecular biology of the cell*. 2008;19(3):833-42.

132. Barceló-Coblijn G, Kitajka K, Puskás LG, Hőgyes E, Zvara A, Hackler Jr L, et al. Gene expression and molecular composition of phospholipids in rat brain in relation to dietary n-6 to n-3 fatty acid ratio. *Biochimica et Biophysica Acta (BBA)-Molecular and Cell Biology of Lipids*. 2003;1632(1-3):72-9.
133. Rizo J, Xu J. The synaptic vesicle release machinery. *Annual review of biophysics*. 2015;44:339-67.
134. Lee H-C, Inoue T, Sasaki J, Kubo T, Matsuda S, Nakasaki Y, et al. LPIAT1 regulates arachidonic acid content in phosphatidylinositol and is required for cortical lamination in mice. *Molecular biology of the cell*. 2012;23(24):4689-700.
135. Jennings BH. *Drosophila—a versatile model in biology & medicine*. *Materials today*. 2011;14(5):190-5.
136. Arias AM. *Drosophila melanogaster and the development of biology in the 20th century*. *Drosophila*. 2008:1-25.
137. Roberts DB. *Drosophila melanogaster: the model organism*. *Entomologia experimentalis et applicata*. 2006;121(2):93-103.
138. Heigwer F, Port F, Boutros M. RNA interference (RNAi) screening in *Drosophila*. *Genetics*. 2018;208(3):853-74.
139. Marcogliese PC, Wangler MF. *Drosophila as a model for human diseases*. *Encyclopedia of Life Sciences*. 2001.
140. Heckscher ES, Lockery SR, Doe CQ. Characterization of *Drosophila* larval crawling at the level of organism, segment, and somatic body wall musculature. *Journal of Neuroscience*. 2012;32(36):12460-71.
141. Bellen HJ, Tong C, Tsuda H. 100 years of *Drosophila* research and its impact on vertebrate neuroscience: a history lesson for the future. *Nature Reviews Neuroscience*. 2010;11(7):514-22.
142. McGuire SE, Roman G, Davis RL. Gene expression systems in *Drosophila*: a synthesis of time and space. *TRENDS in Genetics*. 2004;20(8):384-91.
143. Brand AH, Perrimon N. Targeted gene expression as a means of altering cell fates and generating dominant phenotypes. *development*. 1993;118(2):401-15.
144. Duffy JB. GAL4 system in *Drosophila*: a fly geneticist's Swiss army knife. *genesis*. 2002;34(1-2):1-15.
145. Stewart B, Atwood H, Renger J, Wang J, Wu C-F. Improved stability of *Drosophila* larval neuromuscular preparations in haemolymph-like physiological solutions. *Journal of Comparative Physiology A*. 1994;175(2):179-91.
146. Krzeptowski W, Górska-Andrzejak J, Kijak E, Gorlich A, Guzik E, Moore G, et al. External and circadian inputs modulate synaptic protein expression in the visual system of *Drosophila melanogaster*. *Frontiers in Physiology*. 2014;5:102.

147. Angius A, Cossu S, Uva P, Oppo M, Onano S, Persico I, et al. Novel NALCN biallelic truncating mutations in siblings with IHPRF1 syndrome. *Clinical genetics*. 2018;93(6):1245-7.
148. Gal M, Magen D, Zahran Y, Ravid S, Eran A, Khayat M, et al. A novel homozygous splice site mutation in NALCN identified in siblings with cachexia, strabismus, severe intellectual disability, epilepsy and abnormal respiratory rhythm. *European Journal of Medical Genetics*. 2016;59(4):204-9.
149. Lozic B, Johansson S, Lovric Kojundzic S, Markic J, Knappskog PM, Hahn AF, et al. Novel NALCN variant: altered respiratory and circadian rhythm, anesthetic sensitivity. *Annals of Clinical and Translational Neurology*. 2016;3(11):876-83.
150. Yeh S-Y, Huang W-H, Wang W, Ward CS, Chao ES, Wu Z, et al. Respiratory network stability and modulatory response to substance P require Nalcn. *Neuron*. 2017;94(2):294-303. e4.
151. Chong JX, McMillin MJ, Shively KM, Beck AE, Marvin CT, Armenteros JR, et al. De novo mutations in NALCN cause a syndrome characterized by congenital contractures of the limbs and face, hypotonia, and developmental delay. *The American Journal of Human Genetics*. 2015;96(3):462-73.
152. Sedensky MM, Meneely PM. Genetic analysis of halothane sensitivity in *Caenorhabditis elegans*. *Science*. 1987;236(4804):952-4.
153. Ou M, Zhao W, Liu J, Liang P, Huang H, Yu H, et al. The general anesthetic isoflurane bilaterally modulates neuronal excitability. *Science*. 2020;23(1):100760.
154. Yang Y, Ou M, Liu J, Zhao W, Zhuoma L, Liang Y, et al. Volatile anesthetics activate a leak sodium conductance in retrotrapezoid nucleus neurons to maintain breathing during anesthesia in mice. *Anesthesiology*. 2020;133(4):824-38.
155. Singaram VK. *The Role of Neuronal Leak Channels in Anesthesia: Case Western Reserve University*; 2012.
156. Speca DJ, Chihara D, Ashique AM, Bowers MS, Pierce-Shimomura JT, Lee J, et al. Conserved role of unc-79 in ethanol responses in lightweight mutant mice. *PLoS genetics*. 2010;6(8):e1001057.
157. Krishnan K, Nash HA. A genetic study of the anesthetic response: mutants of *Drosophila melanogaster* altered in sensitivity to halothane. *Proceedings of the National Academy of Sciences*. 1990;87(21):8632-6.
158. Mir B, Iyer S, Ramaswami M, Krishnan K. A genetic and mosaic analysis of a locus involved in the anesthesia response of *Drosophila melanogaster*. *Genetics (USA)*. 1997.
159. Guan Z, Scott R, Nash H. A new assay for the genetic study of general anesthesia in *Drosophila melanogaster*: use in analysis of mutations in the X-chromosomal 12E region. *Journal of neurogenetics*. 2000;14(1):25-42.

160. King AN, Sehgal A. Molecular and circuit mechanisms mediating circadian clock output in the *Drosophila* brain. *European Journal of Neuroscience*. 2020;51(1):268-81.
161. Allada R, Chung BY. Circadian organization of behavior and physiology in *Drosophila*. *Annual review of physiology*. 2010;72:605.
162. Lear BC, Lin J-M, Keath JR, McGill JJ, Raman IM, Allada R. The ion channel narrow abdomen is critical for neural output of the *Drosophila* circadian pacemaker. *Neuron*. 2005;48(6):965-76.
163. Pierce-Shimomura JT, Chen BL, Mun JJ, Ho R, Sarkis R, McIntire SL. Genetic analysis of crawling and swimming locomotory patterns in *C. elegans*. *Proceedings of the National Academy of Sciences*. 2008;105(52):20982-7.
164. Campbell DB, Nash HA. Use of *Drosophila* mutants to distinguish among volatile general anesthetics. *Proceedings of the National Academy of Sciences*. 1994;91(6):2135-9.
165. Nash HA, Campbell DB, Krishnan K. New mutants of *Drosophila* that are resistant to the anesthetic effects of halothane. *Annals of the New York Academy of Sciences*. 1991;625(1):540-4.
166. Sloan TB. Anesthetics and the brain. *Anesthesiology Clinics of North America*. 2002;20(2):265-92.
167. Platholi J, Hemmings HC. Effects of general anesthetics on synaptic transmission and plasticity. *Current Neuropharmacology*. 2022;20(1):27-54.
168. Rickman C, Davletov B. Arachidonic acid allows SNARE complex formation in the presence of Munc18. *Chemistry & biology*. 2005;12(5):545-53.
169. Parisi M, Li R, Oliver B. Lipid profiles of female and male *Drosophila*. *BMC research notes*. 2011;4(1):1-5.
170. Ruiz S, Ferreiro MJ, Menhert KI, Casanova G, Olivera A, Cantera R. Rhythmic changes in synapse numbers in *Drosophila melanogaster* motor terminals. *PloS one*. 2013;8(6):e67161.
171. Gilestro GF, Tononi G, Cirelli C. Widespread changes in synaptic markers as a function of sleep and wakefulness in *Drosophila*. *science*. 2009;324(5923):109-12.
172. Huang S, Piao C, Beuschel CB, Götz T, Sigrist SJ. Presynaptic active zone plasticity encodes sleep need in *Drosophila*. *Current Biology*. 2020;30(6):1077-91. e5.
173. Sugie A, Hakeda-Suzuki S, Suzuki E, Silies M, Shimosono M, Möhl C, et al. Molecular remodeling of the presynaptic active zone of *Drosophila* photoreceptors via activity-dependent feedback. *Neuron*. 2015;86(3):711-25.
174. Xin X. Neuronal activation contributes to the regulation of synaptic strength in circadian networks: Brandeis University; 2019.

175. Korn H, Triller A, Mallet A, Faber DS. Fluctuating responses at a central synapse: n of binomial fit predicts number of stained presynaptic boutons. *Science*. 1981;213(4510):898-901.
176. Silver RA, Lubke J, Sakmann B, Feldmeyer D. High-probability unquantal transmission at excitatory synapses in barrel cortex. *Science*. 2003;302(5652):1981-4.

8. APPENDIX

Appendix 1: Summary of the Statistics

For the sake of simplicity only comparisons in which values are significantly different from each other are included in the tables

FIGURE	4.15. BRP and glutamate receptor oscillate with the same pattern (C)						
DESCRIPTION	1st vial, Mean BRP, Per NMJ Data						
Hour	0	7	9	12	17	19	
Mean \pm SEM	0.1121 \pm 0.0099	0.03076 \pm 0.0016	0.04683 \pm 0.0033	0.06022 \pm 0.0035	0.08242 \pm 0.012	0.08849 \pm 0.0096	
Multiple Comparisons	Hour	P value	Hour	P value	Hour	P value	Test
	0 vs. 7	<0.0001	7 vs. 12	0.0039	9 vs. 19	0.0060	Kruskal Wallis with Dunn's Multiple Comparison Test
	0 vs. 9	<0.0001	7 vs. 17	<0.0001			
0 vs. 12	0.0097	7 vs. 19	<0.0001				

FIGURE	4.15. BRP and glutamate receptor oscillate with the same pattern (C)						
DESCRIPTION	1st vial, Integrated BRP, Per NMJ Data						
Hour	0	7	9	12	17	19	
Mean \pm SEM	761.3 \pm 95.97	199.6 \pm 18.05	327.9 \pm 24.21	376.9 \pm 35.46	515.9 \pm 105.7	572.8 \pm 84.18	
Multiple Comparisons	Hour	P value	Hour	P value	Hour	P value	Test
	0 vs. 7	<0.0001	0 vs. 12	0.056	7 vs. 17	0.0121	Kruskal Wallis with Dunn's Multiple Comparison Test
	0 vs. 9	0.0073	7 vs. 12	0.051	7 vs. 19	0.0004	

FIGURE	4.15. BRP and glutamate receptor oscillate with the same pattern (C)						
DESCRIPTION	1st vial, Mean GluRIID, Per NMJ Data						
Hour	0	7	9	12	17	19	
Mean ±SEM	0.0025±0.0002	0.00092±0.0001	0.0018±0.0002	0.0017±0.0002	0.0022±0.0004	0.0025±0.0004	
Multiple Comparisons	Hour	P value	Hour	P value	Hour	P value	Test
	0 vs. 7	0.0005	7 vs. 19	0.0068			Kruskal Wallis with Dunn's Multiple Comparison Test

FIGURE	4.15. BRP and glutamate receptor oscillate with the same pattern (C)						
DESCRIPTION	1st vial, Integrated GluRIID, Per NMJ Data						
Hour	0	7	9	12	17	19	
Mean ±SEM	663.0±78.43	241.1±26.66	463.8±52.88	437.4±60.47	564.5±122.8	649.7±114.7	
Multiple Comparisons	Hour	P value	Hour	P value	Hour	P value	Test
	0 vs. 7	0.0005	7 vs. 19	0.0068			Kruskal Wallis with Dunn's Multiple Comparison Test

FIGURE	4.15. BRP and glutamate receptor oscillate with the same pattern (C)						
DESCRIPTION	1st vial, Mean BRP, Per AZ Data						
Hour	0	7	9	12	17	19	
Mean ±SEM	0.06685±0.0057	0.02761±0.002	0.04758±0.005	0.04912±0.005	0.06347±0.011	0.06609±0.0081	
Multiple Comparisons	Hour	P value	Hour	P value	Hour	P value	Test
	0 vs. 7	<0.0001	7 vs. 12	0.0351	7 vs. 19	0.0001	Kruskal Wallis with Dunn's Multiple Comparison Test
	7 vs. 9	0.0577	7 vs. 17	0.0047			

FIGURE	4.15. BRP and glutamate receptor oscillate with the same pattern (C)						
DESCRIPTION	1st vial, Integrated BRP, Per AZ Data						
Hour	0	7	9	12	17	19	
Mean ±SEM	3.546±0.3120	1.368±0.1202	2.561±0.2637	2.532±0.2791	3.439±0.6520	3.496±0.4209	
Multiple Comparisons	Hour	P value	Hour	P value	Hour	P value	Test
	0 vs. 7	<0.0001	7 vs. 12	0.0897	7 vs. 19	0.0002	Kruskal Wallis with Dunn's Multiple Comparison Test
	7 vs. 9	0.0516	7 vs. 17	0.0058			

FIGURE	4.15. BRP and glutamate receptor oscillate with the same pattern (C)						
DESCRIPTION	1st vial, Mean GluRIID, Per AZ Data						
Hour	0	7	9	12	17	19	
Mean ±SEM	0.06685±0.0057	0.02761±0.0019	0.04758±0.0049	0.04912±0.0049	0.06347±0.011	0.06609±0.0081	
Multiple Comparisons	Hour	P value	Hour	P value	Hour	P value	Test
	0 vs. 7	<0.0001	7 vs. 12	0.0351	7 vs. 19	0.0001	Kruskal Wallis with Dunn's Multiple Comparison Test
	7 vs. 9	0.0577	7 vs. 17	0.0047			

FIGURE	4.15. BRP and glutamate receptor oscillate with the same pattern (C)						
DESCRIPTION	1st vial, Integrated GluRIID, Per AZ Data						
Hour	0	7	9	12	17	19	
Mean ±SEM	3.546±0.3120	1.3686±0.1202	2.5616±0.2637	2.5326±0.2791	3.4396±0.6520	3.4966±0.4209	
Multiple Comparisons	Hour	P value	Hour	P value	Hour	P value	Test
	0 vs. 7	<0.0001	7 vs. 12	0.0897	7 vs. 19	0.0002	Kruskal Wallis with Dunn's Multiple Comparison Test
	7 vs. 9	0.0516	7 vs. 17	0.0058			

FIGURE	4.15. BRP and glutamate receptor oscillate with the same pattern (C)						
DESCRIPTION	2 nd vial, Mean BRP, Per NMJ Data						
Hour	0	7	9	12	17	19	
Mean ±SEM	0.1222±0.011	0.03872±0.0044	0.04196±0.0041	0.05076±0.0031	0.1015±0.0087	0.1078±0.01041	
Multiple Comparisons	Hour	P value	Hour	P value	Hour	P value	Test
	0 vs. 7	<0.0001	7 vs. 17	<0.0001	12 vs. 17	0.0002	One way ANOVA with Tukey's Multiple Comparison Test
	0 vs. 9	<0.0001	7 vs. 19	<0.0001	12 vs. 19	<0.0001	
	0 vs. 12	<0.0001	9 vs. 19	<0.0001			

FIGURE	4.15. BRP and glutamate receptor oscillate with the same pattern (C)						
DESCRIPTION	2 nd vial, Integrated BRP, Per NMJ Data						
Hour	0	7	9	12	17	19	
Mean ±SEM	931.3±99.57	216.0±23.18	239.4±33.28	283.7±29.58	644.1±64.02	716.7±106.4	
Multiple Comparisons	Hour	P value	Hour	P value	Hour	P value	Test
	0 vs. 7	<0.0001	0 vs. 17	0.0384	9 vs. 17	0.0009	One way ANOVA with Tukey's Multiple Comparison Test
	0 vs. 9	<0.0001	7 vs. 17	0.0006	9 vs. 19	<0.0001	
	0 vs. 12	<0.0001	7 vs. 19	<0.0001	12 vs. 17	0.0053	
					12 vs. 19	0.0005	

FIGURE	4.15.BRP and glutamate receptor oscillate with the same pattern (C)						
DESCRIPTION	2 nd vial, Mean GluRIID, Per NMJ Data						
Hour	0	7	9	12	17	19	
Mean ±SEM	0.0042±0.0005	0.0009±0.0001	0.0011±0.0001	0.0011±0.0001	0.0029±0.0003	0.0030±0.0005	
Multiple Comparisons	Hour	P value	Hour	P value	Hour	P value	Test
	0 vs. 7	<0.0001	7 vs. 17	0.0003	9 vs. 19	0.0153	Kruskal Wallis with Dunn's Multiple Comparison Test
	0 vs. 9	<0.0001	7 vs. 19	0.0034	12 vs. 17	0.0067	
	0 vs. 12	<0.0001	9 vs. 17	0.0015			

FIGURE	4.15.BRP and glutamate receptor oscillate with the same pattern (C)						
DESCRIPTION	2 nd vial, Integrated GluRIID, Per NMJ Data						
Hour	0	7	9	12	17	19	
Mean ±SEM	1104±134.6	242.9±27.89	288.5±40.05	300.9±32.28	766.2±82.30	788.1±149.1	
Multiple Comparisons	Hour	P value	Hour	P value	Hour	P value	Test
	0 vs. 7	<0.0001	7 vs. 17	0.0003	9 vs. 19	0.0154	Kruskal Wallis with Dunn's Multiple Comparison Test
	0 vs. 9	<0.0001	7 vs. 19	0.0034	12 vs. 17	0.0067	
	0 vs. 12	<0.0001	9 vs. 17	0.0015	12 vs. 19	0.053	

FIGURE	4.15. BRP and glutamate receptor oscillate with the same pattern (C)						
DESCRIPTION	2 nd vial, Mean BRP, Per AZ Dat						
Hour	0	7	9	12	17	19	
Mean ±SEM	0.1106±0.001	0.03498±0.004	0.03801±0.004	0.04548±0.003	0.09106±0.008	0.09696±0.009	
Multiple Comparisons	Hour	P value	Hour	P value	Hour	P value	Test
	0 vs. 7	<0.0001	7 vs. 17	<0.0001	9 vs. 19	<0.0001	One way ANOVA with Tukey's Multiple Comparison Test
	0 vs. 9	<0.0001	7 vs. 19	<0.0001	12 vs. 17	0.0002	
	0 vs. 12	<0.0001	9 vs. 17	<0.0001	12 vs. 19	<0.0001	

FIGURE	4.15. BRP and glutamate receptor oscillate with the same pattern (C)						
DESCRIPTION	2 nd vial, Integrated BRP, Per AZ Data						
Hour	0	7	9	12	17	19	
Mean ±SEM	6.402±0.5479	2.261±0.2306	2.298±0.2055	2.744±0.1507	5.363±0.4154	5.803±0.5302	
Multiple Comparisons	Hour	P value	Hour	P value	Hour	P value	Test
	0 vs. 7	<0.0001	7 vs. 17	<0.0001	9 vs. 19	<0.0001	One way ANOVA with Tukey's Multiple Comparison Test
	0 vs. 9	<0.0001	7 vs. 19	<0.0001	12 vs. 17	0.0001	
	0 vs. 12	<0.0001	9 vs. 17	<0.0001	12 vs. 19	<0.0001	

FIGURE	4.15. BRP and glutamate receptor oscillate with the same pattern (C)						
DESCRIPTION	2 nd vial, Mean GluRIID, Per AZ Data						
Hour	0	7	9	12	17	19	
Mean ±SEM	0.1007±0.0111	0.0323±0.0036	0.0369±0.0037	0.0399±0.0034	0.0797±0.0083	0.0774±0.0092	
Multiple Comparisons	Hour	P value	Hour	P value	Hour	P value	Test
	0 vs. 7	<0.0001	7 vs. 17	0.0001	9 vs. 19	0.0052	Kruskal Wallis with Dunn's Multiple Comparison Test
	0 vs. 9	<0.0001	7 vs. 19	0.0007	12 vs. 17	0.0065	
	0 vs. 12	<0.0001	9 vs. 17	0.0013	12 vs. 19	0.0223	

FIGURE	4.15. BRP and glutamate receptor oscillate with the same pattern (C)						
DESCRIPTION	2 nd vial, Integrated GluRIID, Per AZ Data						
Hour	0	7	9	12	17	19	
Mean ±SEM	5.732±0.7397	1.600±0.1696	1.979±0.2026	1.965±0.1862	4.478±0.4721	4.139±0.5331	
Multiple Comparisons	Hour	P value	Hour	P value	Hour	P value	Test
	0 vs. 7	<0.0001	7 vs. 17	<0.0001	9 vs. 19	0.0098	Kruskal Wallis with Dunn's Multiple Comparison Test
	0 vs. 9	<0.0001	7 vs. 19	0.0005	12 vs. 17	0.0011	
	0 vs. 12	<0.0001	9 vs. 17	0.0009	12 vs. 19	0.0112	

FIGURE	4.19. Changing diet has an impact on AZ shape and intensity.						
DESCRIPTION	Normal Food, Mean BRP, Per NMJ Data						
Hour	17.30	21	3	9	15		
Mean ±SEM	0.09535±0.01064	0.08924±0.01280	0.08175±0.008828	0.1027±0.009634	0.09533±0.01231		
Multiple Comparisons	Hour	P value	Hour	P value	Hour	P value	Test
	All values n.s.						Kruskal Wallis with Dunn's Multiple Comparison Test

FIGURE	4.19. Changing diet has an impact on AZ shape and intensity.						
DESCRIPTION	Normal Food, Integrated BRP, Per NMJ Data						
Hour	17.30	21	3	9	15		
Mean ±SEM	557.1±68.90	603.1±81.08	470.0±46.71	574.3±61.55	446.2±51.88		
Multiple Comparisons	Hour	P value	Hour	P value	Hour	P value	Test
	All values n.s.						Kruskal Wallis with Dunn's Multiple Comparison Test

FIGURE	4.19. Changing diet has an impact on AZ shape and intensity.						
DESCRIPTION	Normal Food, Mean GluRIID, Per NMJ Data						
Hour	17.30	21	3	9	15		
Mean ±SEM	0.0036±0.0004	0.003433±0.0006	0.002154±0.0002	0.003448±0.0003	0.003072±0.0005		
Multiple Comparisons	Hour	P value	Hour	P value	Hour	P value	Test
	17.30 vs. 3	0.0176	3 vs. 9	0.0126			Kruskal Wallis with Dunn's Multiple Comparison Test

FIGURE	4.19. Changing diet has an impact on AZ shape and intensity.						
DESCRIPTION	Normal Food, Integrated GluRIID, Per NMJ Data						
Hour	17.30	21	3	9	15		
Mean ±SEM	943.0±125.3	900.0±145.7	564.5±53.62	903.9±90.42	805.4±131.5		
Multiple Comparisons	Hour	P value	Hour	P value	Hour	P value	Test
	17.30 vs. 3	0.0176	3 vs. 9	0.0125			Kruskal Wallis with Dunn's Multiple Comparison Test

FIGURE	4.19. Changing diet has an impact on AZ shape and intensity.						
DESCRIPTION	Special Food, Mean BRP, Per NMJ Data						
Hour	17.30	21	3	9	15		
Mean ±SEM	0.1323±0.0082	0.09883±0.0075	0.1056±0.0068	0.1224±0.0082	0.1264±0.0090		
Multiple Comparisons	Hour	P value	Hour	P value	Hour	P value	Test
	All values n.s.						One way Anova with Tukey's Multiple Comparison Test

FIGURE	4.19. Changing diet has an impact on AZ shape and intensity.						
DESCRIPTION	Special Food, Integrated BRP, Per NMJ Data						
Hour	17.30	21	3	9	15		
Mean ±SEM	774.1±49.38	648.3±73.52	597.6±52.59	673.9±59.55	753.8±72.19		
Multiple Comparisons	Hour	P value	Hour	P value	Hour	P value	Test
	All values n.s.						Kruskal Wallis with Dunn's Multiple Comparison Test

FIGURE	4.19. Changing diet has an impact on AZ shape and intensity.						
DESCRIPTION	Special Food, Mean GluRIID, Per NMJ Data						
Hour	17.30	21	3	9	15		
Mean ±SEM	0.0049±0.0004	0.0046±0.00068	0.004254±0.00046	0.004369±0.0004	0.004088±0.0003		
Multiple Comparisons	Hour	P value	Hour	P value	Hour	P value	Test
	All values n.s.						Kruskal Wallis with Dunn's Multiple Comparison Test

FIGURE	4.19. Changing diet has an impact on AZ shape and intensity.						
DESCRIPTION	Special Food, Integrated GluRIID, Per NMJ Data						
Hour	17.30	21	3	9	15		
Mean ±SEM	1273±115.5	1213±178.3	1115±120.6	1145±128.2	1072±82.08		
Multiple Comparisons	Hour	P value	Hour	P value	Hour	P value	Test
	All values n.s.						Kruskal Wallis with Dunn's Multiple Comparison Test

FIGURE	4.19. Changing diet has an impact on AZ shape and intensity.						
DESCRIPTION	Normal Food, Mean BRP, Per AZ Data						
Hour	3	9	15	17.30	21		
Mean ±SEM	0.07606±0.0080	0.09411±0.0088	0.08746±0.01151	0.08776±0.010	0.08271±0.012		
Multiple Comparisons	Hour	P value	Hour	P value	Hour	P value	Test
	All values n.s.						Kruskal Wallis with Dunn's Multiple Comparison Test

FIGURE	4.19. Changing diet has an impact on AZ shape and intensity.						
DESCRIPTION	Normal Food, Integrated BRP, Per AZ Data						
Hour	3	9	15	17.30	21		
Mean ±SEM	4.591±0.4562	5.699±0.4608	5.118±0.5707	4.943±0.5253	5.045±0.6212		
Multiple Comparisons	Hour	P value	Hour	P value	Hour	P value	Test
	All values n.s.						Kruskal Wallis with Dunn's Multiple Comparison Test

FIGURE	4.19. Changing diet has an impact on AZ shape and intensity.						
DESCRIPTION	Normal Food, Mean GluRIID, Per AZ Data						
Hour	3	9	15	17.30	21		
Mean ±SEM	0.06843±0.006652	0.1136±0.01250	0.1163±0.02047	0.1131±0.01353	0.09766±0.01403		
Multiple Comparisons	Hour	P value	Hour	P value	Hour	P value	Test
	3 vs. 9	0.0088	3 vs. 15	0.0931	3 vs. 17.3	0.0278	Kruskal Wallis with Dunn's Multiple Comparison Test

FIGURE	4.19. Changing diet has an impact on AZ shape and intensity.						
DESCRIPTION	Normal Food, Integrated GluRIID, Per AZ Data						
Hour	3	9	15	17.30	21		
Mean ±SEM	3.643±0.3900	6.350±0.6842	6.511±1.172	6.407±0.8190	5.328±0.7576		
Multiple Comparisons	Hour	P value	Hour	P value	Hour	P value	Test
	3 vs. 9	0.0067	3 vs. 17.3	0.0226			Kruskal Wallis with Dunn's Multiple Comparison Test

FIGURE	4.19. Changing diet has an impact on AZ shape and intensity.						
DESCRIPTION	Special Food, Mean BRP, Per AZ Data						
Hour	3	9	15	17.30	21		
Mean ±SEM	0.09546±0.0063	0.1097±0.0073	0.1162±0.0083	0.1212±0.0077	0.0906±0.0068		
Multiple Comparisons	Hour	P value	Hour	P value	Hour	P value	Test
	All values n.s.						One way Anova with Tukey's Multiple Comparison Test

FIGURE	4.19. Changing diet has an impact on AZ shape and intensity.						
DESCRIPTION	Special Food, Integrated BRP, Per AZ Data						
Hour	3	9	15	17.30	21		
Mean ±SEM	5.158±0.3064	5.847±0.3197	6.330±0.4018	6.320±0.4057	4.948±0.3531		
Multiple Comparisons	Hour	P value	Hour	P value	Hour	P value	Test
	All values n.s.						One way Anova with Tukey's Multiple Comparison Test

FIGURE	4.19. Changing diet has an impact on AZ shape and intensity.						
DESCRIPTION	Special Food, Mean GluRIID, Per AZ Data						
Hour	3	9	15	17.30	21		
Mean ±SEM	0.1247±0.01050	0.1288±0.01103	0.1275±0.0096	0.1471±0.01233	0.1232±0.01032		
Multiple Comparisons	Hour	P value	Hour	P value	Hour	P value	Test
	All values n.s.						Kruskal Wallis with Dunn's Multiple Comparison Test

FIGURE	4.19. Changing diet has an impact on AZ shape and intensity.						
DESCRIPTION	Special Food, Integrated GluRIID, Per AZ Data						
Hour	3	9	15	17.30	21		
Mean ±SEM	6.560±0.5680	6.536±0.5808	6.537±0.4822	7.555±0.6718	6.618±0.5128		
Multiple Comparisons	Hour	P value	Hour	P value	Hour	P value	Test
	All values n.s.						Kruskal Wallis with Dunn's Multiple Comparison Test

FIGURE	4.21. Spanning a period of time results in gradual brp and glutamate receptor change and a change in brp and glutamate receptor morphologies.					
DESCRIPTION	SF (BRP) Mean Intensity, per image					
Hour	9	10	12	13	14	
Mean ±SEM	0.06854±0.00	0.09901±0.01153	0.1124±0.0058	0.1251±0.0073	0.1165±0.0099	
	1					
Multiple Comparisons	Hour	P value	Hour	P value		Test
	9 vs. 12	0.0012	9 vs. 13	0.0014		One way Anova with Tukey's Multiple Comparison Test
	9 vs. 14	0.0056				

FIGURE	4.21. Spanning a period of time results in gradual brp and glutamate receptor change and a change in brp and glutamate receptor morphologies.					
DESCRIPTION	Special Food, Integrated BRP, Per NMJ Data					
Hour	9	10	12	13	14	
Mean ±SEM	317.3±44.99	444.5±55.66	662.7±49.29	735.8±82.82	611.6±30.24	
Multiple Comparisons	Hour	P value	Hour	P value		Test
	9 vs. 12	<0.0001	10 vs. 12	0.0423		One way Anova with Tukey's Multiple Comparison Test
	9 vs. 13	<0.0001	10 vs. 13	0.0223		
	9 vs. 14	0.0035				

FIGURE	4.21. Spanning a period of time results in gradual brp and glutamate receptor change and a change in brp and glutamate receptor morphologies.					
DESCRIPTION	Special Food, Mean GluRIID, Per NMJ Data					
Hour	9	10	12	13	14	
Mean ±SEM	0.0017±0.0002	0.0026±0.0004	0.0025±0.0003	0.00079±0.0001	0.0007±0.0001	
Multiple Comparisons	Hour	P value	Hour	P value		Test
	10 vs. 13	0.0460	12 vs. 13	0.0243		One way Anova with Tukey's Multiple Comparison Test
	10 vs. 14	0.0374	12 vs. 14	0.0176		

FIGURE	4.21. Spanning a period of time results in gradual brp and glutamate receptor change and a change in brp and glutamate receptor morphologies.					
DESCRIPTION	Special Food, Integrated GluRIID, Per NMJ Data					
Hour	9	10	12	13	14	
Mean ±SEM	453.3±64.85	673.6±110.4	651.1±103.2	207.0±41.69	186.4±41.73	
Multiple Comparisons	Hour	P value	Hour	P value		Test
	10 vs. 13	0.0460	12 vs. 13	0.0243		One way Anova with Tukey's Multiple Comparison Test
	10 vs. 14	0.0375	12 vs. 14	0.0176		

FIGURE	4.21. Spanning a period of time results in gradual brp and glutamate receptor change and a change in brp and glutamate receptor morphologies.					
DESCRIPTION	Special Food, Mean BRP, Per AZ Data					
Hour	9	10	12	13	14	
Mean ±SEM	0.06281±0.008	0.09058±0.010	0.1024±0.0056	0.1157±0.0071	0.1077±0.0094	
Multiple Comparisons	Hour	P value	Hour	P value		Test
	9 vs. 12	0.0012	9 vs. 13	0.0011		One way Anova with Tukey's Multiple Comparison Test
	9 vs. 14	0.0043				

FIGURE	4.21. Spanning a period of time results in gradual brp and glutamate receptor change and a change in brp and glutamate receptor morphologies.					
DESCRIPTION	Special Food, Integrated BRP, Per AZ Data					
Hour	9	10	12	13	14	
Mean ±SEM	3.090±0.4478	4.457±0.4542	5.047±0.2544	5.482±0.2926	5.032±0.3728	
Multiple Comparisons	Hour	P value	Hour	P value		Test
	9 vs. 12	0.0008	9 vs. 14	0.0126		One way Anova with Tukey's Multiple Comparison Test
	9 vs. 13	0.0021				

FIGURE	4.21. Spanning a period of time results in gradual brp and glutamate receptor change and a change in brp and glutamate receptor morphologies.					
DESCRIPTION	Special Food, Mean GluRIID, Per AZ Data					
Hour	9	10	12	13	14	
Mean ±SEM	0.05478±0.0075	0.09143±0.0110	0.08730±0.0079	0.06675±0.011	0.06790±0.016	
Multiple Comparisons	Hour	P value	Hour	P value		Test
	All values n.s.					One way Anova with Tukey's Multiple Comparison Test

FIGURE	4.21. Spanning a period of time results in gradual brp and glutamate receptor change and a change in brp and glutamate receptor morphologies.					
DESCRIPTION	Special Food, Integrated BRP, Per AZ Data					
Hour	9	10	12	13	14	
Mean ±SEM	2.810±0.3964	4.744±0.6310	4.648±0.4467	4.284±0.8516	4.139±1.040	
Multiple Comparisons	Hour	P value	Hour	P value		Test
	9 vs. 12	0.0341				Kruskal Wallis with Dunn's Multiple Comparison Test

FIGURE	4.15. BRP and glutamate receptor oscillate with the same pattern (B)						
DESCRIPTION	1st day, Mean BRP, Per NMJ Data						
Hour	0.5	3.5	6.5	7.5	11	22	
Mean ±SEM	0.07012±0.004	0.05012±0.0021	0.06995±0.0053	0.06101±0.008	0.1053±0.009	0.06753±0.01108	
Multiple Comparisons	Hour	P value	Hour	P value	Hour	P value	Test
	22 vs. 11	0.0032	3.5 vs. 11	<0.0001	7.5 vs. 11	0.0011	One way Anova with Tukey's Multiple Comparison Test
	0.5 vs. 11	0.0049	6.5 vs. 11	0.0076			

FIGURE	4.15. BRP and glutamate receptor oscillate with the same pattern (B)						
DESCRIPTION	1st day, Integrated BRP, Per NMJ Data						
Hour	0.5	3.5	6.5	7.5	11	22	
Mean ±SEM	421.8±41.90	282.3±33.29	343.0±42.88	278.8±47.65	542.9±58.61	432.1±69.64	
Multiple Comparisons	Hour	P value	Hour	P value	Hour	P value	Test
	3.5 vs. 11	0.0034	6.5 vs. 11	0.0769	7.5 vs. 11	0.0108	One way Anova with Tukey's Multiple Comparison Test

FIGURE	4.15. BRP and glutamate receptor oscillate with the same pattern (B)						
DESCRIPTION	1st day, Mean GluRIID, Per NMJ Data						
Hour	0.5	3.5	6.5	7.5	11	22	
Mean \pm SEM	0.0018 \pm 0.0001	0.0005 \pm 6.832e-005	0.0015 \pm 0.0002	0.0012 \pm 0.0002	0.0026 \pm 0.00035	0.002 \pm 0.0002	
Multiple Comparisons	Hour	P value	Hour	P value	Hour	P value	Test
	22 vs. 3.5	<0.0001	3.5 vs. 6.5	0.0332	6.5 vs. 11	0.0428	One way Anova with Tukey's Multiple Comparison Test
	22 vs. 7.5	0.0356	3.5 vs. 11	<0.0001	7.5 vs. 11	0.0045	
	0.5 vs. 3.5	0.0026					

FIGURE	4.15. BRP and glutamate receptor oscillate with the same pattern (B)						
DESCRIPTION	1st day, Integrated GluRIID, Per NMJ Data						
Hour	0.5	3.5	6.5	7.5	11	22	
Mean \pm SEM	469.3 \pm 50.57	129.2 \pm 17.91	409.4 \pm 64.59	312.5 \pm 67.65	675.5 \pm 90.57	609.4 \pm 74.76	
Multiple Comparisons	Hour	P value	Hour	P value	Hour	P value	Test
	22 vs. 3.5	<0.0001	3.5 vs. 6.5	0.0333	6.5 vs. 11	0.0428	One way Anova with Tukey's Multiple Comparison Test
	22 vs. 7.5	0.0355	3.5 vs. 11	<0.0001	7.5 vs. 11	0.0045	
	0.5 vs. 3.5	0.0026					

FIGURE	4.15. BRP and glutamate receptor oscillate with the same pattern (B)						
DESCRIPTION	1st day, Mean BRP, Per AZ Data						
Hour	0.5	3.5	6.5	7.5	11	22	
Mean \pm SEM	0.06443 \pm 0.003961	0.04546 \pm 0.001850	0.06316 \pm 0.004763	0.05533 \pm 0.007409	0.09532 \pm 0.008326		0.06543 \pm 0.009888
Multiple Comparisons	Hour	P value	Hour	P value	Hour	P value	Test
	0.3 vs. 11	0.0067	6.3 vs. 11	0.0073	11 vs. 22	0.0158	One way Anova with Tukey's Multiple Comparison Test
	3.3 vs. 11	<0.0001	7.3 vs. 11	0.0010			

FIGURE	4.15. BRP and glutamate receptor oscillate with the same pattern (B)						
DESCRIPTION	1st day, Integrated BRP, Per AZ Data						
Hour	0.5	3.5	6.5	7.5	11	22	
Mean \pm SEM	3.866 \pm 0.1995	2.860 \pm 0.1303	3.766 \pm 0.2516	3.453 \pm 0.3593	5.465 \pm 0.3994	3.696 \pm 0.4897	
Multiple Comparisons	Hour	P value	Hour	P value	Hour	P value	Test
	0.3 vs. 11	0.0040	6.3 vs. 11	0.0034	11 vs. 22	0.0020	One way Anova with Tukey's Multiple Comparison Test
	3.3 vs. 11	<0.0001	7.3 vs. 11	0.0008			

FIGURE	4.15. BRP and glutamate receptor oscillate with the same pattern (B)						
DESCRIPTION	1st day, Mean GluRIID, Per AZ Data						
Hour	0.5	3.5	6.5	7.5	11	22	
Mean \pm SEM	0.05815 \pm 0.003	0.01958 \pm 0.0026	0.05884 \pm 0.006	0.05014 \pm 0.0101	0.09686 \pm 0.012	0.07067 \pm 0.012	
Multiple Comparisons	Hour	P value	Hour	P value	Hour	P value	Test
	0.3 vs. 3.3	<0.0001	3.3 vs. 11	<0.0001	3.3 vs. 22	<0.0001	Kruskal Wallis with Dunn's Multiple Comparison Test
	3.3 vs. 6.3	0.0003	3.3 vs. 7.3	0.0464			

FIGURE	4.15. BRP and glutamate receptor oscillate with the same pattern (B)						
DESCRIPTION	1st day, Integrated GluRIID, Per AZ Data						
Hour	0.5	3.5	6.5	7.5	11	22	
Mean \pm SEM	3.260 \pm 0.2058	1.074 \pm 0.2002	3.081 \pm 0.3294	2.560 \pm 0.4452	4.985 \pm 0.6232	3.649 \pm 0.5705	
Multiple Comparisons	Hour	P value	Hour	P value	Hour	P value	Test
	0.3 vs. 3.3	<0.0001	3.3 vs. 7.3	0.0775	3.3 vs. 22	<0.0001	Kruskal Wallis with Dunn's Multiple Comparison Test
	3.3 vs. 6.3	0.0007	3.3 vs. 11	<0.0001	7.3 vs. 11	0.0537	

Appendix 2: Thesis Originality Report



Dijital Makbuz

Bu makbuz ödevinizin Turnitin'e ulaştığını bildirmektedir. Gönderiminize dair bilgiler şöyledir:

Gönderinizin ilk sayfası aşağıda gönderilmektedir.

Gönderen: Rukiye Karatepe
 Ödev başlığı: Moleküler metab
 Gönderi Başlığı: PhD_Thesis
 Dosya adı: ABSTRACT.docx
 Dosya boyutu: 7.69M
 Sayfa sayısı: 95
 Kelime sayısı: 22,421
 Karakter sayısı: 128,782
 Gönderim Tarihi: 18-Ağu-2022 11:51ÖÖ (UTC+0300)
 Gönderim Numarası: 1883879237

ABSTRACT

Karatas, R., Investigating the Effects of Neurometabolic Disease-Causing Genes on Synaptic Function in *Drosophila melanogaster*, Program of Molecular Metabolism Doctor of Philosophy Thesis, Ankara, 2022. Our group has identified several patients that harbor mutations in genes that hold the potential for being important players of synaptic function, UNC79 and MBOAT7 being two of them. UNC79 is one of the accessory subunits of a sodium leak channel, NALCN, which is composed of NALCN, UNC80 and UNC79 subunits. It is widely expressed in the brain and known to inhibit neurons in *Drosophila*. MBOAT7, on the other hand, is an enzyme that attacks preferentially arachidonic acid to ω -3 positions of phospholipids (PL) in specifically brain tissues of mammals. PLs are relevant players of synaptic function. In the light of information, we aimed to reveal the effects of UNC79 and MBOAT7 knockdowns on synapse size, number and morphology via combination of molecular biology and imaging techniques by using fruit fly as a model organism.

Pan-neuronal and motorneuron silencing of NALCN channel components - NALCN, UNC79, and UNC80 - and motorneuron silencing MBOAT7 ortholog in *Drosophila 2nd* instar larvae resulted in discrepancies in both brp and glutamate receptor levels and morphologies compared to control groups. Besides, pan-neuronal silencing MBOAT7 ortholog has no effect on brp and glutamate receptor intensities.

Dissecting wild-type larvae in a time-dependent fashion showed that brp and glutamate receptor levels oscillate in 2d neuromuscular junctions. Silencing motorneuronally silenced no in a time-dependent fashion showed a shift in brp and glutamate receptor intensities compared to control groups. On the other hand no changes in both brp and glutamate receptor levels were observed in pan-neuronally silenced fly larvae.

Keywords: Rare metabolic disease, GAL4/UAS, RNAi, brp, Glutamate receptor.

[*] This work was supported by TÜBİTAK 3000 (Project Number: 320Z188) and The German Academic Exchange Service (DAAD) Scholarship (57442043).

Appendix 3: Digital Receipt

PhD_Thesis

ORJİNALLİK RAPORU

% 7	% 5	% 5	% 2
BENZERLİK ENDEKSİ	İNTERNET KAYNAKLARI	YAYINLAR	ÖĞRENCİ ÖDEVLERİ

BİRİNCİL KAYNAKLAR

1	pubman.mpd.mpg.de İnternet Kaynağı	<% 1
2	refubium.fu-berlin.de İnternet Kaynağı	<% 1
3	www.biorxiv.org İnternet Kaynağı	<% 1
4	www.ncbi.nlm.nih.gov İnternet Kaynağı	<% 1
5	flybase.org İnternet Kaynağı	<% 1
6	journals.plos.org İnternet Kaynağı	<% 1
7	hdl.handle.net İnternet Kaynağı	<% 1
8	d-nb.info İnternet Kaynağı	<% 1
9	www.nature.com İnternet Kaynağı	<% 1

9. CV

Rukiye Karatepe

Employment History

Research Fellow , Leibniz Institute for Molecular Pharmacology (FMP), Berlin, Germany	September 2019-May2021
Research & Teaching Assistant , Sağlık Bilimleri University, Medical Faculty, Department of Medical Biology& Histology, Istanbul, Turkey	May2017-Present
Research & Teaching Assistant , Fatih University, Biology Department, Istanbul, Turkey	October2009-August2011

Education

PhD, Hacettepe University, Department of Pediatric Basic Sciences, Molecular Metabolism Unit, Ankara, Turkey	September 2014-Present
MSc, Fatih University, Biology Department, Istanbul, Turkey	October2009-December2011
BSc, Istanbul Technical University, Molecular Biology and Genetics, Istanbul, Turkey	September2003-June2009

Research and Teaching Experience

Graduate Student, Leibniz Institute for Molecular Pharmacology (FMP), Berlin	September2019-May2021
We identified patients that harbor de novo mutations causing neurometabolic diseases putatively affecting synaptic transmission. In this project with our collaborator, Prof. Alexander Walter, we wanted to find out if the candidate gene changes synapse shape, morphology, and synaptic protein abundance, by using Drosophila as a model organism	
Research & Teaching Assistant, Sağlık Bilimleri University , Istanbul	May2017-Present
Teaching Assistant for Histology and Anatomy labs during 2016-2019 time course to Medical students, Military Medical Students, ,Dentistry students.	
Graduate Student, Hacettepe University, Ankara	September2014-Present
Executed mutation screens of patients with inborn metabolic diseases. Performing my PhD studies in the topic "Investigation of Synapse Function in Neurometabolic Diseases"	

<p>Research Intern, Heidelberg University, Heidelberg, Germany</p> <p>Studied the effects of acute ethanol intoxication on in vitro dissociated hippocampal neurons</p>	<p>August2013- June2014</p>
<p>Research and Teaching Assistant, Fatih University, Istanbul, Turkey</p> <p>Assisted Laboratory work and helped create curriculum, composed exams, graded all written work and determined final grades for: General Biology Lab I General Biology Lab II Biochemistry Lab I/II Biochemistry Lab II Cell Biology Lab</p> <p>Performed Master's Thesis under supervision of Assoc. Prof. Lokman Alpsoy in the topic "Cytotoxic and genotoxic effects of Prunus armeniaca seed extracts in vitro"</p>	<p>October2009' August2011</p>
<p>Bachelor's Thesis, Istanbul Technical University, Istanbul, Turkey</p> <p>Performed Bachelor's Thesis under supervision of Assoc. Prof. Alper Tunga Akarsubaşın the topic "Microbial Community Analysis in Marmara Sea Sediments"</p>	<p>2008-2009</p>

Awards and Honors

<p>TUBITAK 1002-Short Term R&D Funding, Hacettepe University, Ankara, Turkey.</p>	<p>October2020- July2021</p>
<p>DAAD Short-Term Research Grant, Scholarship for Performing my PhD studies in FMP Berlin, Germany.</p>	<p>December2019- May2020</p>
<p>Project of Scientific Investigation (BAP) Fellowship, Fatih University, Istanbul, Turkey.</p>	<p>2010-2011</p>
<p>M.Sc. Scholarship Full scholarship (Scholarship, exempt from Master's fee, free transportation, free meal), Fatih University, Istanbul, Turkey</p>	<p>2009-2011</p>
<p>High School Scholarship, Turgut Ozal College, Malatya, Turkey</p>	<p>1999-2002</p>

Books

Vellay C. (1913). *Le Probleme Meditteraneeen* (M. Karatepe, R. Karatepe, V. Karatepe, Trans.), Ankara: Turk Diyanet Vakfi Publication (In Press).

Papers

Karatepe, R, Akal, ZU, Alpsoy, L. (2015). Genotoxic and Cytotoxic Effects of *Prunus Armeniaca* seed extracts in vitro, *Fresenius Environmental Bulletin*, 24(8), 2549-2555.

Computer Skills

R Programming, Fortran, GraphPad Prism, ImageJ, Adobe Illustrator, Cell Profiler, DB Browser for SQLite, Microsoft Power BI